The Mississippi River Source-to-Sink System: Perspectives on Tectonic, Climatic, and Anthropogenic Influences, Miocene to Anthropocene

S.J. Bentley Sr.[1*], M.D. Blum[2], J. Maloney[1], L. Pond[3], R. Paulsell[3]
[1]Coastal Studies Institute and Department of Geology and Geophysics, Louisiana State University, Baton Rouge LA 70803 USA,
[2] Department of Geology, University of Kansas, Lawrence, KS 66045 USA
[3] Louisiana Geological Survey, Louisiana State University, Baton Rouge LA 70803 USA
*Corresponding Author, sjb@lsu.edu, +1-225-578-5735

Keywords: Mississippi; source-to-sink; alluvial valley; Mississippi Delta; Mississippi Fan; Miocene; Pleistocene; Holocene; Anthropocene

Abstract

The Mississippi River fluvial-marine sediment-dispersal system (MRS) has become the focus of renewed research during the past decade, driven by the recognition that the channel, alluvial valley, delta, and offshore regions are critical components of North American economic and ecological networks. This renaissance follows and builds on over a century of intense engineering and geological study, and was sparked by the catastrophic Gulf of Mexico 2005 hurricane season, the 2010 Deep Water Horizon oil spill, and the newly recognized utility of source-to-sink concepts in hydrocarbon exploration and production. With this paper, we consider influences on the MRS over Neogene timescales, integrate fluvial and marine processes with the valley to shelf to deepwater regions, discuss MRS evolution through the late Pleistocene and Holocene, and conclude with an evaluation of Anthropocene MRS morphodynamics and source-to-sink connectivity in a time of profound human alteration of the system. In doing so, we evaluate the effects of tectonic, climatic, and anthropogenic influences on the MRS over multiple timescales.

The Holocene MRS exhibits autogenic process-response at multiple spatial and temporal scales, from terrestrial catchment to marine basin. There is also ample evidence for allogenic influence, if not outright control, on these same morphodynamic phenomena that are often considered hallmarks of autogenesis in sedimentary systems. Prime examples include episodes of enhanced Holocene flooding that likely triggered avulsion, crevassing, and lobe-switching events at subdelta to delta scales.

The modern locus of the Mississippi fluvial axis and shelf-slope-fan complex was established by Neogene crustal dynamics that steered sediment supply. Dominant Miocene sediment supply shifted west to east, due to regional subsidence in the Rockies. Then, drier

conditions inhibited sediment delivery from the Rocky Mountains, and Appalachian epeirogenic uplift combined with wetter conditions to enhance sediment delivery from the Appalachians.

Climatic influences came to the forefront during Pleistocene glacial-interglacial cycles. The fluvial system rapidly responded to sea-level rises and falls with rapid and extensive floodplain aggradation and fluvial knickpoint migration, respectively. More dramatically, meltwater flood episodes spanning decades to centuries were powerful agents of geomorphic sculpting and source-to-sink connectivity from the ice edge to the deepest marine basin. Differential sediment loading from alluvial valley to slope extending from Cretaceous to present time drove salt-tectonic motions, which provided additional morphodynamic complexity, steered deep-sea sediment delivery, diverted and closed canyons, and contributed to modern slope geometry.

Despite the best efforts from generations of engineers, the leveed, gated, and dammed Mississippi still demonstrates the same tendency for self-regulation that confronted 19th century engineers. This is most apparent in the bed-level aggradation and scour associated with changes in sediment cover and stream power in river channels, and in the upstream migration of channel depocenters and fluvial and sediment outlets at the expense of downstream flow, that will ultimately lead to delta backstepping. Like other source-to-sink systems, upstream control of sediment supply is impacting downstream morphology. Even within the strait-jacketed confines of the modern flood control system, the Mississippi River still retains some independence.

1.0 Introduction

On January 30, 1878, James Buchanan Eads spoke on the Mississippi River to the St Louis Merchant's Exchange, "We . . . see that the Creator has, in His mysterious wisdom, endowed the grand old river with almost sentient faculties for its preservation. By these it is able to change, alter, or abandon its devious channels, elevate or lower its surface slopes, and so temper the force which impels its floods to the sea" (McHenry, 1884). Eads was the leading fluvial engineer of his time, having developed the engineered levee system used to control the mouths of the Mississippi for navigation purposes. He recognized the self-regulating properties that have made the Mississippi a premier global example of a meandering river and fluvially dominated deltaic system. Scientific study of the river not new, and many of the most important understandings date from research conducted over a century ago. In this review we will examine these self–regulating, or autogenic, properties of the Mississippi River system, as well as the external, or allogenic, processes that control delivery of water and sediment to the Mississippi and its tributaries, within the context of source-to-sink connectivity.

Despite more than 150 years of investigations, there is still much to be learned about the Mississippi system by new research, and continued study of its linked alluvial, deltaic, and offshore components is of critical importance for several reasons. First, 10-20% of the world's population resides on or near large deltas (Vorosmarty et al., 2009), and most of these deltas are disappearing due to the combined effects of rising sea level, natural deltaic processes, and anthropogenic interference (e.g., Syvitski et al., 2009). The Mississippi has a massive record of intensive research on which to ground plans for coastal landscape conservation and restoration.

However, much previous research was conducted to understand deltaic environments as analogs for hydrocarbon production, maintain the river channel for river-borne commerce, and prevent flooding of adjacent flood plains and flood basins for agricultural purposes. A more detailed understanding, using modern tools, techniques, and increasingly complex numerical analysis is required to address controversial scientific issues and successfully implement conservation and restoration plans.

As a result, the Mississippi River fluvial-marine sediment-dispersal system (MRS; Fig. 1, Table 1) has become the focus of renewed research during the past decade, driven by the recognition that the channel, alluvial valley, delta, and offshore environments are critical components of North American economic and ecological networks (Day et al., 2014). This renaissance follows and builds on previous intense engineering and geological study, but has been triggered by the catastrophic Gulf of Mexico 2005 hurricane season, the 2010 Deep Water Horizon oil spill, and increased interest in the potential utility of source-to-sink concepts in hydrocarbon exploration and production. A number of basic-research studies and one major review paper (Blum and Roberts, 2012) have resulted from this renaissance. Individual studies have been wide ranging in focus, from climatology to ecology of the alluvial valley to shelf and slope studies.

With this paper, we consider influences on the MRS over Neogene timescales, integrate marine processes and the shelf to deepwater stratigraphic record, and more explicitly discuss the contribution of the Mississippi sediment routing system to development of the Gulf of Mexico continental margin. In doing so, we evaluate the effects of tectonic, climatic, and anthropogenic influences on the MRS over multiple timescales, and the relative roles of allogenic forcing versus autogenic self-organization. We first briefly describe the longer-term integration of the

Mississippi system, then focus on the Miocene Epoch (Fig. 2), when Earth's continents assumed their modern configuration (Potter and Szatmari, 2009), and the ancestral Mississippi River assumed a continental-scale, polyzonal tributary network resembling that of the present. We then explore the Pleistocene and early Holocene stratigraphic record, when global climate change brought about continental-scale glaciations (and deglaciations) and coupled high-amplitude cycles of global sea-level rise and fall. Last, we turn to the late Holocene and the time period of strong anthropogenic influences: we first outline processes and products before large-scale human alteration in the early 19th century, and contrast this with the strong anthropogenic impacts on the river basin, valley, and delta from the 19th century to the present.

1.1 The Mid-Cretaceous to Oligocene Mississippi Embayment and ancestral Mississippi System

Recent detrital-zircon studies of ancient Gulf of Mexico fluvial deposits (e.g., Mackey et al., 2012; Craddock and Kylander-Clark, 2013; Blum and Pecha, 2014) provide insights on Gulf of Mexico drainage integration that add to views developed from more traditional means (e.g., as summarized in Galloway et al., 2011), and complement new insights from continued exploration of the deepwater Gulf of Mexico. These studies show the Cretaceous was a period of regional-scale drainage integration only, with Gulf of Mexico drainage restricted to the area south of the Appalachian-Ouachita orogenic system; much of North America instead drained to the Boreal Sea through the Western Canada foreland-basin system (Blum and Pecha, 2014; Bhattacharya et al., this volume) (Fig. 2). At this time, the largest system discharging to the Gulf of Mexico flowed into the eastern Mississippi embayment, through what is now southwest Mississippi and south Louisiana. Farther west, a series of smaller river systems drained the Ouachita mountains in Arkansas and Oklahoma, and delivered sediments to the Houston embayment and west-central Gulf of Mexico (Fig. 2).

By the Paleocene, large-scale drainage reorganization in North America was well underway, establishing the basic template that persists today (Figs. 1, 2, and 3). Through the Paleocene and early Eocene, the eastern Gulf of Mexico was fed by the ancestral Tennessee River. By this time, an ancestral Mississippi system had developed as well, including tributaries from the northern Rocky Mountains and the northern margins of the Appalachians, and flowed north to south through the Mississippi embayment. At this time, however, the primary Gulf of Mexico sediment-routing system was located to the west, discharging sediment to the Gulf of Mexico in the vicinity, and just to the west of, present-day Houston, Texas (Winker, 1982; Galloway et al., 2011). This Paleocene system has long been recognized to have drained much of the rapidly uplifting southern and central Laramide Rocky Mountains, but detrital zircon signatures suggest headwaters extended west to include the Sierra Nevada in present-day California (Blum and Pecha, 2014; Fig. 2). In aggregate, these axes of sediment input from a truly continental-scale drainage basin produced the extensive basin-floor fan systems of the Wilcox trend in the central and western deepwater Gulf of Mexico, with their prolific hydrocarbon resources (Meyer et al., 2005; Sweet and Blum, 2011).

Much of the Eocene is poorly represented in the deepwater Gulf of Mexico, most likely due to globally high sea levels and flooding of the early Eocene Wilcox shelves (Galloway et al, 2011). Through the Paleogene, the shelf margin for the ancestral Mississippi system was located under present-day south Louisiana, roughly at the latitude of New Orleans (Galloway et al., 2000). This general understanding is over five decades old (Rainwater, 1964; Curtis, 1970), but details and fundamental controls are being better defined by new approaches to terrestrial geological questions and technology for deepwater exploration (Wu and Galloway, 2002; Combellas-Bigott and Galloway, 2006; Galloway et al., 2011; Snedden et al., 2012; Gallen et al., 2013; Miller et al., 2013; Craddock and Kylander-Clark, 2013).

As noted above, through the Paleocene and Eocene, the primary locus of allochthonous sediment accumulation in the Gulf of Mexico basin was along the northwestern margin (Fig. 3b). Extension commenced in the Rio Grande Rift in late Oligocene time, associated with peripheral uplift around the rift zone. Galloway et al. (2011) refer to this as emplacement of a “moat and dam” for sediment around and west of the rift, effectively truncating the large fluvial systems that had been building the NW Gulf of Mexico continental margin since the Paleocene. By this time, Laramide uplift had ceased, and fluvial systems within and draining the Rocky Mountains shifted to a mode of regional aggradation, filling basins with thick deposits of coarse fluvial sediment, reducing sediment supply to the Gulf of Mexico (McMillan et al., 2006; Table 2).

2.0 The Miocene Epoch: Establishment of the Modern Mississippi Fluvial Axis

By the Early Miocene, the continental-scale river system entering the Gulf of Mexico shifted eastward from the earlier Wilcox trend to the modern Mississippi fluvial axis, integrating drainage from the Appalachian Mountains to the northern and central Rocky Mountains. The Mississippi system became one of the dominant sources of sediment to the Gulf of Mexico basin at this time (Figs. 4 and 5), along with a paleo-Tennessee (Xu et al., 2014) that was later captured by the Mississippi. That drainage pattern continues to the present day. During the Miocene, ~200 km of shelf-margin progradation occurred, producing the foundation for the modern alluvial-deltaic system; the extensive Mississippi fan system was established as the dominant feature in the deepwater Gulf of Mexico (Winker, 1982; Galloway et al., 2011) (Figs. 2-5) (Table 2).

Miocene evolution of the ancestral MRS was most recently evaluated by Galloway et al. (2011). Our objective here is to use those insights as a starting point, and to re-evaluate their conclusions, in light of more recent published studies, as well earlier research. From early to mid Miocene time, fluvial sediment yield from the Appalachians increased (Boettcher and Milliken, 1994; Pazzaglia et al., 1997), despite the lack of active Appalachian tectonic activity for nearly 200 million years. The Appalachian rejuvenation at least doubled sediment delivery to the Mississippi fluvial axis (Galloway et al., 2011). The combined effects of Rio Grande uplift and rifting, reduction of sediment supply from the central and northern Rockies to the NW Gulf of Mexico margin, increased Appalachian sediment yield and increased sediment supply to the north-central Gulf of Mexico margin, made the Mississippi fluvial axis the dominant source of allochthonous sediment to the Gulf of Mexico by the middle Miocene (Galloway et al., 2000, 2011) (Figs. 3-5; Table 2), to the present day.

Both the decline of Rocky Mountain sediment delivery and the increase of Appalachian sediment yield have been attributed to climate. Aridity of Miocene climate (Zachos et al., 2001) has been suggested as the primary cause of reduced sediment discharge from western tributaries of the ancestral Mississippi (Galloway et al., 2011). In the Appalachian Mountains, increased Miocene precipitation has been suggested as a possible driver of increased sediment yield at that time (Poag and Sevon, 1989; Boettcher and Milliken, 1994). However, recent geomorphological and paleoclimatic studies in both the Rockies and Appalachians offer alternative explanations for the observed changes in sediment supply, discussed in following paragraphs.

Chapin (2008) documented arid conditions in the region of the Rocky Mountain Orogenic Plateau during much of Miocene time. From these observations, Galloway et al. (2011) attributed reduced sediment supply from the Rockies to loss of stream power, primarily due to climatic conditions. A contrasting view of the Miocene Rocky Mountains and northern Great Plains is proposed by Retallack (2007), who studied paleosols across Montana, Idaho, Nebraska, South Dakota, and Kansas, spanning the time frame of 40 Ma to Recent, to produce paleoclimate records from paleosol-based proxies. Using transfer functions, Retallack (2007) determined that climate of the middle Miocene (ca. 19-16 Ma) Rockies and Great Plains was generally warm and wet (with high interannual variability), shifting to cooler and drier conditions during the late Miocene (Table 2). These results were found to closely track the observed records of fossil plant and mammal community structure in the study areas. The same paleoecological records (Alroy et al., 2000; Barnosky and Carrasco, 2002; Prothero, 2004) did not track the more global paleoclimatic proxy record of Zachos et al. (2001) for the Miocene, suggesting important regional climate divergence from global patterns. Retallack's findings cannot shed much detail on stream power for the region, but these findings do suggest that rivers draining this region may have had at least episodic strong flows and sediment transport. Based on these two perspectives, the issue of climatic control of stream power forcing reduction in sediment discharge appears unresolved, and other potential controls should be considered.

McMillan et al. (2006) addressed this question directly, exploring the roles of interacting climate and tectonics for the Rocky Mountain Orogenic Plateau, in a study of Miocene fluvial aggradation, stream incision, and paleoelevation reconstruction for the Rockies and adjacent Great Plains. McMillan et al. (2006) reconstructed Miocene patterns of post-Laramide basin filling (by coarse fluvial sediments exceeding 1500 m thickness) and subsequent incision (up to 1500 m incision). They identified regional patterns that were best explained by regional slow subsidence after the Laramide orogeny to ca. 3-8 Ma (with coherent spatial variability), followed by regional doming. This shift from a period of subsidence (during which basins filled and valleys aggraded) to uplift (when incision increased and sediment discharge to Mississippi tributaries increased) overlaps with the regional climate shift from relatively warm and wet, to cooler and dryer in later Miocene time (Retallack, 2007; Chapin, 2008). This suggests that regional crustal motion played an important role in controlling sediment discharge to rivers, a role that may have been interwoven with climatic influences on erosion and sediment transport (McMillan et al., 2006).

Increased sediment yield from the Appalachian Mountains during the Miocene, attributed by numerous studies to increased precipitation or seasonality (Boettcher and Milliken, 1994; Galloway et al., 2011), has also been investigated with respect to the possible role of mantle-driven surface uplift. Gallen et al. (2013) and Miller et al. (2013) conducted independent studies of Miocene to recent stream incision and erosion in the unglaciated central and southern Appalachians, respectively, using comparable geomorphic analyses of stream-knickpoint migration and relief production. Results spanning ~1000 km along the Appalachian range yield remarkably consistent results, suggesting that relief production (and associated sediment yield) is most consistent with a period of epeirogenic uplift beginning well prior to ca. 3.5 Ma (early Pliocene) and as early as ca 15 Ma (early-middle Miocene). Patterns of incision and erosion are incompatible with geomorphic erosion style associated with increased precipitation. Further, much erosion apparently predates pronounced climate change ca. 4 Ma, and is of greater magnitude than can be explained by coastal-margin flexure or eustasy (Pazzaglia and Gardner, 2000; Rowley et al., 2011). No single geophysical explanation for such surface motions has achieved prominence, but several explanations based on mantle dynamics have been proposed (Gallen et al., 2013; Miller et al., 2013, and references therein). In summary, the dominant supply of sediment to the Miocene MRS shifted from west to east during Miocene time, due to large-scale uplift and rejuvenation of the Appalachians during a wet climate phase in that region (both increasing sediment yield), and reduced sediment supply from the Rocky Mountain Orogenic Plateau, due to early Miocene regional subsidence that reduced stream gradients (albeit during a relatively wet climate phase) and then drying (reducing stream discharge) during a later Miocene phase of regional tectonic doming.

Coastal and deepwater sediment accumulation in Middle and Late Miocene time created an extensive central Gulf of Mexico composite delta system, with a slope apron to the southwest of coastal deltas, and a channelized lobate fan complex to the southeast (Winker, 1982; Galloway et al., 2000; Wu and Galloway, 2002; Combellas-Bigott and Galloway, 2006) (Fig. 5, Table 2) that provided the foundation for later shelf-edge progradation and basinal accumulation in the northern Gulf of Mexico (NGoM). Regional sediment isopachs (Wu and Galloway, 2002) and more recent detrital zircon studies of terrestrial outcrops (Xu et al., 2014) suggest that several major terrestrial-to-marine delivery conduits may have existed, possibly simultaneously. Strong longitudinal variations in isopach thickness (up to 4.9 km of accumulation) and structure (Wu and Galloway, 2002) also indicate that sediment depocenters and accommodation were influenced by syndepositional faulting in western regions of the deepwater depocenters and salt migration in eastern deepwater regions.

Large-scale gravity-driven extensional and compressional deformation began in Miocene time, as large masses of sediment delivered to the NGoM margin at that time moved downslope into the basin; this continued through the Pleistocene (Winker, 1982; Galloway et al., 2000). Simultaneous with large-scale deformation driven by unstable terrigenous deposits, Mesozoic salt deposits deformed from the Cretaceous onward to produce varied and extensive seascapes (Combellas-Bigott and Galloway, 2006). Examples include: the Sigsbee escarpment, formed from laterally migrating salt tongues that locally thrust over older Pleistocene fan deposits (Weimer, 1990); km-scale pillows and basins that in some cases deformed and closed-off active deep-sea canyon systems and created slope minibasins (Weimer and Buffler, 1988; Tripsanas et al., 2007); and more extensive ridges with valleys that captured turbidity currents, possibly encouraging canyon development and shifting the loci of fan development (Weimer, 1990; Combellas-Bigott and Galloway, 2006; Pilcher et al., 2011; Snedden et al., 2012).

3.0 Pleistocene to Early Holocene: Continental Glaciation, Glacio-Fluvial Processes and Global Sea-Level Changes

The Pleistocene Epoch spans 2.6 My, and is subdivided into ~50 stages based on the $\delta^{18}O$ record from foraminiferal tests in marine sediments (hereafter referred to as Marine Isotope Stages, or MIS); these stages are interpreted to represent significant changes in global ice volume and sea level (e.g., Lisiecki and Raymo, 2005). In contrast to the smaller ice volumes and lower-amplitude climate shifts of the Miocene and Pliocene worlds, the high-amplitude Pleistocene cycles are commonly assumed to represent strong drivers for sediment-dispersal systems in general, and especially for the Mississippi system. However, sedimentary records of these events are more difficult to unravel. Uniformitarian reasoning suggests that processes active over recent glacial cycles were similar to those before (see Jaeger and Koppes, this volume), but a relatively detailed geochronologically constrained understanding of rates and forcing mechanisms in the Mississippi source-to-sink system only exists for the last 125 kyr, designated MIS 5 through 1.

3.1 Pleistocene Overview, 2.6-0.1 Ma

The oldest identified glacial deposits within the Mississippi drainage are represented by tills in Missouri, deposited ~2.4 Ma just north and west of the present Missouri-Mississippi confluence (Balco et al., 2005). This corresponds reasonably well to $\delta^{18}O$ records in Gulf of Mexico sediments that place the first measureable incursions of glacial meltwater at ~2.3 Ma (Joyce et al., 1993). Through the early Pleistocene, the marine isotope record indicates that cycles of global ice volume and globally coherent sea-level change followed the ~43 kyr cycle of changes in axial tilt, whereas the middle and late Pleistocene was dominated by the ~100 kyr eccentricity cycle (Imbrie and Imbrie, 1980; Martinsen et al., 1987; Lisiecki and Raymo, 2005) (Fig. 6). It is common to discuss ice volumes and sea-level in terms of end-member interglacials and highstands or glacials and lowstands, but it is important to recognize that the majority of the Pleistocene is represented by intermediate ice volumes (Porter, 1989) (Fig. 6a), with sea level and shorelines in mid-shelf positions (Fig. 6b)(Blum and Hattier-Womack, 2009). In fact, the mean Pleistocene sea-level position is -62 m (Blum et al., 2013), and full-glacial or interglacial positions represent only ~10-15% of the time. The same level of detail has never been recognized in the fragmentary, net erosional record of the continental interiors (Fig. 7). Twelve Plio-Pleistocene glaciations are now recognized for North America as a whole (e.g. Rutter et al., 2013), but it remains uncertain how many glacial events advanced far enough to the south to directly impact the Mississippi sediment dispersal system.

Galloway et al. (2000) subdivide phases of Pleistocene deposition based on the first downhole appearance of the foraminifer *Trimosina* A in offshore wells, which is typically dated at ~0.6 Ma, and corresponds roughly with the transition from the dominantly ~43 ky to the dominantly 100 ky Milankovitch forcing: strata below this marker are referred to as the Post

Trimosina A (PTA) depositional episode (~1.6-0.6 Ma), whereas strata above are referred to as the Post Sangamon (PS) episode (0.6-0.1 Ma). Weimer (1990) further subdivides marine strata in the Mississippi Fan into 17 seismic sequences, of which sequences 1-10 (oldest to youngest) correspond in part to Galloway et al.'s (2000) PTA, but extend into late Pliocene time; sequences 12-17 correspond generally to the PS depositional episode (Fig. 6). The Mississippi Fan subdivisions of Bouma et al. (1986) (Figs. 6, 8, and 9) are comparable to those of Weimer (1990) (Figs. 6 and 10).

Apart from uncertainties about glacial chronology and history, the terrestrial record for this time as a whole is significantly less complete due to its fragmentary record, and limits on geochronological techniques. However, ice advance into the North American interior has long been inferred to have rerouted the Mississippi's two largest tributaries, the Missouri and Ohio rivers, from their former outlets in the Hudson Bay lowlands, to the Mississippi valley and Gulf of Mexico (e.g., Licciardi et al., 1999). It was recognized early on that the Missouri had, for example, flowed east-northeast from North Dakota to Canada, and was diverted to the south as an ice-marginal stream during the Pleistocene, likely during the middle Pleistocene (Bluemle, 1972). Similarly, the Ohio headwaters are thought to have flowed west then north through the subsurface Teays valley in Indiana until diverted south by ice advance. Timing of this diversion is also poorly constrained, but it likely occurred during the middle Pleistocene as well. Hence, an early Pleistocene Mississippi drainage would have included the Platte River in Nebraska as its northwestern tributary, and the Tennessee and Cumberland rivers as northeastern tributaries.

Within the coastal plain, two contrasting interpretations of early Pleistocene fluvial axes have been published for what is now the modern Mississippi catchment. Saucier (1994a), for example, interpreted surface features and subsurface stratigraphy (from Corps of Engineers borings) to represent one axial river (the ancestral Mississippi) that drains the entire region, with the primary outlet entering the Gulf of Mexico in southwest Louisiana, several hundred kilometers west of the modern alluvial valley. In this model, the Arkansas, Red, and Tennessee rivers join the Mississippi as tributaries well inland from the coast. Saucier (1994a, illustrated in Plate 28a in that volume) in turn hypothesized that multiple large distributaries (not necessarily coeval) in late Pleistocene time dispersed sediments across >300 km of the present-day coastal plain, which would have created a broader swath of sediment dispersal to deepwater environments.

By contrast, Galloway et al. (2000 and 2011)(using more marine data sources than the primarily terrestrial observations of Saucier) interpret the early Pleistocene to include distinct Tennessee and Red rivers flowing to Gulf, east and west the Mississippi, producing shelf and slope strata that interfinger laterally with contemporary Mississippi coastal and marine deposits (Fig. 7). These proposed courses are hypothesized to have existed since the Miocene (Mississippi and Tennessee) and Pliocene (Red) (Galloway et al., 2011).

It is possible that both models are correct. Saucier's (1994a) detailed mapping demonstrates that within the Holocene, the Red River tributary has joined the Mississippi near its present confluence (Fig. 7), and at other times has either discharged directly to the Gulf of Mexico or joined much farther downstream. Similarly, the Arkansas River tributary now joins the Mississippi ~300 km north of its former late Pleistocene confluence, as does the Appalachian-derived Ohio-Tennessee River. A simpler explanation would therefore recognize the intrinsic scales over which avulsions occur. Resultant alluvial-deltaic headlands are constructed over millions of years, which, in continental-scale systems like the Mississippi, can extend hundreds of kilometers alongshore (Blum et al., 2013). In this alternative interpretation based on autogenic surface dynamics, the triangular-shaped Plio-Pleistocene alluvial-deltaic plain of the Mississippi system extends > 300-400 km across all of south Louisiana, with wider swaths in shelf and slope environments. In this sense, the deepwater fan of the Mississippi system theoretically incorporates the Mississippi fan, as formally named, and fed by eastern Mississippi channels, and the Bryant Fan farther west, fed by the Red and associated river channels entering Gulf of Mexico (Fig. 7).

Regardless of the lack of detail and conflicting interpretation of the terrestrial stratigraphic record, early Pleistocene sediment delivery to the marine basin was substantial. Galloway et al. (2011) add detail to a narrative by Winker (1982), and report 20-60 km of shelf-margin progradation during the PTA episode, mostly centered on ~91° W longitude and decreasing eastward (Fig. 7, south of the Red River fluvial axis). Estimates of early Pleistocene deep-sea fan accumulation range from 30 to 50% of total Quaternary fan thickness (up to 2000 m) (Feeley et al., 1990; Weimer, 1991) comprising approximately seven distinct seismic sequences (number of sequences during this time depending on the age model used: Weimer, 1990 versus Feeley et al., 1990). These sequences (based primarily on seismic data) are likely comprised of lithofacies typical of basin-floor fans, including sandy and muddy proximal channel-levee facies with interspersed mass-transport deposits) that transition basinward over hundreds of kilometers into sand-rich lobe complexes. Most sands and mixed sand-mud lithologies likely represent deposition during lower stages of sea level, when the Mississippi extended to the shelf margin and directly connected to slope canyons. Sand-rich successions that represent active fan construction can be separated from each other by condensed sections of hemipelagic carbonate-rich muds that accumulate during sea-level highstands, when fluvial sediments were mostly trapped on the inundated shelf. As has been the case through the Neogene, growth faults and mobile salt continued to steer sediment to the basin, and also caused syn- and post-depositional deformation (Weimer, 1990).

Although fan deposits older than ~100 ka are more difficult to correlate laterally, owing to subsequent erosion by younger channel systems, and deformation by salt tectonics (Bouma et al., 1986; Weimer and Buffler, 1988), changes in sediment delivery patterns during the last ~500 ky of Pleistocene time are apparent in lateral shifts of the depocenter location (Figs. 8 and 9) and canyon and submarine channel axes (Figs. 7 and 10). Compensational stacking of fan sequences is in some ways reminiscent of lobe switching associated with the Holocene Mississippi Delta discussed below. However, these shifts occur over timescales more closely aligned to Milankovitch forcing (compare timeline of Fig. 6 with submarine channel thalweg and depocenter locations in Figs. 8-10), suggesting at least some allogenic control. The most dramatic examples are massive glacigenic meltwater floods that are well documented in both terrestrial and marine settings for latest Pleistocene and early Holocene time (and discussed in section 3.2). Uniformitarian thought suggests such flows must have occurred during earlier deglacial periods (Fig. 6).

3.2 Late Pleistocene to Early Holocene, ca. 125-9 ka: Record of a Complete Glacial Cycle

A wide range of terrestrial and marine studies document specific landforms and deposits for ~125-9 ka that in some cases identify broad patterns of behavior, and in other cases identify specific events that reformed the alluvial valley and deltaic plain. These landforms and deposits reflect changes in sediment transfer and storage through the Mississippi source-to-sink system (Fig. 6b and Table 3). Datasets with the most robust time control (Table 2) come from the Lower Mississippi Valley and Pleistocene delta plain (Rittenour et al., 2007; Shen et al., 2012) or the slope and fan (Weimer, 1990; Feeley et al., 1990; Weimer and Dixon, 1994 Aharon, 2003; Tripsanas et al., 2007).

3.2.1 The Last Interglacial Period – MIS 5 (ca. 130-71 ka)

MIS 5 represents the ~130-71 ka time span (Fig. 6), and is commonly viewed as the last interglacial interval, when global ice volumes were small, and eustatic sea level was relatively high. During this time, ice-volume equivalent sea levels oscillated from +6 to -45 m, with a mean value of -27 m (Waelbroeck et al., 2002). MIS 5e, ca. 130-118 ka, represents the last time in Earth history prior to the Holocene when global sea level was at or slightly above present levels (+6 m)(Fig. 6a), whereas MIS 5c (peak ca. 96 ka) and 5a (peak ca. 82 ka) represent global high sea levels of smaller scale, -19 to -28 m relative to present. Intervening increases in ice volume occurred during MIS 5d and 5b, when global sea levels reached -49 and -44 m, respectively (Waelbroeck et al., 2002).

The MIS 5 stratigraphic record of the Lower Mississippi Valley is represented by a series of erosional terrace remnants that display meandering channel patterns similar in scale (and so possibly in discharge) to those of the modern channel (Rittenour et al., 2007; Shen et al., 2012), and date to MIS 5e and 5a. Along the coastal plain, MIS 5 valley aggradation and deltaic deposition produced the widespread apron of sediments known as the Prairie Complex (Autin et al., 1991; Shen et al., 2012) or alternately the Prairie Allogroup (Heinrich, 2006a). Elevations of MIS 5 fluvial deposits near the northern edge of the MIS 5 alluvial-deltaic plain are 10-20 meters above sea level (latitude 30.25-30.5°N), and up to 10 m above the adjacent Holocene Mississippi floodplain, whereas coeval deltaic and coastal strata dip below and are onlapped by Holocene deltaic and coastal deposits farther to the south. This long profile is interpreted to reflect flexural isostatic uplift upstream, with flexural subsidence farther south, as driven by sediment loading at the shelf margin (Heinrich, 2006a; Shen et al., 2012). Shen et al. (2012) argue that fluvial aggradation during this time interval (and also during the previous highstand at MIS 7; Fig. 6a) extended ~500 km inland from the modern coast, and, following earlier work by Blum and Tornqvist (2000), attributed such a far-reaching response to the low gradient of the Lower Mississippi Valley combined with the large sediment discharge likely comparable to late Holocene sediment discharge (Fig. 14). However, these ideas are based on limited field evidence. More broadly, the MIS 5 pattern within the Mississippi valley is consistent with the view in Blum et al. (2013), where the upstream limits of aggradation scale to backwater-induced changes in channel gradients forced by sea-level change and shoreline regression and transgression.

Basinward, on the Mississippi Fan (central and eastern Fan), MIS 5 is represented by condensed sections of hemipelagic deposits, as described above for earlier Pleistocene highstands (Horizon 30 of Bouma et al., 1986, and seismic sequence boundary 16-15 of Weimer, 1990, and Dixon and Weimer, 1998)(Figs. 6a, and 8-10; Table 3). During MIS 6, Bryant Canyon, on the western edge of the Mississippi shelf-slope-basin complex, delivered turbidity currents to Bryant Fan (Figs. 7 and 10). This direct conduit was closed during MIS 5, when salt motion beneath the slope deformed the local seabed, blocking the canyon, and producing a network of intraslope basins still evident today. These basins have recorded subsequent sediment delivery to the slope (Tripsanas et al., 2007).

3.2.2 The Last Glacial Period – MIS 4-early MIS 1 (ca. 71-9 ka)

The last glacial period commenced ca. 71 ka, and lasted some 60 kyrs, during which time global ice volumes were significantly larger, and eustatic sea level was significantly lower than today. During the first ~40 kyrs of the last glacial period, MIS 4-3, ca. 71-29 ka, global sea levels were lower (Fig. 6b) and oscillated between -90 and -40 m, but no so low as the last glacial maximum (LGM) during MIS 2. Also during this time, the Mississippi within the northern alluvial valley was transformed from a meandering non-glacial to a braided pro-glacial fluvial system, transporting glacigenic water and sediment from the Rocky Mountains and the Laurentide ice sheet margin. At the same time, in the southern alluvial valley, the Mississippi responded to global sea-level fall by valley incision through the previous inner shelf deltaic clinothem, with abandonment of Prairie depositional surfaces, and extension of the river mouth across the newly emergent shelf (Fisk, 1944; Saucier, 1994a; Autin et al., 1991; Blum, 2007; Rittenour et al., 2007).

Beyond a general chronology for ice advance and retreat, and loess deposition within the Mississippi catchment, upstream controls in the broader Mississippi drainage remain poorly known for MIS 4-3. Changes in provenance and style of sedimentation in the northern catchment suggest that expanding glacial lobes diverted the upper Mississippi and enhanced sediment production (Curry, 1998). However, there are no independent controls on sediment supply to the Mississippi system that can tell us whether glacial advance and retreat, coupled with a generally colder climate, resulted in more or less sediment production. In fact, early workers traditionally ignored the effects of glaciation or climate changes within the drainage basin itself, and inferred the lower Mississippi valley was directly controlled by glacial-eustatic base level controls. Fisk's (1944) classic and widely cited model, for example, inferred that valley incision from base-level fall and resultant non-deposition characterized the entire glacial period, with braided-stream deposition commencing during the period of deglacial sea-level rise.

Subsequent work by Saucier (summarized in Saucier, 1994), Blum et al. (2000), and Rittenour et al. (2004, 2007) demonstrated instead that braided-stream deposition occurred during the glacial period, and was linked in a process-response sense to glaciation rather than base-level fall. Moreover, valley incision was clearly step-wise, punctuated by at least 3 distinct periods of braided channel migration and channel-belt deposition during MIS 4 and 3, separated by intervening periods of renewed valley incision. Sea-level fall certainly had influence, but the Mississippi was subject to both upstream controls (on water and sediment flux) and downstream controls (on base level). In fact, it is difficult to avoid the conclusion that the overall trend of valley deepening during MIS 4-2 was a result of sea-level fall. Braided stream surfaces from MIS 4 (ca. 65 ka) occur below MIS 5a (ca. 85 ka) meander-belt surfaces at distances of ~650 km upstream of the present highstand shoreline. This indicates that a modest amount of incision propagated rapidly over this distance in a period of ~20 kyrs. Farther downstream, MIS 3 braided stream surfaces occur at elevations above the modern flood plain, and considerably higher than buried MIS 2 surfaces, at distances of 300 km from the present shoreline, illustrating that maximum depths of incision did not propagate that far upstream, in spite of ~80-90 m of sea-level fall. In sum, the length scales of Mississippi River incision in response to sea-level fall are not as great as envisioned in earlier work by Fisk (1944), but are impressive nevertheless.

Mapping in Saucier (1994) and Blum et al. (2000), revised with geochronological data in Rittenour et al. (2007), make it clear that lower Mississippi River during the MIS 4 and 3 was a large braided-stream system, with its course located on the western margin of the valley, within what is known as the Western Lowlands, and it was not joined by the Ohio River for some 300 km downstream of the present confluence. Three major MIS 4 and 3 braided-stream surfaces have been identified, mapped, and dated within the Western Lowlands and farther downstream. These surfaces form an overall degradational stair-step pattern in the landscape, at elevations lower than the previous MIS 5 flood plain and delta plain, and they must have therefore been graded to shorelines at a lower elevation, and farther seaward than present. Hence, the river's response to sea-level fall served to route sediment through, and export previously stored sediments from, the MIS 5 highstand alluvial valley and inner shelf clinothem (Blum et al., 2013), and shift the depocenter to the shelf margin, slope and the deep Gulf of Mexico.

Turning basinward, MIS 4-3 deltaic deposits of the Mississippi have been interpreted based on their position relative to known sea level (e.g., Suter and Berryhill, 1985), but geochronological controls are generally lacking. However, regressive deltaic systems from MIS 4-3 are well-known to the east, where they are referred to as the Lagniappe Delta, and to the west, offshore Texas (Anderson, 2005; Anderson et al., this volume). The Lagniappe system has been the subject of extensive seismic analyses and core study (Sydow et al., 1992; Roberts et al., 2004). During MIS 5 to MIS 2, coastal plain rivers (possibly the combined Mobile and Pascagoula rivers) developed a valley network that cut across the emergent shelf, and fed an outer-shelf to shelf-margin delta complex, building delta lobes seaward as the coast regressed southwards. Although the typical grain size of the Lagniappe delta complex is substantially sandier than the Holocene Mississippi River Delta (MRD), the lobate morphology and compensational 3D clinothem architectures are nevertheless strikingly similar. Cyclic progradation, abandonment, and marine planation of delta lobes have been shown for the Lagniappe, and are similar to the lobe-switching responses that have characterized the Holocene MRD at a much larger scale (Roberts, 1997; Roberts et al., 2004).

Dixon and Weimer (1998) and Tripsanas et al. (2007) argue that sea level during MIS 4 and 3 remained sufficiently high to limit the consistent delivery of large volumes of sediment from the Mississippi to the deep sea. Nevertheless, episodic sediment transport brought Mississippi sediments to the Bryant Canyon region, with four specific turbidites of Mississippi origin documented by Tripsanas et al. (2007) during MIS 3. Sufficient sediment reached the central and eastern Mississippi Fan to deposit recognizable seismic packages of this age. Bouma et al. (1986) estimated the age of seismic boundary 20 as mid MIS 3 (Figs. 6a, 8, 9). The more localized study of Weimer and Buffler (1988; and Weimer, 1990) used a more dense grid of borings and seismic data than had Bouma et al. (1986), and determined their Sequence 16 to date from late MIS 3 (Fig. 6a). Both studies noted the difficulty of establishing unambiguous geochronological control and regional correlations in fan strata of this age, owing to complex geometry of stratal surfaces, extensive erosion during early stages of fan-lobe deposition, and incomplete/poorly defined isotope stratigraphy and biostratigraphy.

Regardless of difficulties in correlation and age control, Bouma et al. (1986) and Weimer and others (Weimer and Buffler, 1988; Weimer, 1990; Dixon and Weimer, 1998) document extensive deep-sea sediment delivery at this time (isopach of unit 20-30 in Fig. 9, Table 3) and specific to Weimer's work, an extensive channel-levee network that extended >200 km from the toe-of-slope onto the basin floor at this time (Sequence 16 channels in Fig. 10). Although the chronological control on surfaces in Bouma et al. (1986) includes much uncertainty, an estimate of sediment mass delivery during the time span for unit 20-30 (Table 4, 20-60 ky) is 85-468 Mt/y, comparable to or greater than the late Holocene to present discharge of the Mississippi River (see sections 5.1-5.2). This deposit would have been fed by a falling-stage Mississippi River that was increasing in gradient, sediment supply, and water discharge (Shen et al., 2012).

Weimer (1990) suggested that the seismic sequence boundaries in his Mississippi Fan studies were primarily demarcated by hemipelagic deposits during periods of relative reduced delivery of terrigenous sediments. In the case of the 17-16 boundary (ca. 24 ka: Weimer, 1991), such a definition seems problematic, as the MIS 3-2 transition was more likely marked by accelerating sediment delivery, owing to the increased gradient of the Mississippi River, and lower sea level (pushing the river mouth closer to the shelf edge). One possible explanation is that the 17-16 boundary is an erosional discontinuity produced by accelerating sediment delivery and erosive power of turbidity currents (such as identified by Weimer [1990] at many other boundaries).

The MIS 2 (ca. 29-14 ka) Last Glacial Maximum records ice volume maxima and sea level minima (-120 m from ca. 29-18 ka) during the last 100 ky glacial cycle (Waelbroeck et al., 2002). During the LGM, the Lower Mississippi Valley was the primary conduit for meltwaters and glacigenic sediments from the North American ice sheet, whereas during deglaciation, meltwater was episodically ponded in large ice margin lakes and routed south to the Mississippi and Gulf of Mexico, east through the St. Lawrence seaway, or north to the Mackenzie River (Smith and Fisher, 1993; Fisher, 1994). Rapid deglaciation and corresponding sea-level rise at mean rates of >10 m/kyr occurred from ca. 18-6 ka, after which time ice volumes have remained relatively stable, and rates of sea-level rise decelerated significantly.

Glaciation and deglaciation and associated phenomena left a lasting imprint on the MRS. Early MIS 2 is preserved as a discontinuous series of terrace fragments in the upper Mississippi valley, but an extensive and well-preserved braided-stream surface has been mapped and dated within the Western Lowlands of the Lower Mississippi Valley (the Ash Hill terrace of Rittenour et al., 2007). The LGM then witnessed the first of two dramatic changes in course for the northern half of the LMV, when the Mississippi River broke through a bedrock gap and abandoned the Western Lowlands in favor of a course to the east, known as the Eastern Lowlands. Terraces with braided-stream patterns have been dated to the LGM, and correlated from northern reaches between Wisconsin and Minnesota (the Savannah terrace of Flock, 1983; Knox, 2007) through the Eastern Lowlands to the central Lower Mississippi Valley (the Sikeston terrace of Rittenour et al., 2007). Within the Western Lowlands, an extensive succession of eolian sand dunes accumulated on older braided stream surfaces, and the entrance to the Western Lowlands was filled with a large crevasse splay that permanently sealed that course from Mississippi River flows (Blum et al., 2000; Rittenour et al., 2007). Farther south, beginning in the central LMV, the Sikeston terrace disappears into the subsurface, onlapped and buried by younger floodplain strata associated with Holocene sea-level rise, but the equivalent surface can generally be traced in the subsurface through the lower valley where it is buried by up to 40 m of younger strata under the Holocene delta plain (Blum, 2007; Rittenour et al., 2007). These deposits are interpreted to represent a proglacial Mississippi, attached to the ice sheet in the north, but graded to the LGM shoreline at the shelf edge at -120 m below present-day sea level (Rittenour et al., 2007; Blum, 2007). It is worth noting, however, that associated Mississippi shelf-margin deltaic and shoreline strata have never been clearly identified or dated.

With ice-margin retreat, meltwaters were impounded in Glacial Lake Agassiz, located between the ice and former terminal moraines. This lake drained episodically, and meltwaters were routed through the Mississippi system until the eastern St Lawrence or northern MacKenzie River outlets were unblocked (Smith and Fisher, 1993; Fisher, 1994) Initial meltwater floods ca. 18-16 ka resulted in abandonment of the Sikeston depositional surface, and renewed valley incision. During subsequent meltwater shutdown, a new braided-stream surface formed at a lower level (the Kennett braid-belt of Rittenour et al., 2007). A second major period of meltwater discharge occurred ca. 14-12.5 ka, and resulted in renewed valley incision. Meltwater shutdown again resulted in renewed braided-stream deposition from ca. 12.5-12 ka (the Morehouse braid belt of Rittenour et al., 2007). The Kennett and Morehouse braided-stream surfaces are of a spatial scale that is unparalleled in more recent valley history, exceeding 20 km in width. The periods of incision and braided stream deposition recorded by the Kennett and Morehouse terraces have been interpreted to represent rapid response to meltwater discharges that were an order of magnitude greater than the Holocene Mississippi, and comparable in scale to the present-day Amazon. Farther downstream, each of these depositional surfaces is also onlapped and buried by Holocene strata, but can be traced to the southern valley beneath the modern delta plain. The age of these deposits farther downstream are inferred from stratigraphic relations. If this interpretation is correct, then meltwater-controlled millennial-scale periods of braid-belt formation and incision were transmitted far downstream >800 km, in spite of rapid sea-level rise.

A number of workers report that sediment delivery to the Mississippi fan continued through this period of deglaciation and rapid sea-level rise (Kolla and Perlmutter, 1993; Tripsanas et al., 2007; Covault and Graham, 2010). Indeed, the impacts of meltwater discharge and sediment delivery continued in the Gulf of Mexico into the Holocene. The last documented meltwater events occurred ca. 9.16 ka (Aharon, 2003), by which time global sea level had risen to within ~24 m of its present elevation (Waelbroeck et al., 2002). The meltwater discharges documented from isotope data in the Gulf of Mexico by Aharon (2003) correlate to the periods of valley incision documented by Rittenour et al. (2007), and to the youngest large-scale deposits in the Bryant Canyon and Fan, produced by both flood plumes and contour currents that advected

Mississippi sediment from the east (Tripsanas et al., 2007) (Fig. 6). In aggregate, the volumes of sediment eroded and exported basinward from the previous MIS 5 alluvial valley and delta plain, which would have added to the normal flux, has been estimated at ~50 Mt/yr over the ~60,000 year glacial period, ~10-12% of the pre-dam Mississippi sediment load (Blum et al., 2013). Such volumetric estimates are key to the source-to-sink approach (Walsh et al., this volume) and highlight how storage and/or excavation are can help control signal transfer (Romans et al., this volume).

Contemporaneous with and following meltwater routing to the St. Lawrence and Mackenzie River outlets, the Mississippi was transformed to its interglacial mode, and the lower valley began to aggrade, filling space created during the glacial period. The youngest braid belts in formed ca. 11-13 ka, and can be traced down ~800 km in the LMV (Rittenouer et al., 2007). These braided deposits were transported by huge flood pulses, the largest of which (melt water flood, labeled MWF-4 in Table 4) is estimated by Aharon (2003) to have had an average discharge rate ~2.3 times the record discharge rate of the 2011 Mississippi Flood, with a duration of ~1,000 years (Table 4). These floods undoubtedly helped incise and broaden the deep (20-30 m below shelf) and wide (~100 km) incised valley (Autin, 1991; Saucier, 1994b; Kulp et al., 2002). This valley experienced marine inundation earlier than the more elevated adjacent continental shelves, with the oldest dated marine transgressive deposits formed ca. 15-10 ka. During this time, meltwater floods continued to be discharged to the Gulf of Mexico (Coleman and Roberts, 1988a).

The Pleistocene intervals of combined sea level lowstand and massive meltwater discharges are thought to have been an important time for incision of deep-sea canyons into shelf and slope deposits (Prather et al., 1998). Prather et al. (1998) document ~13 individual buried canyon systems of Pleistocene age, some of which incise >100 km into the shelf/slope. Better age control exists for the channel-levee complexes fed by these canyons, documented for the Pleistocene Mississippi Fan by Weimer and Buffler (1988) (Fig. 10). Weimer (1990) notes that the repeated incision, infilling, and new incision of Mississippi deepwater canyon systems is relatively unique among most fluvial-marine dispersal systems, which more commonly connect to a smaller number of canyons (perhaps only one) that have remained active over longer periods of time. It is possible that both the erosive power and huge sediment volumes of meltwater floods (Tables 4 and 5), combined with the subsurface dynamics of salt migration, make both canyon incision and infill/closure more rapid than is the case for other river systems not connected to continental-scale glacial plumbing. This shifting arrangement poses challenges for defining source-to-sink behavior and connections over longer time scales.

Both Weimer and Buffler (1988) and Bouma et al. (1986) identify sequences in the Missisippi Fan associated with the LGM (unit 0-20 of Bouma, and Sequence 17 of Weimer), with similar bounding ages (Fig. 6a). By the LGM, the eastern fan was dormant, and Sequence 17 of the central fan (the youngest fan deposits) was downlapping eastward onto the eastern Fan Sequence 16 surface (Dixon and Weimer, 1998).

In sediments of the distal Orca Basin (on the slope southwest of the main body of the Mississippi Delta, Figs. 1 and 10), a decline in grain size, clay content, and number of reworked nannofossils from ~12 ka (near the time of melt water flood 4) to ~8 ka (after the last recorded meltwater floods: Table 5) suggests the declining sedimentary influence of episodic deglacial Mississippi flooding on the deep Gulf of Mexico basin (Brown and Kennett, 1998; Aharon, 2003) and the onset of hemipelagic sedimentation characteristic of the Mississippi Fan for the rest of Holocene time.

3.3 Comparison of Sediment Discharge and Fan Accumulation

Table 5 contains discharge rate and duration estimates for massive meltwater floods studied by Aharon (2003), along with estimates of water volume (product of flux and duration: this study) and sediment discharge (this study). Aharon (2003) estimates the average discharge for the smallest of these events (MWF-5 a to g, Table 5) to be 0.07-0.1 x 10^6 m^3/s, with durations of 80-260 y. For comparison, the average discharge of the 2011 Mississippi flood over the ~60 d span of the flood was 0.065 x 10^6 m^3/s.

Sediment mass is calculated here for each of the fan lobes mapped by Bouma et al. (1986)(Table 4). Only unit 0-20 corresponds to a time interval for which approximations of river-sediment discharge are available (Tables 4 and 5). Bouma et al. (1986) estimated the age of seismic surface 20 to be ~40-55 ka, indicating that fan lobe 0-20 incorporates sediments deposited considerably earlier than the oldest meltwater floods of Aharon (2003), which span a time interval of ~6.8 ky. The total sediment mass estimated for fan lobe 0-20 is 23,221 x 10^9 t (Table 4), or 422-581 Mt/y. The total sediment mass from meltwater flood delivery is 5,205 10^9 t, or 765 Mt/y, including pauses in meltwater delivery (Table 5). In other words, meltwater floods spanning 12-17% of the time in which unit 0-20 formed could have deposited 22% of the total sediment mass. Although these results are based on poorly constrained chronostratigraphy and span relatively long periods of time for discharge estimates, both the fan mass accumulation rate and the average rate of meltwater flood sediment delivery are the same order of magnitude as sediment loads of the pre-dam Mississippi River (Kesel et al., 1992; Meade and Moody, 2010). Because these long-term estimates of sediment discharge and accumulation include periods of reduced discharge, episodic discharge and accumulation rates were likely higher at times.

4.0. Later Holocene, 9.16-0.2 ka: Meanders, Delta Lobes, and Floods

The Holocene evolution (pre-Anthropocene) of the Mississippi alluvial valley and subaerial delta has been evaluated in detail during the last two decades by Roberts (1997), Blum (2007) and Blum and Roberts (2009, 2012). Holocene climatic conditions in the Upper Mississippi Valley have been reviewed by Knox (2003) and further evaluated by Montero-Serrano et al. (2010). The present study uses these studies as a starting point, and then expands to provide: (1) an overall summary of the Holocene evolution of the MRS system as a whole; (2) an evaluation of possible climatic influences on a fluvio-deltaic system that has generally been considered to be autogenic during this time.

4.1 Holocene Overview

Early in the Holocene, meltwater discharge was routed to the north away from the UMV, global sea-level rise decelerated and then stabilized ca. 9-6 ka (Fig. 6b), and the iconic characteristics of the modern Mississippi system began to develop. The dominant features of the northern and central Lower Mississippi Valley include the wide, rapidly-migrating, and laterally-amalgamated meander belts (Fisk, 1944; Holbrook et al., 2006, and many other references) that first developed ca. 10 ka (Rittenour et al, 2007). Near 300-400 km upvalley from the coastline, these wide channel belts transition to narrow distributary channel belts that grow and avulse, with the transition zone and first avulsion node roughly corresponding to the beginning of the backwater reach (Gouw and Autin, 2008; Blum et al., 2013). Downvalley, avulsion followed by abandonment is linked with cyclic construction and abandonment of extensive deltaic headlands on the inner shelf (Fisk, 1944; Frazier, 1967; Penland et al., 1988; Roberts, 1997, and many other studies). The oldest well-documented period of Holocene shelf deltaic construction is referred to as the Maringouin Delta, beginning ca. 7.5 ka, whereas the modern Plaquemines-Balize “birdsfoot” delta has been active since ca. 0.8 ka, and a new delta began to develop at the end of the Atchafalaya distributary during the last century (Fisk, 1944; Frazier, 1967; Saucier, 1994a; Roberts, 1997; Tornqvist et al., 1996; Kulp et al., 2005, and others). As alluded to above, with sea-level rise and deltaic development confined mostly to the inner and mid shelf, sediment delivery to the shelf margin, slope, and deepwater has been minimal, and restricted to the mud fraction. In Figure 11, we summarize major Holocene geomorphic developments and climatic events from the upper catchment to the continental shelf.

Chrono- and lithostratigraphic studies of the southern LMV and delta show that valley aggradation was very rapid following the rerouting of meltwater, with near-present floodplain levels reached by ca. 3.5 ka (Kesel, 2008) near the latitude of Baton Rouge. Farther downstream, following 14 ka, the present delta region was a coastal embayment that initially filled with coastal and shallow-marine deposits (Coleman and Roberts, 1988a; Autin et al., 1991; Kulp et al., 2002) and subsequently fluvio-deltaic sediments (Saucier, 1994a). The coastal region rapidly transformed from an embayed coast undergoing transgression to prograding delta composed of multiple headlands (Fig. 12). As the growing delta captured sediment along the inner edge of the wide Holocene continental shelf, outer shelf and slope sediment accumulation slowed, except in close proximity to active delta lobes, where river-sediment plumes contributed to slightly higher rates of hemipelagic sediment accumulation (Coleman and Roberts, 1988a, b).

The effects of high and relatively stable Holocene sea level extended well upstream in the LMV, reaching ~700 km from the present river mouth and ~400 km inland of the regional shoreline, where the modern channel intersects sea level and floodplain sediments presently onlap the Pleistocene Sikeston-Kennett braid belts (Rittenour et al., 2007). Shen et al. (2012) point out the remarkable similarity in the length scales of sea-level influence at both sea-level lowstands (inland knickpoint migration) and highstands (onlap by floodplain deposits), both in the range of 500-600 km upstream. As noted above, the tremendous upstream distances over which sea level has influenced the Mississippi River is attributable to the high sediment load of the Holocene Mississippi River, interacting with the low gradient of the lower river (Saucier, 1994a; Blum and Tornqvist, 2000; Blum, 2007; Shen et al., 2012), and the related backwater length (Blum et al., 2013). As noted in Jerolmack and Swenson (2007), lengths of marine-attached avulsions also scale to backwater conditions. Figure 13 illustrates this, wherein backwater effects influence meander migration rates (Hudson and Kesel, 2000), channel-belt width-to-thickness ratios (Blum et al., 2013)(Fig. 13), and the location of nodal avulsions (cf. Aslan et al., 2005; Nittrouer et al., 2012). Here, major course changes and resultant delta lobe-switching develop and propagate downstream (Fig. 12).

Long before backwater concepts were recognized as significant for avulsion, the phenomenon of lobe switching was documented by Fisk (1944), and has been the focus of many studies that have helped refine the concepts (Kolb and van Lopik, 1958; Saucier, 1994a; Penland et al., 1988, and many others) and chronostratigraphic models (Fisk et al., 1954; Frazier, 1967; Tornqvist et al., 1996; Kulp et al., 2005) (Fig, 12). This body of work is the basis for the "Delta Cycle" of Roberts (1997) that canonizes the MRD as the end-member system for river-dominated fluvio-deltaic successions. Within this model (Roberts, 1997), a delta lobe builds seaward, filling available accommodation and extending channel networks to the point where the hydraulic efficiency of the extensive distributary network is reduced, and the river seeks a more efficient and direct path to base level via avulsion (Fig. 12). While a new delta lobe builds, the abandoned lobe is degraded by the combined factors of reduced sediment supply, subsidence from self-weight consolidation of young, muddy, high-porosity sediments, and reworking by marine processes. This cycle has been repeated 5-6 times during the Holocene, the exact number of cycles depending on the definition of individual lobes by different researchers (e.g., Fisk, 1944; Frazier, 1967; Saucier, 1994a, and others). Each lobe cycle since the Teche lobe has left visible imprint on the subaerial landscape. This is where most human settlement is presently located, and has been concentrated for millennia (McIntire, 1958).

Although numerous absolute age models for the Holocene MRD exist (some shown in Fig. 11), the basic relative chronology of delta-lobe development is well established (Fig. 12). Most age models show at least two delta lobes that have been active river outlets at the same time (Fig. 11). Also, while some active lobes of the pre-Anthropocene MRD were building, other regions were in transgressive or equilibrium stages. This observation has great relevance to present public understanding and policies for stabilization and conservation of the modern system (Bentley et al., 2014). Simply put, the Mississippi River has never sustained a prograding front along the entire delta coastline. Like the pre-Anthropocene sediment budgets developed for the MRD by Blum and Roberts (2009, 2012), this observation forms an important initial condition for the Anthropocene MRD. These concepts are important to communicate to the public regarding shoreline stabilization and landscape restoration of the MRD, as embodied in Louisiana's Coastal Master Plan for coastal restoration and conservation (LA-CPRA, 2012).

A unique and non-geological perspective on the condition and extent of the MRD during the earliest stages of European exploration and colonization is offered by Condrey et al. (2014), who compiled and spatially calibrated observations of early Spanish and French explorers and surveyors, yielding a portrait of the coastal-deltaic landscape ca. 1537-1807. Collectively, these observations demonstrate that during the period of 1537-1807, major distributaries discharging abundant fresh water emerged from the modern locations of the Atchafalaya, Lafourche, Balize, and St. Bernard delta lobes. Such flows are generally supported by the prominence of distributaries shown in maps and charts of this time frame (Condrey et al., 2014; Blum and Roberts, 2012). Much of the MRD coast from the western edge of the Lafourche delta lobe (near the Atchafalaya River) to the modern Balize lobe may have been prograding, or was quasi-stable (Fig. 12D-E). This is a striking contrast to the much more limited distributary network and modest land-building of the present-day MRD (Fig. 12F).

4.2 Autogenic Versus Allogenic: Climatic Influence on Holocene Delta Morphodynamics?

Millennial-scale climatic control on Pleistocene processes in the MRS was documented in terrestrial records by Saucier (1994a, b), Blum et al. (2000), Blum (2007), and Rittenour et al. (2007) along with many other studies. As discussed above, the geomorphic evidence for glacial/deglacial impacts is clear because of an excellent geochronological framework for MIS 5-2 (Rittenour et al., 2007; Shen et al., 2012). Holocene geochronology is less well-developed, but key events are reasonably well-constrained. Moreover, interpretation of Holocene history is complemented by records of late Holocene floods and pronounced droughts in the upper Mississippi catchment (compiled in Knox, 2003) shown graphically in Figure 11. These studies collectively suggest a late Holocene history of strong variations in catchment precipitation/drought and river discharge over timescales of 500-700 y.

Terrestrial climatic records from the upper Mississippi drainage are complemented by interpretations of Pleistocene-Holocene fluvial discharge as recorded in the offshore Orca and Pigmy intraslope basins of the northern Gulf as well as the Bryant Canyon and Fan (Figs. 1 and 10)(Brown and Kennett, 1998; Aharon, 2003; Montero-Serrano et al., 2009, 2010; Tripsanas et al., 2007, 2013). For example, the $\delta^{18}O$ excursions of -0.5 to -2 per mil identified by Brown et al. (1999) are comparable to some deglacial $\delta^{18}O$ excursions identified by Aharon (2003), which prompted Brown et al. (1999) to suggest that the late Holocene megafloods (Fig. 11) may have been comparable in discharge to the smaller deglacial floods in Table 4. Taken at face value, these late Holocene floods would be unprecedented in the instrumented historic record; flows were much larger, for example, than the 2011 Mississippi Flood (Table 5). The terrestrial climate reconstructions of Knox (2003), coupled with interpretations of the isotope record from the Gulf of Mexico slope and basin, suggest century-scale variations in the delivery of hemipelagic sediments by massive river plumes during the late Holocene (Montero-Serrano et al., 2010; Tripsanas et al., 2013). For comparison, the initial deposit of the 2011 flood was largely confined to the shallow shelf (Kolker et al., 2014; Xu et al., 2014).

How did these high-magnitude floods drive geomorphological responses? How is this record of strong allogenic forcing linked with the autogenic avulsion and self-organization that is inherent to fluvial-deltaic systems? Some workers (e.g. Knox, 1985; 2003) have long inferred that major avulsions and deltaic headland abandonment were triggered by climatically-controlled changes in flood magnitudes in the Mississippi drainage basin. Other workers use the time scales of Mississippi avulsion and delta abandonment as empirical benchmarks for autogenetic processes (Slingerland and Smith, 2004). Blum et al. (2013) note that this persistent discussion about the relative influences of allogenic forcing vs. autogenic dynamics takes place within the context of some researchers in climate science consistently shortening the time scales over which major climate changes can be documented, while some experimentalists and theoreticians push for longer autogenic timescales (Wang et al., 2011).

Unfortunately, the precision and accuracy of age models for terrestrial records of climate change, or the record inferred from deep-sea sediments, are generally much higher than what is available for the terrestrial geomorphic record (Romans et al., this volume). For the Mississippi River and delta, the resolution of age models is not sufficient to argue that climate forcing preceded or followed geomorphic response. So, we cannot match specific avulsion events with specific periods of flooding in a true cause and effect manner. Also, it has been recognized since the early work of Fisk (1952) that avulsion of the Mississippi-Atchafalaya system, with complete abandonment of one deltaic headland and development of another, does not happen instantaneously, but instead takes centuries to go to completion (Aslan et al., 2005; Edmonds, 2012). Hence, the stratigraphic signature of an event like a major avulsion transgresses space and time. Nevertheless, comparison of river and delta age models with times of known paleofloods does not preclude interpretation of coeval flooding and avulsion with delta switching. Specifically, in Fig. 11, the lobe-shift transitions of Frazier (1967) are highlighted in yellow, and are broadly coincidental with some flooding events documented by Knox (2003), Brown et al. (1999), and Montero-Serrano et al. (2010). Also, the potentially more reliable dates from Tornqvist et al. (1996) for the onset of Balize and Lafourche delta construction agree with flooding events identified by Brown et al. (1999) and Montero-Serrano et al. (2010) within the limits of resolution.

Blum (2007) raised the possibility that higher-frequency climate and flood-magnitude changes may be recorded by smaller event-scale deposits, as described for tributaries to the Amazon by Aalto et al. (2003), where widespread crevasse-splay deposition appears to coincide with El Nino events. For the Mississippi system, Tornqvist et al. (2008) cored and dated two relatively extensive crevasse-splay complexes of the Lafourche delta (Napoleonville and Paincourtville splays), and identified two periods of rapid aggradation centered on 0.8±0.2 ka, and 1.15±0.15 ka. These aggradational episodes compare favorably with upper Mississippi regional flooding of Knox (2003) ca. 1.0-0.75 ka, the megaflood of Brown et al. (1999) at ca. 1.2 ka, and flooding of Montero-Serrano et al. (2010) at 0.8-0.6 ka. If such detailed, calibrated geochronology were more widely available for other delta lobes of the MRD, then more conclusive links between high-frequency climate patterns and delta morphodynamics might be identified. Such studies should be goals of future research.

5.0 Anthropocene

The Anthropocene (Zalasiewicz et al., 2011) can be defined in a source-to-sink context as the time frame during which human activities dominate signals of the production, transfer, and storage of water and sediment (Syvitski and Kettner, 2011; Romans et al., this volume). This is most apparent at the global scale since ca. 1800-1850 CE and is distinctive in the MRS (Kesel et al., 1992; Samson and Knopf, 1994; Knox, 2006; Meade and Moody, 2010; Blum and Roberts, 2009, 2012).

5.1. A Channelized River with High Sediment Loads and Few Distributaries: ca. 1850-1950

The first century of extensive human modifications to the lower Mississippi River resulted in channelization by engineering structures, straightening of the main channel through numerous engineered meander cutoffs, and development of the initial low-relief man-made levee system. Natural and engineered cutoffs were described by Mark Twain in Life on the Mississippi (1883): *"In the space of one hundred and seventy-six years the Lower Mississippi has shortened itself two hundred and forty-two miles. That is an average of a trifle over one mile and a third per year. Therefore, any calm person, who is not blind or idiotic, can see that in the Old Oolitic Silurian Period,' just a million years ago next November, the Lower Mississippi River was upwards of one million three hundred thousand miles long, and stuck out over the Gulf of Mexico like a fishing-rod. And by the same token any person can see that seven hundred and forty-two years from now the Lower Mississippi will be only a mile and three-quarters long, and Cairo* [Illinois] *and New Orleans will have joined their streets together, and be plodding comfortably along under a single mayor and a mutual board of aldermen. There is something fascinating about science . . . ."* Twain could not have foreseen the unsteadiness of engineering practices to come, but clearly he appreciated the scale at which river engineering had started to impact the Mississippi channel itself. Yet, through the 1800's, these effects were mostly restricted to the channel, and major floods continued to breach natural and low artificial levees, depositing sediment across the floodplains (Table 6; Davis, 1993).

However, within the delta plain, connections between the Mississippi channel and its major distributaries were severed as early as 1814, initially for defensive purposes (e.g. Bayou Manchac; Barry, 1997) and later for flood control (e.g. Bayou Lafourche in 1904; LBSE, 1904). Most of these activities were undertaken by the United States Army Corps of Engineers (US-ACE), for the combined purposes of enhancing navigation and controlling devastating floods

(Barry, 1997; Reuss, 2004) (Table 6), and were conducted under the Mississippi River & Tributaries Project (Reuss, 2004), authorized by the United States Congress in the 1928 Flood Control Act. This legislation followed the Great Flood of 1927, the catastrophic events of which are well-described in Barry's (1997) book "Rising Tide." This project was extended and strengthened in several phases (Moore, 1972; Smith and Winkley, 1996) to create a unified system of levees, channels and control structures to improve navigation and enhance public safety. Moreover, the 1927 flood included failure of the extant network of levees and flood control structures, and led to a reappraisal of the US-ACE strategy for river management that would feature construction of an extensive and continuous network of broader, higher-relief levees.

Therefore, the most significant impact of engineering activities on sediment transfer during the early to mid-20th century was the engineered isolation of the river and its sediments from its adjacent delta plain. Corthell (1897) predicted the consequences of this effort: *"No doubt, the great benefit to the present and two or three following generations accruing from a complete system of absolutely protective levees, excluding the flood waters entirely from the great areas of the lower delta country, far outweighs the disadvantages to future generations from the subsidence of the Gulf delta lands below the level of the sea and their gradual abandonment due to this cause."* Clearly, Corthell (1897) viewed these activities to be justifiable because of the broader range of societal benefits that would ensue, but now, more than a century later, the degradation and submergence of hydrologically isolated regions of the delta plain predicted by Corthell (1897) are real, and are being accelerated by rapid relative sea-level rise (Blum and Roberts, 2009, 2012; Day et al., 2014).

Channel shortening, discontinuous levee construction, and distributary closure during ~1850-1950 coincided with high sediment loads (Fig. 14) from a still mostly undammed catchment (Kesel et al., 1992; Meade and Moody, 2010). We also note that it has been argued that sediment loads from this period may have been inflated by intensive agricultural activity (Meade et al., 1990; Knox, 2003)(Table 6), but this is difficult to document given the existing instrumental record. Kemp et al. (2014) contend that the levee system served to produce more efficient sediment transfer to the delta, although this is difficult to verify with data.

Regardless, sediment delivery to the modern Balize delta produced some of the features that make it iconic within the broader deltaic literature. The well-known birdsfoot morphology is not, in itself, a byproduct of engineering, because it had already developed by the time of early European exploration (Coleman et al., 1991; Blum and Roberts, 2012; Condrey et al., 2014), and historical coastal surveys document rapid extension of distributaries from 1764 to 1959 (e.g., Southwest Pass; Figs. 15 and 16). Moreover, upstream from river mouths, subdeltas extended the subaerial extent of the delta plain through progradation followed by autogenic lobe switching (Gagliano and van Beek, 1976), but over timescales of decades and spatial scales of 100-200 km^2 (Figs. 17 and 18), compared to 1000-2000 y and >10,000 km^2 of major deltaic headland construction (Fig. 12). Indeed, much of the delta plain between the Bohemia Spillway and Head of Passes (shown in Fig. 15) was built from subdelta expansion during the 19^{th} and early 20^{th} centuries (Coleman and Gagliano, 1964), during what may have been a period of peak anthropogenically enhanced sediment delivery. This land then largely disappeared between 1932 and 2010 (Couvillion et al., 2011)(Fig. 19). These distributary levees and bars extended over a foundation produced by mudflows on the subaqueous prodelta (Figs. 19-21)(Fisk et al., 1954; Coleman and Gagliano, 1964; Coleman et al., 1980).

5.2 Dams, Reduced Sediment Load, River Training, and Flood-Control Structures, 1953 to Present

The period 1953-present has seen profound anthropogenic impacts in the Mississippi system that reflect engineering activities that were either implemented or envisioned earlier but taken to completion during this time. Collectively, these projects have fundamentally altered the water and sediment delivery system for the lower Mississippi River and delta to its present state (Allison et al., 2012).

Numerous authors note that dam construction has drastically impacted sediment supply to the lower Mississippi River and delta, a process started in the early 1900's (Anfinson, 1995). Three notable early events are (Autobee, 1996; Billinton et al., 2005): (1) Pathfinder Dam and Reservoir, initially completed on the North Platte River in eastern Wyoming in 1909 by the United States Bureau of Reclamation, which trapped sediment from 38,000 km^2 of the North Platte's Rocky Mountain source in north-central Colorado; (2) Fort Peck Dam and Reservoir, completed on the upper Missouri River in north-central Montana in 1940, which trapped sediment from ~150,000 km^2 of the Missouri's Rocky Mountain headwaters; and (3) Kentucky Dam on the Tennessee River, which was completed in 1944 and trapped sediments from almost all of the Tennessee drainage area of ~105,000 km^2. *Hence, by 1944, the majority of the mountainous highlands throughout the Mississippi drainage were no longer contributing sediments to the lower Mississippi River and delta*.

The total number of dams and reservoirs today is truly astounding. For example, by the late 1990's, Graf (1999) estimated 40,000 dams in the Mississippi drainage. However, the effects of dams on the Mississippi River's sediment supply cannot be placed in proper context without understanding the history of dams on the Missouri River, which still contributes the majority of sediment to the lower Mississippi River *per se* (Figs. 14 and 22). In this context, the most significant dams were constructed on the upper Missouri River under the auspices of the Pick-Sloan Flood Control Act of 1944 (Fig. 1). In fact, we define the beginning time for this section as 1953, because completion of Fort Randall Dam in central South Dakota effectively trapped sediment from 683,000 km^2 of the upper Missouri drainage, and had the single largest impact on sediment supply to the lower river (Meade and Moody, 2010). This was followed by Gavins Point Dam in southeastern South Dakota in 1955, which remains the lowermost dam on the Missouri River. Figure 22 illustrates the effects of these two dams on total suspended-sediment loads measured at Omaha, Nebraska, ~300 river kilometers downstream from Gavins Point, as well as the Missouri River tributary as a whole.

Collectively, these dams initiated almost instantaneously a period of rapid decline in total suspended load (Fig. 22) and the sand fraction (Blum and Roberts, 2014) for the lower Mississippi River as well (although see Nittrouer and Viparelli, 2014), after which the decline continued at a more gradual pace until ca. 1970 (Meade and Moody, 2010; Heimann et al., 2010; 2011). Meade and Moody (2010) attribute this rapid then gradual decline of sediment load to the combined effects of dams (the rapid component) and river response to channel and floodplain engineering (the gradual component). Although pre-dam records are short, the overall sediment-load reduction from both river-training and dam construction, as measured at Tarbert Landing, MS, was from 463 Mt/yr for total suspended load during the period 1950-1953, to ~130 Mt/yr for 1970 to 2013 (reduction of 72%), and from 78 Mt/yr for the suspended sand fraction only for 1950-1953 to 28 Mt/yr for 1970-2013 (reduction of 65%) (Fig. 22). However, even in its current condition, the Missouri system below Gavins Point Dam still supplies ~65% of the total suspended load and the suspended sand fraction for the lower Mississippi River. About 60% of the Missouri's contribution is produced between Gavins Point Dam and Omaha, Nebraska, a stretch of ~300 river kilometers during which no major tributaries join. The source of this sediment is therefore likely dominated by bed scour, which has been inferred by decadal-scale decreases in elevations of water surfaces over a range of discharges (Fig. 23; see Pinter and Heine, 2005; Jacobsen and Galat, 2006; Jemberie et al., 2008; Jacobson et al., 2009; Alexander et al., 2011). From data used to generate Figure 23, we estimate that ~1.05 Gt of sediment were eroded from the Missouri bed between 1954 and the mid 1990's, sufficient to account for ~26 Mt/yr of the total sediment load, with most of that derived from the reach above Omaha. The remaining part of the Missouri contribution to the overall Mississippi system is derived from the reach between Omaha and the Missouri-Mississippi confluence at St. Louis (~800 river kilometers), which includes a number of major tributaries. By comparison, the combined loads of the upper Mississippi drainage above the Missouri confluence, plus the Ohio and Arkansas rivers, are less than half of that contributed by the dammed Missouri system. The Anthropocene lower Mississippi River is today therefore a heavily supply-limited system relative to its Holocene counterpart, with this supply-limited condition corresponding to engineering activities more than 2000 km upstream.

This 1953-present time period also witnessed completion of the extensive and continuous network of improved, higher-relief levees developed through the Mississippi River & Tributaries Project. Moreover, the evolving US-ACE strategy for river management, exemplified by the Mississippi River & Tributaries, also featured spillways and flood-control structures to allow flood-water release into distributary basins, so as to ease pressure on levees (Moore, 1972), and begin to reverse the century-old practice of closing distributaries (Moore, 1972). The two most important of these are the Old River Control Structure, which connects the Mississippi River to the Atchafalaya Basin Floodway, and the Bonnet Carré Spillway, which connects the Mississippi River to Lake Pontchartrain (Figs. 1, 12F, and 15). The Old River Control Structure (ORCS) was completed in 1963, then reinforced and added to following a near failure during the flood of 1973. This series of structures took advantage of the natural ongoing avulsion of the Mississippi into the Atchafalaya basin, which had begun some 500 years ago (initially recognized by Fisk, 1952), through an "old" course of the Red River (Aslan et al., 2005). Construction of the ORCS was the last major step in creating the present flood-control network, and is mandated to maintain flows in the Atchafalaya River at 30% of the combined latitudinal flows of the Red and Mississippi rivers (Reuss, 2004). The present extent of the Mississippi River & Tributaries levee network downstream from Old River is shown in Figure 12F, with major outlets and gauging stations indicated in Figure 15.

Since the mid-20th century, channels within the Mississippi system have displayed strong morphodynamic responses to anthropogenic alteration of sediment supply, and routing of water and sediment. A particularly well-studied case is that of the Missouri River below Gavins Point Dam, where Jacobsen and Galat (2008; see also Alexander et al., 2011) document significant changes in water surface elevations over a range of discharges (Fig. 23). Decreases in bed elevation are attributed to bed scour below Gavins Point Dam, as well as channelization of the lower Missouri River. Discharge-specific stage increases of > 3 m are documented in various parts of the Mississippi main stem, from Minnesota to Louisiana (Wasklewicz et al., 2004; Remo et al., 2009). The US-ACE has recognized and addressed this problem by increasing the height (and breadth) of main-stem levees, beginning in 1897 (4m), then in 1928 (7m), 1972 (9 m), and 1978 (10.5 m) (Smith and Winkley, 1996).

For the lower river, recent river-stage analysis by the US-ACE (2014b) for river reaches near to and downstream from ORCS and the adjacent Morganza Floodway (completed in 1955, and operated only during the 1973 and 2011 floods) shows that for the period 1951-2010, river stages for specific flows at St. Francisville (~66 km downstream from ORCS and the Morganza Floodway; Fig. 15) have risen by 1.5 m at 8400 m^3/s flow to 4 m at 28,000 m^3/s. Allison et al. (2012) studied this same reach for water years 2008-2010 and identified an average loss of suspended sediment load of ~67 Mt/yr. They propose two hypotheses to explain this loss of sediment load: (1) seasonal sedimentation in flood plains that are not leveed, and (2) bed aggradation from loss of stream power downstream from ORCS. This part of the lower river corresponds to the backwater reach, where morphodynamics are affected by the ocean surface. In the upstream parts of the backwater reach, where the Allison et al. (2012) data was collected, rivers are inherently net depositional and characterized by avulsion, whereas in the lower parts of the backwater reach, increases in shear stress necessarily result in scour (Nittrouer et al., 2012).

Smith and Bentley (2014) conducted a pilot study of floodplain sediment accumulation along this reach and determined that accumulation of mud during seasonal flooding can account for <10% of the total suspended-load deficit. This indicates that >90% of the sediment deficit along this reach must be accounted for by river-bed aggradation, or another sediment reservoir not yet identified. If the total suspended-sediment deficit for 2008-2010 were deposited as a uniform sediment layer with porosity of 0.6, annual spatially averaged accumulation would be approximately 0.8-1.0 m/yr. This rate is an order of magnitude greater than the long-term rate of increase in stage documented by the US-ACE (2014b) for this reach, so the entire volume of sediment is not being trapped annually in the riverbed. However, this is conceptually consistent with the hypothesis that increase in stage along this reach is associated with channel-bed aggradation.

5.5 Morphodynamic Response of the Balize Lobe Delta Plain and Front, ca. 1953-Present

The majority of the delta plain has been undergoing submergence during this time period (Couvillon et al., 2011). The only notable exceptions consist of the two regions that still receive direct fluvial sediment supply: the Balize Delta and the outlets of the Atchafalaya River (Wax Lake and Atchafalaya River outlets). The Balize Delta projects seaward across the shelf and is prograding into deeper water, whereas the Atchafalaya and Wax Lake Deltas are bayhead deltas, prograding into water of a few meters depth. Accordingly, these two deltas display strongly contrasting delta-plain and prodelta dynamics during this period. Paola et al. (2011) postulated that the equilibrium surface area of a river delta is a function of: fluvial sediment supply, sediment retention rate (how much sediment delivered is retained to build land), local organic contribution from vegetative growth in delta soils, sediment porosity, eustatic sea level rise, and local subsidence. Delta land-area stability or growth is promoted by increasing sediment supply, retention, and organic production, by decreasing local subsidence (due to self-weight consolidation or other processes), and by sea-level fall or stability. Rate-changes in the opposite direction promote diminution of equilibrium land area. The longer-term land-area prospects for the delta plain have been evaluated in this context by Blum and Roberts (2009; 2012), and results strongly suggest overall land-area reduction for the delta plain will continue and accelerate as rates of sea-level rise accelerate.

For the Balize lobe since ca. 1953, the combined effects of these factors suggest reduction in equilibrium land area. The Balize lobe has built nearly to the shelf edge in water >100 m deep, such that subaerial land development must be preceded by filling accommodation with mostly muddy sediments that possess extremely low angles of repose (Figs. 20 and 21)(Coleman et al., 1980), and are routinely redistributed by tropical cyclones (Walsh et al., 2006, 2013; Guidroz, 2009; Goni et al., 2007). Sediment supply has been reduced (Fig. 22) and multiple factors have accelerated relative sea level rise. Reduction in land area (Fig. 19) between the old Plaquemines lobe shoreline (Fig. 12E) and Head of Passes (Fig. 15) has created a network of open bays subject to fair-weather wind-wave resuspension as well as storm waves and currents (such as West Bay; Andrus, 2007; Andrus and Bentley, 2007; Kolker et al., 2012) that has reduced sediment retention rate. Although subdeltas built during previous times of high sediment supply have largely disappeared (Figs. 17-19), the passes and distributary channels that created these subdeltas persist (such as Cubits Gap and Baptiste Collette Pass), generally remain unobstructed, are outlined by skeletal natural levees, and are presently used for local navigation.

Figure 16 shows that the Southwest Pass distributary had been prograding for at least 200 years of historic observations, but appears to have ceased progradation in the past half century, based on the close proximity of the 10-m isobaths mapped in 1959, 1979, and multiple NOAA surveys 2000-2010 (Maloney et al., 2014). Kemp et al. (2014) report that for the 2010-2013 period, the US-ACE dredging program within the Southwest Pass channel was unable to keep pace with rapid channel sedimentation, resulting in a navigation channel narrower than desired for the primary large-vessel entrance of the Mississippi River. This channel infilling is likely associated with a recent reduction in stream power for this reach, discussed in the following paragraphs.

Concurrent with reduction in land area between Head of Passes and the older Plaquemines shoreline and the end of Southwest Pass progradation, water discharge to the ocean from older subdelta outlets upstream from Head of Passes has increased since ca. 1960 (Kemp et al., 2014)(Fig. 24). More recently, flow was opened and persistently increased through newer outlets in the same section of river (manmade West Bay diversion; natural Fort St. Philip pass, Mardi Gras Pass and Bohemia Spillway)(Allison et al., 2012; Kemp et al., 2014). Simultaneously, discharge through two historically important Mississippi River outlets (South Pass and Pass a Loutre) have declined (Fig. 24). During this same period, the channel bed of lower Mississippi River reaches between Belle Chasse and West Bay (see Fig. 15 for location) have aggraded (Fig. 25A) at rates that increase downstream (Fig. 25B). It appears that the Mississippi is abandoning the outlets below Head of Passes, in favor of upstream outlets, i.e., backstepping. This deltaic response to changing sediment supply, among other factors, provides another example of how source-to-sink analysis can inform our understanding of morphodynamics.

5.6. Atchafalaya-Wax-Lake Deltas and Chenier Coast: Coupled Accretionary Delta-Shelf-Coastal System

The second main region of modern coastal accretion includes the coupled Atchafalaya and Wax Lake Deltas (hereafter referred to as the AWL deltas), the muddy Chenier Plain, and shelf prodelta extending between these two depocenters (Fig. 26). The AWL deltas have developed since the mid 20^{th} century. Primary controls on delta development have been the reactivation of the Atchafalaya River distributary system by clearing of logjams in the mid-19^{th} century, followed by rapid infilling of accommodation within the Atchafalaya Basin (Roberts, 1998; Patterson et al., 2003), and establishing controlled discharge down the Atchafalaya River at 30% of the total latitudinal flow of the Red and Mississippi rivers at the Old River Control Structure (McPhee, 1989; Reuss, 2004). Both deltas became subaerial following the Mississippi flood of

1973 (that nearly destroyed the Old River Control Structure; McPhee, 1989), and since then have grown at a combined rate of ~2 km^2/yr (Roberts, 1998; Allen et al., 2012), punctuated by more rapid growth following large river floods (Allen et al., 2012).

The AWL deltas form at outlets of the Atchafalaya River (Fig. 26). The Atchafalaya Delta is located at the main river outlet, which is used for extensive shipping and is dredged regularly (Roberts, 1997). The Wax Lake Delta is at the mouth of the Wax Lake Outlet of the river, constructed in 1944 to provide flood relief for Morgan City. The Wax Lake Outlet was originally dredged to ~10 m depth (Roberts, 1998), but has deepened erosively to >35 m in some locations. It shoals rapidly where the channel enters the delta and Atchafalaya Bay (water depths < 3 m) (Shaw et al., 2013). This sandy, friction-dominated delta is in a basically natural state, with no human channel maintenance, and is widely used as both a modern analogue for ancient shallow-water delta systems (Wellner et al., 2005), as well as a prime example of deltaic land-building potential from a large river-sediment diversion for coastal restoration (Kim et al., 2009; Bentley et al., 2014).

The AWL deltas are the third major Holocene delta complex to develop at that location, preceded by the Teche and Maringouin deltas several thousand years earlier (Figs. 11 and 12), which collectively define the western boundary of the subaerial MRD. The modern Atchafalaya and older distributaries have supplied muddy sediment to the coastal current system that has built an active sedimentary depocenter to the west, the Chenier Plain (Gould and McFarlan, 1959), and a muddy inner-shelf depocenter extending along the coast from Atchafalaya Bay towards the Chenier Plain (Fig. 26)(Draut et al., 2005a; Neill and Allison, 2005).

The Chenier Plain is named for the low oak-forested sand/shell ridges that occur in the region (“chêne” being French for oak tree), separated by expanses of muddy fresh and brackish marsh. The area was first investigated in depth by Howe et al. (1935) and Russell and Howe (1935). Gould and McFarlan (1959) expanded the 1935 studies, developing the hypothesis that wetlands originated as open-coast mudflats when MRD delta building is concentrated along the western half of the MRD (Teche, Lafourche, and modern AWL), providing an abundant proximal source of muddy sediment. In contrast, the cheniers represent erosional remnants of transgression during periods when major river discharge occurred on the eastern edge of the MRD (Fig. 11). Gould and McFarlan (1959) confirmed this, providing the first radiocarbon age model for the region (Fig. 11).

With the modern Chenier Plain presently in a net progradational phase (Huh et al., 2001), the adjacent muddy inner-shelf clinothem is a seaward subaqueous extension of coastal mudflats, parallel to oblique to the modern shoreline trend (Rotondo and Bentley, 2003; Draut et al., 2005b; Neill and Allison, 2005; Denommee and Bentley, 2013; Kolker et al., 2014). Observations have shown that coastal progradation has occurred during periods of high sediment supply. Fine sediments delivered by a coastal "mud stream" reach the Chenier Plain coast, driven by wind and river flows. High sediment concentrations then dampen wave energy, and allow open-coastal mud deposition during remarkably high-energy conditions (Morgan et al., 1953, 1958; Kemp, 1986; Huh et al., 2001). More recent investigations build on pioneering work by Kemp (1986), and demonstrate that wave attenuation begins well offshore over the fluidized muddy seabed and increases shoreward, coupling with wind-driven and baroclinic currents to produce a landward flux convergence of sediment (Kineke et al., 2006; Elgar and Raubenheimer, 2008; Jaramillo et al., 2009). Rapid short-term subaqueous sediment accretion occurs in association with energetic westward sediment transport from the Atchafalaya River to the clinothem (Rotondo and Bentley, 2003; Draut et al., 2005a; Neill and Allison, 2005; Denommee and Bentley, 2013) and facilitates coastal progradation at up to 70 m/yr (Huh et al., 2001; Draut et al., 2005b). Kolker et al. (2014) and Xu et al. (2014) studied sediment delivery from the 2011 flood, and determined that the 2011 locus of deposition was shifted offshore and downstream from the inner-shelf depocenter mapped earlier by Neill and Allison (2005). Kolker et al. (2014) attribute this to the strong along-shore currents observed in 2011, and the massive freshwater discharge associated with the flood, that would have reduced proximal sediment retention, and promoted transport to downstream locations.

Wells and Kemp's (1981) measurements of westward sediment transport (3.7 Mt/month from bay to shelf and 1.7 Mt/month along the shelf towards the Chenier Plain) were based on three current-meter moorings active for several months each during periods of high river discharge. These estimates undoubtedly incorporated large uncertainties, but are consistent within an order of magnitude with total inner shelf sediment accumulation rates of ~33 Mt/y measured by Neill and Allison (2005) using $^{210}Pb/^{137}Cs$ techniques, which integrate rates over timescales of up to ~100 y (i.e., including pre-1953 times of higher sediment discharge). The best and most recent estimates of Atchafalaya River sediment discharge are 44 Mt/y for 2008-2010 and 46.5 Mt for the 2011 flood (Allison et al., 2012 and Kolker et al., 2014, respectively). These results suggest that the inner shelf prodelta captures up to ~75% of sediment delivered by the Atchafalaya River, which is high for open-shelf dispersal systems (Walsh and Nittrouer, 2009). An alternate explanation is that the prodelta accumulation estimates of Neill and Allison (2005) average over longer periods of higher sediment discharge (pre-1953), and more recent periods of lower sediment discharge (Fig. 22), have a lower trapping efficiency.

6.0. Holocene and Anthropocene Sediment Budgets

Table 7 illustrates a summary of Holocene and Anthropocene patterns of sediment load and storage for the MRS, with references provided for each data source. For the Holocene, the three primary sediment depocenters considered are the alluvial valley and delta plain, Chenier Plain, and continental shelf and slope offshore of the modern delta. Comparison of sediment storage rates indicates that the alluvial valley and delta plain constitute the largest depocenter by far. Uncertainties on the order of 100% for Chenier Plain and shelf and slope sediment storage are likely, based on the type of data and approach used for rate estimation (see caption for Table 7). However, order-of-magnitude increases in storage rates for both settings would still leave the alluvial valley and delta as the dominant depocenter. These results also suggest that substantial quantities of sediment (>200 Mt/y, difference between discharge and storage rates over ky timescales) were exported from the system, beyond the confines of these three sedimentary environments.

Many estimates exist for historical Mississippi discharge and sediment accumulation. To simplify, the most recent estimates from Allison et al. (2012) (spanning water years 2008-2010) are used for sediment load, storage, and discharge by reach and outlet. These are compared to sediment storage rates determined for specific sedimentary environments using ^{210}Pb and ^{137}Cs geochronology. Using these approaches it would be unlikely that source and sink terms would match (and they do not, with apparent accumulation exceeding apparent delivery, owing to the methods used, which average over different spatial and temporal scales). However, results in Table 7 and Figure 27 allow comparison of relative rates for these portions of the dispersal system.

We highlight the following specific points. First, of the total load carried by the combined Mississippi and Atchafalaya rivers below the Old River Control Structure, >50% (103 Mt/y) is retained within the subaerial delta region, yet does not contribute to land growth for the reasons mentioned (Figs. 15 and 27, Table 7). Second, of the total sediment discharge leaving Mississippi and Atchafalaya river outlets, approximately one third exits Atchafalaya River outlets, one third exits the Mississippi below Head of Passes, and one third exits the Mississippi from a large number of small to moderate-sized outlets between Belle Chasse and Head of Passes (Figs. 15 and 27, Table 7). Third, subaqueous prodelta sediment storage for the combined Atchafalaya and Birdsfoot deltas is approximately equal to storage within the terrestrial and fluvial portions of the MRD, with more substantial shelf accumulation during the Anthropocene than evident over longer Holocene timescales (Table 7)(Coleman and Roberts, 1988a, b; Blum and Roberts, 2009). Finally, Anthropocene coastal and subaqueous accumulation along the Chenier Plain is of comparable magnitude to Holocene accumulation, on the order of 5-10% of total sediment storage documented within the Mississippi River system, but over a much shorter timescale.

7.0 Conclusions and Future Directions

Over longest timescales and most extensive spatial scales (Fig. 28, Table 8) in this study, evolution of the MRS shows how tectonics coupled with climatic processes can control development of a source-to-sink system. This is illustrated by the effects of Neogene crustal dynamics that steered sediment supply, especially from the Rocky Mountain Orogenic Plateau, and helped establish the Middle Miocene to Anthropocene locus of the Mississippi fluvial axis and shelf-slope-fan complex. Dominant Miocene sediment supply shifted west to east, due to regional subsidence in the Rockies, then drier conditions (albeit during a phase of uplift) inhibiting sediment delivery from the Rockies, and Appalachian epeirogenic uplift during a wet climate phase enhancing sediment delivery from the Appalachians.

Climatic influences became a dominant source-to-sink control during Pleistocene glacial-interglacial cycles. Sea level change brought rapid floodplain aggradation (rising sea level) and fluvial knickpoint (falling sea level) migration respectively extending 500-600 km inland from the coast. Meltwater floods spanning decades to centuries were powerful agents of geomorphic sculpting and source-to-sink connectivity from the ice edge to the deepest marine basin. These events scoured the valley, deposited vast deep-sea fan deposits, and probably also carved the canyons connecting the fluvial system to the deep basin. Differential sediment loading from alluvial valley to slope during Cretaceous to Anthropocene time drove salt tectonic motions, which provided additional morphodynamic complexity and steered deep-sea sediment delivery, diverted and closed canyons, and remains apparent in modern slope geometry (Fig. 10).

The Holocene Mississippi River source-to-sink system possesses attributes that have been used as primary examples of autogenic process-response at multiple spatial and temporal scales, from catchment to marine basin. These features include but are not limited to meander-belt and avulsion dynamics in both fluvial and deep-sea fan channels, compensational lobe switching at subdelta and delta scales in coastal settings, and over larger spatial and temporal scales in the deep-sea fan (Fig. 28, Table 8). However, there is ample evidence for allogenic influence, if not outright control, on these same morphodynamic phenomena that are often considered hallmarks of autogenesis in sedimentary systems. Prime examples include episodes of enhanced Holocene flooding that likely triggered avulsions and lobe-switching events (Figs. 11, 12, 17, 18, and 28), and influence of Pleistocene meltwater flood discharges on deep-sea fan deposition (Figs. 6, 8-10, Tables 3, 4 and 5).

One goal of extensive and expensive human alteration of the tributary, mainstem, and distributary network during the last two centuries has been to halt autogenic tendencies of channel migration and avulsion, and lobe switching, to make the Mississippi River more predictable for navigation, and to reduce community risk from flooding. Despite the best efforts from generations of engineers, the leveed, gated, and dammed Mississippi still demonstrates the same tendency for self-regulation that Eads wrestled with in the 19th century. This is most apparent in the bed-level aggradation and scour associated with changes in sediment cover and stream power in the LMV and UMV, and in the upstream migration of distributary channel depocenters and fluvial and sediment outlets at the expense of downstream flow, which will collectively lead to delta backstepping. Like other source-to-sink systems, upstream control on sediment supply impacts downstream morphology, and even within the strait-jacketed confines of the modern flood-control system, the Mississippi River still retains some independence.

In this paper we have highlighted source-to-sink connectivity spanning a wide range of scales in time and space, but we also recognize significant knowledge gaps. In our view, the socioeconomic and scientific value of the Mississippi system in North America is great enough that we require a rigorous quantitative understanding of source-to-sink processes and products, so as to manage the system in a sustainable way for human habitation and commerce. This understanding should build on, and go well beyond, the broad and deep empirical conceptual understanding that has developed over the past two centuries. In closing, we suggest three specific areas that should be targeted for future research:

(1) <u>More extensive and intensive application of new and evolving geochronological techniques</u>. Recent high-resolution studies using ^{14}C and optically stimulated luminenscence geochronology (described in sections 4.1 and 4.2) have allowed us to more accurately identify

rates and scales of processes and products within the system, from the alluvial valley (and farther upstream) to the lower delta. Such studies have been few and spatially restricted, but informative. Expanding high resolution geochronological study to other locations in the alluvial valley and delta, as well as the shelf and into deeper water, should be a priority.

(2) New chemostratigraphic and sediment provenance studies. Application of detrital zircon geochronology to provenance has provided important insights connecting sediment sources to downstream morphological development in the Mississippi system (sections 1.1, 2.0, and 3.0). However, this understanding remains skeletal at present, especially for the Plio-Pleistocene, and has focused primarily on sand-sized fractions of sediment load. Expanding such studies in terrestrial and deep-sea settings, through time and space, and including analysis of argillaceous sediments, such as Sr-Nd isotopic analysis, should also be a priority. The volumetrically dominant fine-grained stratigraphic record of the delta plain also represents a repository for information on North American climatic and biotic change that can be exploited by chemostratigraphic techniques.

(3) Improved understanding of the Mississippi shelf margin. The shelf-margin deltaic system from the MIS 2 glacial period, as well as previous glacial-period lowstands, remain largely undocumented, despite representing a critical linkage between the fluvial and deep-sea components of the Mississippi S2S system (section 3.2.2). Newer high-resolution seismic and other subsurface data can, in theory, make it possible to resolve and dissect these features. These data presently exist within the hydrocarbon industry, but are largely inaccessible. A concerted collaborative academic-industry effort to eliminate this knowledge gap, incorporating both seismic and subsurface coring efforts, would be beneficial.

Ideally, these three objectives would be elements of an integrated, community-level, basin-scale source-to-sink research program to develop a detailed and rigorous morphodynamic understanding of the Mississippi system, the flagship system for the North American continent. Such a program would better enable management of risks and resources for the Mississippi delta region of the future, and provide continued export of basic scientific insights from the Mississippi system to studies of other modern and ancient S2S systems.

9.0 Acknowledgements

Support for this paper was provided to SJB by the Billy and Ann Harrison Endowment for Sedimentary Geology of the LSU Foundation, and to SJB from the National Science Foundation via Coastal SEES Award #1427389, to JM from the Bureau of Ocean Energy Management, Cooperative Agreement M13AC00013 with LSU, and to MDB by the Scott and Carol Ritchie Chair at the University of Kansas.

10.0 References

Aalto, R., Maurice-Bourgoin, L., Dunne, T., Montgomery, D. R., Nittrouer, C. A., & Guyot, J. L., 2003. Episodic sediment accumulation on Amazonian flood plains influenced by El Nino/Southern Oscillation. Nature, 425(6957), 493-497.

Aharon, P., 2003. Meltwater flooding events in the Gulf of Mexico revisited: implications for rapid climate changes during the last deglaciation. Paleoceanography, 18(4), 1-14.

Allen, Y.C., Couvillion, B.R., and Barras, J.A., 2012. Using multitemporal remote sensing imagery and inundation measures to improve land change estimates in coastal wetlands. Estuaries and Coasts, 35(1), 190-200.

Alexander, J. S., Wilson, R. C. and Green, W. R., 2012. A brief history and summary of the effects of river engineering and dams on the Mississippi River system and delta. US Geological Survey Circular 1375. 44 p.

Allison, M. A., Demas, C. R., Ebersole, B. A., Kleiss, B. A., Little, C. D., Meselhe, E. A., Powell, N.J., Pratt, T.C., and Vosburg, B. M., 2012. A water and sediment budget for the lower Mississippi–Atchafalaya River in flood years 2008–2010: implications for sediment discharge to the oceans and coastal restoration in Louisiana. Journal of Hydrology, 432, 84-97.

Alroy, J., Koch, P.L. and Zachos, J.C., 2000. Global climate change and North American mammalian evolution. Paleobiology, 26(suppl.), 259–288.

Anderson, J. B., 2005. Diachronous development of Late Quaternary shelf-margin deltas in the northwestern Gulf of Mexico: implications for sequence stratigraphy and deep-water reservoir occurrence. SEPM Special Publication 83, p. 257-276.

Anderson, J.B., Wallace, D.J., Simms, A.R., Rodriguez, A.B. Weight, R.W., and P.Z. Taha. This Volume. Recycling Sediments Between Source and Sink During a Eustatic Cycle: Case Study of Late Quaternary Northwestern Gulf of Mexico Basin

Anfinson, J.O., 1995. The secret history of the Mississippi's earliest locks and dams. Minnesota History, Summer 1995, p. 254-267.

Andrus, T. M., 2007. Sediment flux and fate in the Mississippi River Diversion at West Bay: observation study (MS thesis, Louisiana State University).

Andrus, M., and Bentley, S.J., 2007, Sediment flux and fate in the Mississippi River Diversion at West Bay. ASCE: Coastal Sediments 2007, p. 722-735.

Aslan, A., Autin, W. J., & Blum, M. D., 2005. Causes of river avulsion: insights from the late Holocene avulsion history of the Mississippi River, USA. Journal of Sedimentary Research, 75(4), 650-664.

Autin, W. J., Burns, S. F., Miller, B. J., Saucier, R. T., & Snead, J. I., 1991. Quaternary geology of the lower Mississippi Valley. In: Geological Society of America, Decade of North American Geology, Quaternary nonglacial geology: conterminous US, 2, 547-582.

Autobee,, R., 1996, The North Platte Project. Bureau of Reclamation History Program, 39 p.

Barnosky, A.D. and Carrasco, M.A., 2002. Effects of Oligo-Miocene global climatic changes on mammalian species richness in the northwestern quarter of the USA. Evol. Ecol. Res., 4, 811–841.

Barry, J.M., 1997. Rising tide: the great Mississippi flood of 1927 and how it changed America: New York: Simon and Schuster.

Bentley, S.J., AM Freeman, CS Willson, J Cable, and L Giosan, 2014, Using what we have: optimizing sediment management in Mississippi River Delta restoration to improve the economic viability of the Nation. In John W. Day, G. Paul Kemp, Angelina M. Freeman, and David P. Muth, eds., Perspectives on the Restoration of the Mississippi Delta: The Once and Future Delta. 10.1007/978-94-017-8733-8_6.

Bhattacharya, J.P., Copeland, P., Lawton, T.F., and J.H. Holbrook. This Volume. Estimation of source area, river paleo-discharge, paleoslope and sediment budgets of linked deep-time depositional systems and implications for hydrocarbons.

Billington, D.P., Jackson, D.C., and Melosi, M.V., 2005. The history of large federal dams: planning, design, and construction in the era of Big Dams. United States Department of the Interior, Bureau of Reclamation, 605 p.

Bluemle, J. P., 1972. Pleistocene drainage development in North Dakota. Geological Society of America Bulletin, 83(7), 2189-2193.

Blum MD., 2007. Large rivers and climate change, past and future. In Large Rivers: Geomorphology and Management, ed. A Gupta, pp. 627–60. London: Wiley

Blum, M.D., Guccione, M.J., Wysocki, D.J., Robnett, P.C., 2000. Late Pleistocene evolutionof the Mississippi valley, southern Missouri to Arkansas. Geological Society ofAmerica

Bulletin 112, 221 –235. Blum, M. D., & Hattier-Womack, J., 2009. Climate change, sea-level change, and fluvial sediment supply to deepwater depositional systems. External Controls on Deepwater Depositional Systems: SEPM, Special Publication, 92, 15-39.

Blum, M., Martin, J., Milliken, K., & Garvin, M., 2013. Paleovalley systems: insights from Quaternary analogs and experiments. Earth-Science Reviews, 116, 128-169.

Blum, M., & Pecha, M., 2014. Mid-Cretaceous to Paleocene North American drainage reorganization from detrital zircons. Geology [Boulder], Pre-Issue Publicationdoi:10.1130/G35513.1

Blum, M. D., & Roberts, H. H., 2009. Drowning of the Mississippi Delta due to insufficient sediment supply and global sea-level rise. Nature Geoscience, 2(7), 488-491.

Blum, M. D., & Roberts, H. H., 2012. The Mississippi Delta region; past, present, and future. Annual Review Of Earth And Planetary Sciences, 40655-683. doi:10.1146/annurev-earth-042711-105248

Blum, M. D., & Roberts, H. H., 2014. Is sand in the Mississippi River delta a sustainable resource?. Nature Geoscience, 7(12), 851-852.

Blum, M.D., and Törnqvist, T.E., 2000, Fluvial response to climate and sea-level change: A review and a look forward: Sedimentology, v. 47, p. 2–48, doi: 10.1046/j.1365-3091.2000.00008.x.

Boettcher, S.S. and Milliken, K.L., 1994. Mesozoic–Cenozoic unroofing of the southern Appalachian basin: apatite fission track evidence from Middle Pennsylvanian sandstones: Journal of Geology, 102, 655–663.

Boettcher, S.S., Russell, I.A, Way, N., and West, B.P., 2011. New plays and play extensions revitalize the northern Gulf of Mexico: Gulf Coast Association of Geological Societies Transactions, 61, 543–545.

Bouma A.H., Coleman, J.M. and Meyer, A.W., 1986. Introduction, Objectives, and Principal Results of Deep Sea Drilling Project Leg 96. Deep Sea Drilling Program Initial and Project Reports, doi:10.2973/dsdp.proc.96.102, 96, 15-36.

Bowen, E.A., 1986. Correlation of Quaternary glaciations in the Northern Hemisphere; chart 1: Quaternary Science Reviews, 5.

Brown, P. A., & Kennett, J. P., 1998. Megaflood erosion and meltwater plumbing changes during last North American deglaciation recorded in Gulf of Mexico sediments. Geology, 26(7), 599-602.

Brown, A.P., Kennett, J.P. and Teller, J.T, 1999. Megaflood erosion and meltwater plumbing changes during last North American deglaciation recorded in Gulf of Mexico sediments: Reply, Geology, 27(5), 479 – 480.

Brown G, Callegan C, Heath R, Hubbard L, Little C, Luong P, Martin K, McKinney P, Perky D, Pinkard F, Pratt T, Sharp J, Tubman M, 2009. West Bay sediment diversion effects. ERDC Workplan Report—Draft. Coastal and Hydraulics Lab, U.S. Army Engineer Research and Development Center, Vicksburg, MS. 250 pp., Apps.

Bryant, W., Wetzel, A. and Sweet, W., 1986. Geotechnical Properties of Intraslope Basin Sediments, Gulf of Mexico, Deep Sea Drilling Project Leg 96, Site 619. Deep Sea Drilling Project Reports, doi:10.2973/dsdp.proc.96.153.1986.

Chapin, C.E., 2008. Interplay of oceanographic and paleo-climate events with tectonism during middle to late Miocene sedimentation across the southwestern USA: Geosphere, v. 4, p. 976–991, doi: 10.1130/GES00171.1.

Coleman, J.M. and Gagliano, S.M., 1964. Cyclic sedimentation in the Mississippi River deltaic plain: Gulf Coast Association of Geological Societies Transactions, 14, 67-80.

Coleman, J. M., Prior, D. B., and Garrison, L. E., 1980. Subaqueous sediment instabilities in the offshore Mississippi River delta (p. 60). Bureau of Land Management, New Orleans OCS Office.

Coleman, J.M. and Roberts, H.H., 1988a. Sedimentary development of the Louisiana continental shelf related to sea-level cycles: Part I—Sedimentary sequences: Geo-Marine Letters, 8, 63–108.

Coleman, J.M. and Roberts, H.H., 1988b. Late Quaternary depositional framework of the Louisiana continental shelf and upper continental slope: Gulf Coast Association of Geological Societies Transactions, 38, 407–419.

Coleman, J. M., Roberts, H. H., & Bryant, W. R., 1991. Late Quaternary sedimentation. The Gulf of Mexico Basin: Boulder, Colorado, Geological Society of America, The Geology of North America, 325-352.

Combellas-Bigott, R.I. and Galloway, W.E., 2006. Depositional and structural evolution of the middle Miocene, depositional episode, east-central Gulf of Mexico: The American Association of Petroleum Geologists Bulletin, 90(3), 335–362.

Condrey, R. E., Hoffman, P. E., & Evers, D. E. , 2014. The last naturally active delta complexes of the Mississippi River (LNDM): discovery and implications. In Perspectives on the Restoration of the Mississippi Delta (pp. 33-50). Springer Netherlands.

Corbett, D. R., McKee, B., & Allison, M., 2006. Nature of decadal-scale sediment accumulation on the western shelf of the Mississippi River delta. Continental Shelf Research, 26(17), 2125-2140.

Corthell EL. 1897. The delta of the Mississippi River. Natl. Geogr. Mag. 8, 351–54

Couvillion, B.A., Barras, J.A., Steyer, G.D., Sleavin, W., et al, 2011. Land-Area Change in Coastal Louisiana, 1932–2010: Sci. Investig. Map 3164, US Geol. Surv., Washington, D C.

Covault, J. A., & Graham, S. A. (2010). Submarine fans at all sea-level stands; tectono-morphologic and climatic controls on terrigenous sediment delivery to the deep sea. Geology [Boulder], 38(10), 939-942. doi:10.1130/G31081.1

Craddock, W.H. and Kylander-Clark, A.C., 2013. U-Pb ages of detrital zircons from the Tertiary Mississippi River Delta in central Louisiana: Insights into sediment provenance. Geosphere, 9(6), 1832-1851. doi:10.1130/GES00917.1

Curry, B.B., 1998. Evidence at Lomax, Illinois, for Mid-Wisconsin (~40,000 yr BP) Position of the Des Moines Lobe and for Diversion of the Mississippi by the Lake Michigan Lobe (20,350 yr BP): Quaternary Research, 50, 128-138.

Curtis, D.M., 1970. Miocene deltaic sedimentation, Louisiana Gulf Coast. In: Morgan, J.P., ed., Deltaic sedimentation, modern and ancient. SEPM Special Publication 15, p. 293-308.

Davis, D. W., 1993. Crevasses on the lower course of the Mississippi River. In Coastal Zone'93 (pp. 360-378). ASCE.

Day, J.W., Kemp, G.P., Freeman, A.M., and Muth, D.P, 2014. Perspectives on the Restoration of the Mississippi Delta: The Once and Future Delta. 10.1007/978-94-017-8733-8_6. Springer, Netherlands.

Denommee, K.D., and Bentley, S.J., 2013. Clinoform mechanics on the Southwest Louisiana Continental Shelf, Gulf Coast Association of Geological Societies Transactions, 63, 205-212.

DeSantis, L.R.G. and Wallace, S.C., 2008. "Neogene forests from the Appalachians of Tennessee, USA; geochemical evidence from fossil mammal teeth." Palaeogeography, Palaeoclimatology, Palaeoecology, 266(1-2), 59-68.

Dixon, B. T., & Weimer, P., 1998. Sequence stratigraphy and depositional history of the eastern Mississippi Fan (Pleistocene), northeastern deep Gulf of Mexico. AAPG bulletin, 82(6), 1207-1232.

Draut, A.E., Kineke, G.C., Velasco, D.W., Allison, M.A., and Prime, R.J. 2005a. Influence of the Atchafalaya River on recent evolution of the chenier-plain inner continental shelf, northern Gulf of Mexico. Continental Shelf Research, 25(1), 91-112.

Draut, A.E., Kineke, G.C., Huh, O.K., Grymes III, J.M., Westphal, K.A., and Moeller, C.C. 2005b. Coastal mudflat accretion under energetic conditions, Louisiana chenier-plain coast, USA. Marine Geology, 214(1), 27-47.

Edmonds, D.A**.**, 2012. Stability of backwater influenced bifurcations: a study of the Mississippi–Atchafalaya bifurcation: Geophysical Research Letters, 39, L08402.

Elgar, S., and Raubenheimer, B., 2008. Wave dissipation by muddy seafloors. Geophysical Research Letters, 35(7).

Feeley, M. H., Moore, T. J., Loutit, T. S., & Bryant, W. R., 1990. Sequence stratigraphy of Mississippi Fan related to oxygen isotope sea level index. AAPG Bulletin, 74(4), 407-424.

Feng, J. and Buffler, R.T., 1996. Post mid-Cretaceous depositional history, Gulf of Mexico basin: Gulf Coast Association of Geological Societies Special Publication, pp. 9–25.

Fisher, T. G., 2003. Chronology of glacial Lake Agassiz meltwater routed to the Gulf of Mexico. Quaternary Research, v. 59, p. 271-276.

Fisk H.N., 1944. Geological investigation of the alluvial valley of the lower Mississippi River. illus., War Department, Corps of Engineers, Washington DC, p 78

Fisk H.N. 1952. Geological Investigation of the Atchafalaya Basin and the Problem of the Mississippi River Diversion: Vicksburg, MS: US Army Corps Eng.

Fisk, H., Kolb, C., McFarlan, E.R., and Wilbert, L.R. 1954. Sedimentary framework of the modern Mississippi delta [Louisiana]. Journal Of Sedimentary Petrology, 24(2), 76-99.

Fisk, H. N., 1961. Bar-finger sands of Mississippi Delta. In: Geometry of sandstone bodies--A symposium, 45th annual meeting, Atlantic City, N. J., April 25-28, 1960, p. 29-52.

Flock, M. A., 1983. The late Wisconsinan Savanna Terrace in tributaries to the upper Mississippi River. *Quaternary Research*, *20*(2), 165-176.

Frazier D E. 1967. Recent deltaic deposits of the Mississippi River: their development and chronology. Trans. Gulf Coast A ssoc. Geol. Soc. 17:287–315

Gagliano, S.M., Light, P., and Becker, R.E., 1973. Controlled diversions in the Mississippi Delta system; an approach to environmental management. Hydrologic And Geologic Studies Of Coastal Louisiana, (8), Louisiana State University, Center for Wetland Resources, Coastal Resources Unit : Baton Rouge, LA, United States

Gagliano, S.M., and van Beek, J.L., 1976. Mississippi River sediment load as a resource. In Modern Mississippi Delta; depositional environments and processes; a guide book prepared for the AAPG/SEPM field trip; Mississippi Delta flight. Saxena, R. S., pp. 103-125). United States: New Orleans Geol. Soc.: New Orleans, La., United States.

Gallen, S.F., Wegmann, K.W. and Bohnenstiehl, D.R., 2013. "Miocene rejuvenation of topographic relief in the Southern Appalachians." GSA Today, 23(2), 4-10.

Galloway, W.E., Ganey-Curry, P.E., Li, X. and Buffler, R., 2000. "Cenozoic depositional history of the Gulf of Mexico basin." AAPG Bulletin, 84(11), 1743-1774.

Galloway, W. E., Whiteaker, T. L., & Ganey-Curry, P., 2011. History of Cenozoic North American drainage basin evolution, sediment yield, and accumulation in the Gulf of Mexico basin. Geosphere, 7(4), 938-973.

Goñi, M. A., Y. Alleau, R. Corbett, J. P. Walsh, D. Mallinson, M. A. Allison, E. Gordon, S. Petsch, and T. M. Dellapenna, 2007. The effects of Hurricanes Katrina and Rita on the seabed of the Louisiana shelf. The Sedimentary Record 5, no. 1 (2007): 4-9.

Gould, H.R., and McFarlan, E.J., 1959. Geologic history of the chenier plain, south-western Louisiana. Transactions - Gulf Coast Association Of Geological Societies, 9 261-270.

Gould, H. R., 1970. The Mississippi Delta complex. Special Publication 28 - Society Of Economic Paleontologists And Mineralogists, Deltaic Sedimentation, Modern and Ancient, p. 3-30.

Gouw MJP, Autin WJ., 2008. Alluvial architecture of the Holocene Lower Mississippi Valley (U.S.A.) and a comparison with the Rhine–Meuse d elta (The Netherlands). Sediment. Geol. 204:106–21

Graf, W. L., 1999. Dam nation; a geographic census of American dams and their large-scale hydrologic impacts. Water Resources Research, 35(4), 1305-1312. doi:10.1029/1999WR900016

Guidroz, W.S., 2009. Subaqueous, Hurricane-Initiated Shelf Failure Morphodynamics along the Mississippi River Delta Front, North-Central Gulf of Mexico. Unpublished, Louisiana State University PhD dissertation.

Hallam, A., 1992. *Phanerozoic sea-level changes*. Columbia University Press.

Heimann, D.C., Rasmussen, P.P., Cline, T.L., Pigue, L.M., and Wagner, H.R., 2010, Characteristics of sediment data and annual suspended-sediment loads and yields for selected lower Missouri River mainstem and tributary stations, 1976–2008: U.S. Geological Survey Data Series Report 530, 58 p.

Heimann, D.C., Sprague, L.A., and Blevins, D.W., 2011. Trends in suspended-sediment loads and concentrations in the Mississippi River Basin, 1950-2009. USGS Scientific Investigations Report 2011-5200.

Heinrich, P.V., 2006a. Pleistocene and Holocene fluvial systems of the Lower Pearl River, Mississippi and Louisiana, USA: Gulf Coast Association of Geological Societies Transactions, 56, 267–278.

Heinrich, P.V., 2006b. The White Lake Geologic Quadrangle, 1:100,000 (map). Louisiana Geological Survey, Baton Rouge.

Heinrich, P.V., and Autin, W.J., 2000, The Baton Rouge Geologic Quadrangle, 1:100,000 (map). Louisiana Geological Survey, Baton Rouge.

Heinrich, P.V., Snead, J., and McCulloh, R., 2002. The Lake Charles Geologic Quadrangle, 1:100,000 (map). Louisiana Geological Survey, Baton Rouge.

Heinrich, P.V., Snead, J., and McCulloh, R., 2003. The Crowley Geologic Quadrangle, 1:100,000 (map). Louisiana Geological Survey, Baton Rouge.

Holbrook, J., Autin, W. J., Rittenour, T. M., Marshak, S., & Goble, R. J., 2006. Stratigraphic evidence for millennial-scale temporal clustering of earthquakes on a continental-interior fault: Holocene Mississippi River floodplain deposits, New Madrid seismic zone, USA. *Tectonophysics*, *420*(3), 431-454.

Howe, H.W., Russell, R.J., and McGuirt, J.H., 1935. Geology of Cameron and Vermilion Parishes; physiography of coastal southwest Louisiana. Geological Bulletin [Baton Rouge, La.], 20(6), 1-72.

Huh, O.K., Walker, N.D. and Moeller, C., 2001. Sedimentation along the eastern chenier coast: Down drift impact of a delta complex shift: Journal of Coastal Research, 17(1), 72-81.

Imbrie, J., & Imbrie, J. Z. (1980). Modeling the climatic response to orbital variations. Science, 207(4434), 943-953.

Jacobson, R.B., and Galat, D.L., 2006, Flow and form in rehabilitation of large river ecosystems: An example from the Lower Missouri River: Geomorphology, v. 77, p. 249–269.

Jacobson, R.B., Blevins, D.W., and Bitner, C.J., 2009, Sediment regime constraints on river restoration—An example from the Lower Missouri River, *in* James, L.A., Rathburn, S.L., and Whittecar, G.R., eds., Management and Restoration of Fluvial Systems with Broad Historical Changes and Human Impacts: Geological Society of America Special Paper 451, p. 1–22, doi: 10.1130/2009.2451(01).

Jaeger, J.M., & Koppes, M., 2015. The role of the cryosphere in source-to-sink systems. Earth Sci. Rev. (in this volume).

Jaramillo, S., Sheremet, A., Allison, M.A., Reed, A.H., and Holland, K.T. 2009. Wave-mud interactions over the muddy Atchafalaya subaqueous clinoform, Louisiana, United States: Wave-supported sediment transport. Journal of Geophysical Research: Oceans (1978–2012), 114(C4).

Jemberie, A.A., N. Pinter, and J.W.F. Remo, 2008. Hydrologic history of the Mississippi and Lower Missouri Rivers based upon a refined specific-gage approach. Hydrologic Processes, 22: 7736-4447, doi:10.1002/hyp.7046.

Joyce, J.E., Tjalsma, L.R.C. and Prutzman, J.M., 1993. North American glacial meltwater history for the past 2.3 m.y.: oxygen isotope evidence from the Gulf of Mexico: Geology, 21, 483–486.

Keller, G., and Baldridge, W., 1999. The Rio Grande Rift; a geological and geophysical overview: Rocky Mountain Geology, 34(1), 121-130.

Kemp, G.P. 1986. Mud deposition at the shoreface: wave and sediment dynamics on the chenier plain of Louisiana, 148 p Ph. D. Thesis Department of Marine Science, Louisiana State University, Baton Rouge.

Kemp, G.P., Willson, C.S., Rogers, D.J., Westphal, K.A., and Binselam, A., 2014. Adapting to change in the Lowermost Mississippi River: Implications for navigation, flood control, and restoration of the delta ecosystem. In: Day, J. W., Kemp, G. P., & Freeman, A. M. (eds.) Perspectives on the Restoration of the Mississippi Delta, pp. 51-84. Springer Netherlands.

Kesel RH, Yodis E G, McGraw DJ. 1992. An approximation o f the sediment budget o f the lower Mississippi River prior t o m ajor human m odification. Earth Surf. Process. Landf. 17:711–23

Kesel, R.H., 2008. A revised Holocene geochronology for the lower Mississippi valley: Geomorphology, 101, 78–89

Kim, W., Mohrig, D., Twilley, R., Paola, C., and Parker, G., 2009. Is it feasible to build new land in the Mississippi River Delta?. EOS, Transactions American Geophysical Union, 90(42), 373-374.

Kineke, G.C., Higgins, E.E., Hart, K., and Velasco, D., 2006. Fine-sediment transport associated with cold-front passages on the shallow shelf, Gulf of Mexico. Continental Shelf Research, 26(17), 2073-2091.

Knox, J.C., 1985. Responses of floods to Holocene climatic change in the Upper Mississippi Valley: Quaternary Research, 23(3), 287-300.

Knox, J.C. 2003. North American paleofloods and future floods: responses to climatic change. Paleohydrology: understanding global change. Chichester: Wiley, pp. 143-164.

Knox, J.C. 2006. Floodplain sedimentation in the Upper Mississippi Valley: Natural versus human accelerated. Geomorphology, 79(3), 286-310.

Knox, JC. 2007. The Mississippi River system. In Large Rivers: Geomorphology and Management, pp. 145–81. London: Wiley

Kolb C.R. and Van Lopik J.R., 1958. Geology of the Mississippi River Deltaic Plain, southeastern Louisiana. Vicksburg, MS: U S Army Corps Eng.

Kolla, V., & Perlmutter, M. A., 1993. Timing of turbidite sedimentation on the Mississippi Fan. AAPG Bulletin, 77(7), 1129-1141. doi:10.1306/BDFF8E16-1718-11D7-8645000102C1865D

Kolker, A.S., Allison M.A., and Hameed S., 2011**,** An evaluation of subsidence rates and sea-level variability in the northern Gulf of Mexico: Geophys. Res. Lett., 38, L21404

Kolker, A.S., Miner, M.D., and Weathers, H.D., 2012. Depositional dynamics in a river diversion receiving basin: the case of the West Bay Mississippi River Diversion. Estuarine, Coastal and Shelf Science, 106, 1-12.

Kolker, A.S., Li, C., Walker, N.D., Pilley, C., Ameen, A.D., Boxer, G., Ramatchandirane, C., Ullah, M., and Williams, K., 2014. The impacts of the great Mississippi/Atchafalaya River flood on the oceanography of the Atchafalaya Shelf. Continental Shelf Research, 86, 17–33

Kulp, M., Howell, P., Adiau, S., Penland, S., Kindinger, J. and Williams, S.J., 2002. Latest Quaternary stratigraphic framework of the Mississippi River delta region: GCAGS Transactions, 52, 573-583.

Kulp, M., FitzGerald, D., & Penland, S., 2005. Sand-rich lithosomes of the Holocene Mississippi River Delta Plain. Special Publication - Society For Sedimentary Geology, 83279-293.

LA-CPRA (Louisiana Coastal Protection and Restoration Authority), 2012. Louisiana's Coastal Master Plan for a Sustainable Coast. http://www.coastalmasterplan.louisiana.gov/, accessed Sept 21, 2014.

LBSE (Louisiana Board of State Engineers), 1904. Report of the Board of State Engineers of the State of Louisiana. The Advocate. Baton Rouge, Louisiana, 235 p.

Licciardi, J. M., Teller, J. T., & Clark, P. U., 1999. Freshwater routing by the Laurentide ice sheet during the last deglaciation. Geophysical Monograph, 112177-201.

Lisiecki, L.E., and Raymo, M.E., 2005. A Pliocene-Pleistocene stack of 57 globally distributed benthic d18O records. Paleoceanography, 20, doi:10.1029/2004PA001071.

Love, M.R., Amante, C.J., Eakins, B.W., and Taylor, L.A., 2012. Digital Elevation Models of the Northern Gulf Coast: Procedures, Data Sources and Analysis, NOAA Technical Memorandum NESDIS NGDC-59, U.S. Dept. of Commerce, Boulder, CO, 43 pp.

Mackey, G. N., Horton, B. K., & Milliken, K. L., 2012. Provenance of the Paleocene-Eocene Wilcox Group, western Gulf of Mexico Basin; evidence for integrated drainage of the southern Laramide Rocky Mountains and Cordilleran Arc. Geological Society Of America Bulletin, 124(5-6), 1007-1024. doi:10.1130/B30458.1

Maloney, J. M., Bentley, S. J., Obelcz, J., Xu, K., Miner, M. D., Georgiou, I. Y., Keller, G., 2014. Assessing Subaqueous Mudflow Hazard on the Mississippi River Delta Front, Part 1: A Historical Perspective on Mississippi River Delta Front Sedimentation. In AGU Fall Meeting Abstracts (Vol. 1, p. 1061).

Martinson, D. G., Pisias, N. G., Hays, J. D., Imbrie, J., Moore, T. C., & Shackleton, N. J., 1987. Age dating and the orbital theory of the ice ages: development of a high-resolution 0 to 300,000-year chronostratigraphy. Quaternary research, 27(1), 1-29.

McHenry, E., 1884. Addresses and papers of James B. Eads. Slawson & Co., St Louis.

McIntire, W.G., 1958. Prehistoric Indian Settlements of the Changing Mississippi River Delta: Louisiana State Univ. Press, Baton Rouge, LA.

McKay, D. and Berg, D., 2008. Optical ages spanning two glacial-interglacial cycles from deposits of the ancient Mississippi River, north-central Illinois: Geological Society of America Abstracts with Programs, 40(5), 78 p.

McMillan, M.E., Heller, P.L., and Wing, S.L., 2006, History and causes of post-Laramide relief in the Rocky Mountain orogenic plateau: Geological Society of America Bulletin, v. 118, p. 393–405, doi: 10.1130/B25712.1.

McPhee, J., 1989. The control of nature. Macmillan.

McVey, K.J., 2005. Pleistocene and Early Holocene Aggradation of Mississippi River Tributaries within the Eastern and Western Lowlands of the Mississippi Alluvial Valley [M.S. thesis]: Fayetteville, University of Arkansas, 192 p.

Meade. R.H., Yuzyk, R.R., and Day, T.J., 1990, Movement and storage of sediment in rivers of the United States and Canada. In, Wolman, M.G., and Riggs, H.C., Surface Water Hydrology: Boulder, CO, Geological Society of America, The Geology of North America, v. O-1.

Meade RH, Moody JA, 2010. Causes for the decline of suspended-sed-iment discharge in the Mississippi River system, 1940–2007. Hydrolical Processes 24:35–49

Meyer, D., Zarra, L., and Yun, J., 2007. From BAHA to Jack, evolution of the lower Tertiary Wilcox trend in the deepwater Gulf of Mexico. The Sedimentary Record, 5(3), 4-9.

Miller, S.R., Sak, P.B., Kirby, E. and Bierman, P.R., 2013. Neogene rejuvenation of central Appalachian topography: Evidence for differential rock uplift from stream profiles and erosion rates. Earth and Planetary Science Letters, 369, 1-12.

Montero-Serrano, J. C., Bout-Roumazeilles, V., Sionneau, T., Tribovillard, N., Bory, A., Flower, B. P., & Flower, B., 2010. Changes in precipitation regimes over North America during the Holocene as recorded by mineralogy and geochemistry of Gulf of Mexico sediments. Global And Planetary Change, 74(3-4), 132-143. doi:10.1016/j.gloplacha.2010.09.004

Montero-Serrano, J. C., Bout-Roumazeilles, V., Tribovillard, N., Sionneau, T., Riboulleau, A., Bory, A., & Flower, B., 2009. Sedimentary evidence of deglacial megafloods in the northern Gulf of Mexico (Pigmy Basin). Quaternary Science Reviews, 28(27), 3333-3347.

Moore, N.R., 1972. Improvement of the lower Mississippi River and tributaries, 1931-1972. Vicksburg, Miss.: Mississippi River Commission.

Morgan, J.P, Van Lopik, J.R, and Nichols, L.G, 1953. Occurrence and development of mudflats along the western Louisiana coast. Louisiana State University Coastal Institute Technical Report 2, 34 p.

Morgan, JP, Nichols L.G, and Wright, M, 1958. Morphological effects of Hurricane Audrey on the Louisiana coast. Louisiana State University Coastal Institute Technical Report 10, 53 p.

Neill, C.F., and Allison, M.A. (2005). Subaqueous deltaic formation on the Atchafalaya Shelf, Louisiana. Marine Geology, 214(4), 411-430.

Nittrouer, J.A., Shaw, J., Lamb, M.P. and Mohrig, D., 2012, Spatial and temporal trends for water-flow velocity and bed-material sediment transport in the lower Mississippi River: Geological Society of America Bulletin, 124(3-4), 400-414.

Nittrouer, J. A., & Viparelli, E., 2014. Sand as a stable and sustainable resource for nourishing the Mississippi River delta. Nature Geoscience, 7(5), 350-354.

Nobes, D.C., Villinger, H., Davis, E.E. and Law, L.K., 1986. Estimation of marine sediment bulk physical properties at depth from seafloor geophysical measurements. Journal of Geophysical Research: Solid Earth (1978–2012), 91(B14), 14033-14043.

Paola C, Twilley RR, Edmonds DA, Kim W , Mohrig D, et al. 2011. Natural processes in delta restoration: application to the Mississippi Delta. Annu. Rev. Mar. Sci. 3:67–91

Patterson, L.J., Muhammad, Z., Bentley, S.J., Del Britsch, L., and Dillon, D.L., 2003. ^{210}Pb and ^{137}CS Geochronology of the Lake Fausse Pointe Region of the Lower Atchafalaya Basin. Gulf Coast Association of Geological Societies Transactions, 53, 668-675.

Pazzaglia, F.J., Robinson, R.A.J. and Traverse, A., 1997. "Palynology of the Bryn Mawr Formation (Miocene); insights on the age and genesis of middle Atlantic margin fluvial deposits." Sedimentary Geology, 108(1-4), 19-44.

Pazzaglia, F.J. and Gardner, T.W., 2000. Late Cenozoic landscape evolution of the U.S. Atlantic passive margin: Insights into North American great escarpment, in M. A. Summerfield, ed., Geomorphology and global tectonics: Chichester, United Kingdom, John Wiley and Sons Ltd., 283–306

Penland, P.S., Boyd, R. and Suter, J.R., 1988. Transgressive depositional systems of the Mississippi delta plain; a model for barrier shoreline and shelf sand development: J. Sediment Res., 58, 932–49

Pilcher, R. S., B. Kilsdonk, and J. Trude, 2011. Primary basins and their boundaries in the deep-water northern Gulf of Mexico: Origin, trap types, and petroleum system implication: American Association of Petroleum Geologists Bulletin, v. 95, p. 219-240.

Pinter, N., and Heine, R.A., 2005. Hydrodynamic and morphodynamics response to river engineering documented by fixed-discharge analysis, Lower Missouri River, USA. Journal of Hydrology, v. 302, p. 70-91.

Poag, C.W. and Sevon, W.D., 1989. A record of Appalachian denudation in postrift Mesozoic and Cenozoic sedimentary deposits of the U.S. Middle Atlantic continental margin: Geomorphology, 2, 119–157, doi:10.1016/0169-555X(89)90009-3.

Porter, S. C. (1989). Some geological implications of average Quaternary glacial conditions. Quaternary Research, 32(3), 245-261.

Potter, P. E., & Szatmari, P., 2009. Global Miocene tectonics and the modern world. Earth-Science Reviews, 96(4), 279-295.

Prather, B.E., Booth, J.R., Steffens, G.S. and Craig, P.A., 1998. Classification, lithologic calibration, and stratigraphic succession of seismic facies of intraslope basins, deep-water Gulf of Mexico: AAPG bulletin, 82(5), 701-728.

Prothero, D.R., 2004. Did impacts, volcanic eruptions, or climate change affect mammal evolution? Palaeogeogr. Palaeoclimatol. Palaeoecol, 214, 283–294.

Rainwater, E.H., 1964. Regional stratigraphy of the Gulf Coast Miocene: Gulf Coast Association of Geological Societies Transactions v. 14, p. 271-292.

Remo, J.W., Pinter, N., and Heine, R., 2009. The use of retro-and scenario-modeling to assess effects of 100+ years river of engineering and land-cover change on Middle and Lower Mississippi River flood stages: Journal of hydrology, 376(3), 403-416.

Retallack, G. J. (2007). Cenozoic paleoclimate on land in North America. The Journal of Geology, 115(3), 271-294.

Reuss, M., 2004. Designing the bayous: The control of water in the Atchafalaya Basin, 1800-1995 (No. 4): Texas A&M University Press.

Richmond, G.M. and Fullerton, D.S., 1986. Summation of Quaternary glaciations in the United States of America: Quaternary Science Reviews, 5, 183-196.

Rittenour, T.M., Blum, M.D. and Goble, R.J., 2007. Fluvial evolution of the lower Mississippi River valley during the last 100 k.y. glacial cycle; response to glaciation and sea-level change: Geological Society Of America Bulletin, 119(5-6), 586-608. doi:10.1130/B25934.1

Roberts, H.H., 1997. Dynamic changes of the Holocene Mississippi River delta plain: The delta cycle. Journal of Coastal Research, 13(3), 605-627.

Roberts, H.H, 1998. Delta switching: Early responses to the Atchafalaya River diversion. Journal of Coastal Research, 14(3), 882-899.

Roberts, H. H., Fillon, R., Kohl, B., Robalin, J., & Sydow, J., 2004. Depositional architecture of the Lagniappe (Mobile River) delta: Sediment characteristics, timing of depositional events, and temporal relationship with adjacent shelf-edge deltas. Late Quaternary Stratigraphic Evolution of the Northern Gulf of Mexico Basin, SEPM Special Publication, (79), 141-186.

Romans, B.W., Castelltort, S., Covault, J.A., Fildani, A., and J.P. Walsh. 2015. Environmental signal propagation in sedimentary systems across timescales. Earth Science Reviews, this volume.

Rotondo, K.A. and Bentley, S.J., 2003. Deposition and resuspension of fluid muds on the western Louisiana inner continental shelf: Gulf Coast Association of Geological Societies Transactions, 53, 721-731.

Rowley, D.B., Forte, A.M., Moucha, R., Mitrovica, J.X., Simmons, N.A. and Grant, S.P., 2011. Mantle dynamic impact on passive margin evolution: implications for their architecture and derived sea level histories. In: Friedrich, A. (Ed.), Fragile Earth: Geological Processes from Global to Local Scales and Associated Hazards: Geological Society of America, Boulder, Colorado, pp. A3.

Russell, R.J., & Howe, H.V., 1935. Cheniers of southwestern Louisiana. Geographical Review, 25, 449-461.

Samson, F., & Knopf, F., 1994. Prairie conservation in North America. *BioScience*, 418-421.

Saucier, R.T., 1994a. Geomorphology and Quaternary geologic history of the lower Mississippi Valley: Vicksburg, Mississippi, Mississippi River Commission, 205 p.
Saucier, R.T., 1994b. Evidence of late-glacial runoff in the lower Mississippi Valley: Quaternary Science Reviews, 13, 973–981.
Shaw, J.B., Mohrig, D., and Whitman, S.K., 2013. The morphology and evolution of channels on the Wax Lake Delta, Louisiana, USA. Journal of Geophysical Research: Earth Surface, 118(3), 1562-1584.
Shen, Z., Törnqvist, T. E., Autin, W. J., Mateo, Z. R. P., Straub, K. M., & Mauz, B., 2012. Rapid and widespread response of the Lower Mississippi River to eustatic forcing during the last glacial-interglacial cycle. Geological Society of America Bulletin, 124(5-6), 690-704.
Smith, D. G. and Fisher, T. G., 1993. Glacial Lake Agassiz: the northwestern outlet and paleoflood. Geology, v. 21, p. 9-12.
Smith, M., and Bentley, S.J., Sr., 2014. Sediment capture in floodplains of the Mississippi River: a case study in Cat Island National Wildlife Refuge, Louisiana. In: Sediment Dynamics from the Summit to the Sea, IAHS Special Publication 367, p. 442-446.
Smith, L.M., and Winkley, B.R., 1996. The response of the Lower Mississippi River to river engineering: Engineering Geology, 45(1), 433-455.
Slingerland, R., & Smith, N. D., 2004. River avulsions and their deposits. Annu. Rev. Earth Planet. Sci., 32, 257-285.
Snead, J., and Henrich, P.V., 2012a. The Atchafalaya Bay Geologic Quadrangle, 1:100,000 (map). Louisiana Geological Survey, Baton Rouge.
Snead, J., and Henrich, P.V., 2012b. The Morgan City Geologic Quadrangle, 1:100,000 (map). Louisiana Geological Survey, Baton Rouge.
Snedden, J. W., Galloway, W. E., Whiteaker, T. L., & Ganey-Curry, P. E. (2012). Eastward shift of deepwater fan axes during the Miocene in the Gulf of Mexico: Possible causes and models: Gulf Coast Association of Geological Societies Journal, v. 1, p. 131-144.
Suter, J.R. and Berryhill, H.L., 1985. Late Quaternary shelf-margin deltas, Northwest Gulf of Mexico AAPG Bulletin(January 1985), 69(1), 77-91
Sweet, M. L. and Blum, M. D., 2011. Paleocene-Eocene Wilcox submarine canyons and thick deepwater sands of the Gulf of Mexico: Very large systems in a greenhouse world, not a Messinian-like crisis: Gulf Coast Association of Geological Societies Transactions, 61, 443–450.
Sydow, J., Roberts, H. H., Bouma, A. H., & Winn, R., 1992. Constructional subcomponents of a shelf-edge delta, northeast Gulf of Mexico. Gulf Coast Association of Geological Societies Transactions, 52, 717-726.
Syvitski, J.P. and Kettner, A., 2011. Sediment flux and the Anthropocene: Philosophical Transactions of the Royal Society A: Mathematical, Physical and Engineering Sciences, 369(1938), 957-975.
Tornqvist, T. E., Kidder, T. R., Autin, W. J., van der Borg, K., de Jong, A. M., Klerks, J. W.; Snijders, Els M. A.; Storms, Joep E. A.; van Dam, Remke L.; Wiemann, Michael C., 1996. A revised chronology for Mississippi River subdeltas. Science, 273(5282), 1693-1696.
Tornqvist, T.E., Wallace, D.J., Storms, J.A., Wallinga, J., van Dam, R.L., Blaauw, M., and Snijders, E.A., 2008. Mississippi Delta subsidence primarily caused by compaction of Holocene strata: Nature Geoscience, 1(3), 173-176. doi:10.1038/ngeo129
Tripsanas, E. K., Bryant, W. R., Slowey, N. C., Bouma, A. H., Karageorgis, A. P., & Berti, D., 2007. Sedimentological history of Bryant Canyon area, northwest Gulf of Mexico, during

the last 135 kyr (Marine Isotope Stages 1–6): a proxy record of Mississippi River discharge. Palaeogeography, Palaeoclimatology, Palaeoecology, 246(1), 137-161.

Tripsanas, E. K., Karageorgis, A. P., Panagiotopoulos, I. P., Koutsopoulou, E., Kanellopoulos, T. D., Bryant, W. R., & Slowey, N. C., 2013. Paleoenvironmental and paleoclimatic implications of enhanced Holocene discharge from the Mississippi River based on the sedimentology and geochemistry of a deep core (JPC-26) from the Gulf of Mexico. Palaios, 28(9), 623-636. doi:10.2110/palo.2012.p12-060r

Tyson, C.N., 1981. Peace and prosperity: in, The Red River in southwestern history: Norman, University of Oklahoma Press, 222 p.

Twain, M., 1883. Life on the Mississippi.

US-ACE, 2012, Bonnet Carre Spillway. http://www.mvn.usace.army.mil/Portals/56/docs/Recreation/BCS/Brochures/BCspillwaybooklet.pdf. Accessed 9/27/2014

US-ACE (United States Army Corps of Engineers), 2014a. Mississippi River &Tributaries Project. http://www.mvd.usace.army.mil/Portals/52/docs/04_MRT_WEB.pdf, accessed 9/20/2014).

US-ACE, 2014b, Morganza Floodway Interim Water Control Manual: Proposed Clarifications to the Standing Instructions. US-ACE New Orleans District, http://www.mvn.usace.army.mil/Portals/56/docs/MRT/MorganzaInterimWCMStandingInstructionsSimplifiedFINAL.pdf, accessed 9/30/2014.

Vörösmarty, C.J., Syvitski, J., Day, J., de Sherbinin, A., Giosan, L., Paola, C., 2009. Battling to save the world's river deltas. Bulletin of the Atomic Scientists, 65, (2), 31-43.

Waelbroeck, C., Labeyrie, L., Michel, E., Duplessy, J.C., McManus, J.F., Lambeck, K., Balbon, E. and Labracherie, M., 2002. Sea-level and deep water temperature changes derived from benthic foraminifera isotopic records: Quaternary Science Reviews, 21, 295–305, doi:10.1016/S0277-3791(01)00101-9.

Walker, J.D., Geissman, J.W., Bowring, S.A., and Babcock, L.E., compilers, 2012. Geologic Time Scale v. 4.0: Geological Society of America, doi: 10.1130/2012.CTS004R3C.

Walsh, J. P., Corbett, R., Mallinson, D., Goni, M., Dail, M., Loewy, C., Marciniak, K., Ryan, K., Smith C., and Tesi, T., 2006. Mississippi delta mudflow activity and 2005 Gulf hurricanes. Eos, Transactions American Geophysical Union, 87(44), 477-478.

Walsh, J.P., and Nittrouer, C.A., 2009. Understanding fine-grained river-sediment dispersal on continental margins. Marine Geology, 263(1), 34-45.

Walsh, J.P., Corbett, D.R., Ogston, A.S., Nittrouer, C., Kuehl, S.A., Allison, M.A., and S.L. Goodbred Jr. 2013. Shelf and slope sedimentation associated with large deltaic systems. Editors: T.S. Bianchi, M.A. Allison, and W. Cai, In: Biogeochemical Dynamics at Major River-Coastal Interfaces: Linkages with Global Change. Cambridge University Press, New York, NY, 704 pgs.

Wang Y, Straub, K. and Hajek, E., 2011. Scale-dependent compensational stacking; an estimate of autogenic time scales in channelized sedimentary deposits. Geology [Boulder] [serial online], 39(9), 811-814.

Wasklewicz, T.A., Grubaugh, J., Franklin, S., and Gruelich, S., 2004. 20th century stage trends along the Mississippi River: Physical Geography, 25(3), 208-224.

Weimer, P., 1990. Sequence stratigraphy, facies geometries, and depositional history of the Mississippi Fan, Gulf of Mexico. AAPG Bulletin, 74(4), 425-453.

Weimer, P., 1991. Sequence Stratigraphy of the Mississippi Fan Related to Oxygen Isotope Sea Level Index: Discussion (1). AAPG Bulletin, 75(9), 1500-1507.

Weimer, P. and Dixon, B.T., 1994. Regional sequence stratigraphic setting of the Mississippi fan complex, northern deep Gulf of Mexico: implications for evolution of the northern Gulf basin margin: Gulf Coast SEPM Foundation 15th Annual Research Conference, p. 373–381.

Weimer, P. and Buffler, R.T., 1988. "Distribution and seismic facies of Mississippi Fan channels." Geology 16,(10), 900-903. GeoRef, EBSCOhost (accessed August 1, 2013).

Wellner, R., Beaubouef, R., Van Wagoner, J.C., Roberts, H.H., and Sun, T., 2005. "Jet-plume depositional bodies—The primary building blocks of Wax Lake delta: Transactions of the Gulf Coast Association of Geological Societies, 55, 867-909.

Wells JT, Kemp G P. 1981. Atchafalaya mud stream and recent mudflat progradation: Louisiana chenier plain. Trans. Gulf Coast Assoc. Geol. Soc. 31:409–16

Wells, J.T. and Roberts, H.H., 1980. Fluid mud dynamics and shoreline stabilization: Louisiana chenier plain: American Society of Civil Engineers, Proceedings 17th International Coastal Engineering Conference, p. 1382-1401.

Winker, C.D., 1982. "Cenozoic shelf margins, northwestern Gulf of Mexico." Transactions - Gulf Coast Association Of Geological Societies, 32, 427-448.

Wu, X., Galloway, W.E., 2002. Upper Miocene Depositional History of the Central Gulf of Mexico Basin: Gulf Coast Association of Geological Societies Transactions, 52, 1019-1030.

Xu, J., Snedden, J.W., Fulthorpe, C.S., and Stockli, D.F., 2014. Sediment input pathways from North American highlands to the Gulf of Mexico based on detrital zircon U-Pb and U-Th/He dating, AGU annual meeting, San Francisco, CA, (Dec. 2014)

Zachos, J., Pagani, M., Sloan, L., Thomas, E. and Billups, K., 2001. Trends, rhythms, and aberrations in global climate 65 Ma to present: Science, 292, 686–693, doi: 10.1126/science.1059412.

Zalasiewicz, J., Williams, M., Haywood, A. and Ellis, M., 2011. The Anthropocene: a new epoch of geological time? Philosophical Transactions of the Royal Society A: Mathematical, Physical and Engineering Sciences, 369(1938), 835-841.

Figure Captions

Figure 1. Extent of modern Mississippi River catchment and shelf/slope/fan deposits, showing locations of major dams and spillways. Adapted from Meade and Moody (2010), and Galloway et al. (2011).

Figure 2. Reorganization of North American drainage and sediment routing during the mid-Cretaceous to Paleocene, interpreted from detrital zircons in fluvial sandstones.. This re-routing set the stage for later development of the MRS as the major fluvial drainage for the continent, and establishment of the GoM basin as the major depocenter for the southern half of the continent. After Blum and Pecha, 2014.

Figure 3a. Key for Figures 3B, 5, and 7.

Figure 3. (a)Key for figures 3b, 5, and 7. (b) Frio-Vicksburg depositional episode, 28-35 Ma, after Galloway et al. (2000, 2011): major continental fluvial axes, topographic and structural elements of the North American interior , and major GoM depositional elements. This is the time frame prior to establishment of the Miocene paleo-Mississippi system.

Figure 4. Fluvial sediment supply to the GoM basin, Miocene to Pleistocene, after Galloway et al. 2011.

Figure 5. Late Miocene depositional episode, 12.6-6.4 Ma, after Galloway et al., 2000, 2011: major continental fluvial axes, topographic and structural elements of the North American interior, and major GoM depositional elements. This time interval marks establishment of the ancestral Mississippi system in its present drainage configuration. Galloway's configuration of the paleo- Ohio and -Tennessee fluvial axes are not based on extensive geomorphic or stratigraphic data, and are the subject of some debate, as also is the case for Pleistocene locations of the paleo-Tennessee (see section 3.1). Deep Sea depocenters are better documented, however.

.

Figure 6. Pleistocene timelines. (upper panel) Last 600 ky. (lower panel) detail of last 100 ky. Key to abbreviated references, top to bottom: Tripsanas et al., 2007; Bouma et al., 1986; Weimer, 1991; Dixon and Weimer, 1998; Rittenour et al., 2007. Aharon, 2003; Tripsanas et al., 2007; Bouma et al., 1986.

Figure 7. Late Pleistocene depositional episode (Sangamon, 0.6-0.1 Ma), after Galloway et al., 2000, 2011: major continental fluvial axes, topographic and structural elements of the North American interior, and major GoM depositional elements. This time span, and immediately subsequent MIS 3 and 2, was a time of high sediment discharge to the GoM basin, bringing the Mississippi Fan (and associated Bryant Fan) to its present extent.

Figure 8. Mississippi Fan Structure Maps from Bouma et al., 1986.

Figure 9. Mississippi Fan Isopachs of volumes between surfaces in Figure 10. The thickest deposits trace the locations of channel-levee complexes, which are marked with red arrows to indicate approximate thalweg locations. Related channel networks are shown in Figure 12.

Figure 10. Major late Pleistocene features of the continental shelf, Mississippi, Bryant, and Eastern fans, after Suter and Berryhill (1985), Weimer and Buffler (1988), Weimer (1990), Dixon and Weimer (1998), and Tripsanas et al., (2007). The ages of channel systems 14-17 are indicated in Figure 7a. The canyon systems shown both have surface expression on the modern seafloor. However, at least 11 other mostly Pleistocene canyon systems have been mapped in the subsurface of the Mississippi shelf-slope complex, in addtion to channel complexes 1-13, mapped by Weimer and Buffler (1988) and Dixon and Weimer (1998), all of Pleistocene age.

Figure 11. Synthesis of major Holocene geomorphic developments (italic text) and climatic events (plain text) from the upper catchment to the continental shelf of the MRS. The lobe-shift transitions of Frazier (1967) are highlighted in yellow. The reference B&R 2012 refers to Blum and Roberts, 2012.

Figure 12. Delta lobes and distributaries, after Fisk (1944) and Saucier (1994a). Channels and distributaries of the Maringouin complex (A) drawn by Fisk and Saucier are the least well documented. More recent cross sections identifying specific candidates for these channels are shown in Blum et al. (2007).

Figure 13. Relationships between Mississippi River flow conditions, channel migration rates, and channel-belt morphology. A. Plots of channel-bed elevation, low-flow water, and the flood-stage water surface (after Nittrouer et al., 2012), illustrating changes in water surface slopes as the channel enters its backwater reach. B. Plots of meander-bend migration rate (after Hudson and Kesel, 2000) and channel-belt width-to-thickness ratio (from Blum et al., 2013), illustrating dramatic changes in migration rates and resultant width-to-thickness ratios as the channel enters the backwater reach. Note these morphological changes occur considerably upstream from the limits of saltwarer penetration within the channel. C. , D. LIDAR images of channel-belt planforms at river kilometer 700 (C.), within the upper limits of the backwater reach, and river kilometer 200 (D.), far downstream within the backwater reach, illustrating dramatic changes in morphology that occur within this part of the river system. LIDAR data courtesy of Atlas: The Louisiana Statewide GIS System (http://atlas.lsu.edu)

Figure 14. A)water routing of the Mississippi River, ca. 1980. B) Sediment routing in the Mississippi River, ca. 1800, and ca. 1980. Both figures after Meade and Moody (2010).

Figure 15. Index map of river outlets, and average sediment flux per year at at selected gauging stations in the Lower Mississippi and Atchafalaya River systems, over water years 2008-2010, data from Allison et al. (2012).

Figure 16. Historical progradation of Southwest Pass from 1764-2009, after Maloney et al. (2014). Black lines represent ~10 m depth contours and are labeled by year. These data were digitized from Fisk (1961), Gould (1970), and Coleman et al. (1991), except 1940 and 1979, which were digitized from Coleman et al. (1980). The green line is the 10 m depth contour from NOAA DEMs from 2007-2009. The gap in this contour near the river mouth results from a data gap. The most recent nautical charts (2011) indicate that this area is a dredged material dump site, and therefore contours likely do not reflect natural progradation. First charted extent of jetties in 1901 are plotted as blue stars. Current extent (completed 1913) plotted

with black stars. The NOAA northern gulf coast 1 arc-second DEM is colored and shaded as background (Love et al., 2012).

Figure 17. Subdeltas of modern Balize/Birdsfoot Delta, after Coleman and Gagliano, 1964.

Figure 18. Lifecycle of West Bay subdelta after Gagliano et al. (1973).

Fig. 19. Change in land area within the Balize delta lobe, 1937-2000. Data from Couvillion et al., 2011, after Kemp et al., 2014.

Figure 20. Isopach map illustrating change in bathymetry between 1940 and 1977-79 surveys of Coleman et al., 1980, after Maloney et al. (2014). Negative (blues) values show deepening or loss of sediment and positive values (reds) show shoaling or addition of sediment. The mudlobe zone of Coleman et al. (1980) is located between the two dashed lines. Digitized surfaces from Guidroz (2009).

Figure 21. Block diagram illustrating seabed morphology and structure/stratigraphy of the Balize lobe delta front, based on Coleman, et al. (1980), after Maloney et al. (2014). Bathymetry from Walsh et al. (2006) illustrates mudflow gullies and lobes at intermediate depths (rainbow bathymetric grid).

Figure 22. Time-series of historic-period suspended-sediment loads for the Missouri and upper Mississippi Rivers, and the lower Mississippi River at Tarbert Landing, Mississippi (data from Heimann et al., 2010, 2011), with contributions of each segment represented by different color fills. The Upper Missouri is defined as the reach above Omaha, Nebraska (between Gavins Point Dam and Omaha for the post-dam period), whereas the Lower Missouri is defined as the reach between Omaha and the Mississippi confluence at St. Louis, Missouri. The upper Missouri, between Gavins Point Dam and Omaha, does not include any major tributaries with significant sediment input, and sediment loads recorded at the Omaha gauging station are attributed to bed scour between the Gavins Point Dam and Omaha (see Fig. 23). The Lower Missouri includes the Platte and Kansas River tributaries, as well as other minor tributaries.

Figure 23. Changes in Missouri River stage at various constant discharges for the period 1954 to the mid 1990's, from Gavins Point Dam to just upstream from the Mississippi confluence. Plots are interpreted to represent significant bed scour between Gavins Point Dam and Omaha, Nebraska (~300 river kilometers), and additional scour that has been attributed to channelization for the reach centered on Kansas City, Missouri. Reaches with minor aggradation occur downstream from the reach of intensive bed scour between Gavins Point and Omaha, which is also coincident with Platte River tributary influx, and downstream from the channelized reach centered on Kansas City. Estimated stage value of zero represents the 1954 low-flow stage at 566 m^3s^{-1}, and other stages are relative to that value (from Jacobson and Galat, 2006; Jacobson et al., 2009).

Figure 24. LMR discharge 1960-2009 as a percentage of Tarbert Landing flow. Data from Kemp et al. (2014), adapted from Brown et al. (2009).

Figure 25. (a) River-bed volume change 1962-2004 along undredged reaches of the LMR from Belle Chasse to West Bay (see Fig. X for location); (b) fill rate of the river bed by reach (upstream to downstream) along the same distance of the LMR. Data from Kemp et al. (2014), adapted from Brown et al. (2009).

Figure 26. Chenier Plain and Atchafalaya River outlets, southwest Louisiana. Compiled from Neill and Allison (2005), Wells and Roberts (1980), Wells and Kemp (1981), and the following Louisiana Geological Survey geological maps: Heinrich (2006b); Heinrich and Autin (2000), Heinrich et al. (2002, 2003), and Snead and Heinrich (2012a and b).

Figure 27. Anthropocene sediment loads and storage/accumulation rates for measurement locations (and references) identified in Table 7.

Figure 28. Relative temporal and spatial scales for processes and geomorphic elements of the Mississippi River source to sink system discussed in this paper. Selected references cited in this paper, used for this figure:
modern floods: US-ACE 2012, 2014a, b;
crevasse splays: Coleman and Gagliano, 1964; Davis, 1993; Tornqvist et al., 1996, 2008;
compaction: Dokka et al., 2006; Tornqvist et al., 2008; Blum and Roberts, 2012
subdelta cycle: Coleman and Gagliano, 1964; Gagliano et al., 1973;
deglacial megafloods: Aharon, 2003; Knox, 1985, 2003. 2006 ;
delta lobe cycle: Frazier, 1967; Penland et al., 1988; Weimer, 1990; Tornqvist et al., 1996;
salt tectonics: Feng and Buffler, 1996; Tripsanas et al., 2007; Prather et al., 1998
deep sea fan/lobe sequences: Bouma et al., 1986; Weimer, 1990; Feeley et al., 1990; Weimer, 1991;
glacial sea level cycles: Waelbroeck et al., 2002; Lisiecke and Raymo, 2005;
crustal subsidence/uplift: Gallen et al., 2013; Miller et al., 2013; McMillan et al., 2014;
Neogene secular sea level fall: Hallam, 1992; Lisiecke and Raymo, 2005

Figure 1


Montana
North Dakota
Yellowstone River
South Dakota
Missouri River
Wyoming
Minnesota
Wisconsin
Mississippi
Michigan
Iowa
Omaha
Nebraska
Platte River
Colorado
Kansas
Illinois River
Illinois
Indiana
Ohio
Pennsylvania
West Virginia
Ohio River
St. Louis
Hermann
Missouri
River
Kentucky
Virginia
Arkansas River
Grand Chain
Oklahoma
Arkansas
Tennessee
North Carolina
South Carolina
New Mexico
Red River
Mississippi
Georgia
Alabama
Shreveport
Texas
Louisiana
Natchez
Old River Control Structure
Baton Rouge
Florida
New Orleans
N
Dams
0 100 200 Kilometers
0 100 200 Miles
Mississippi River Basin
Gulf of Mexico
Orca Basin
Shelf, slope and fan

Figure 2

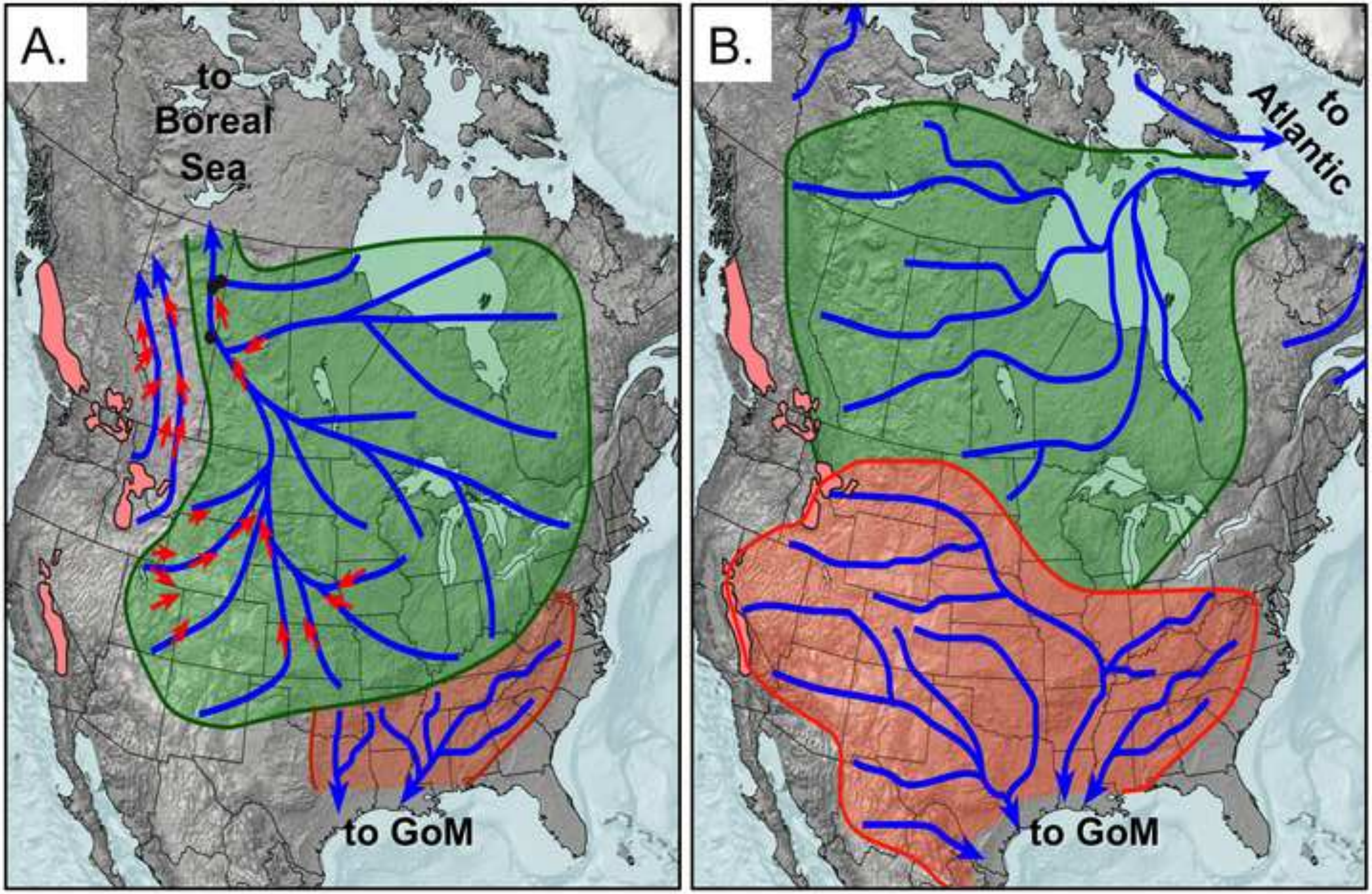

Figure 3a

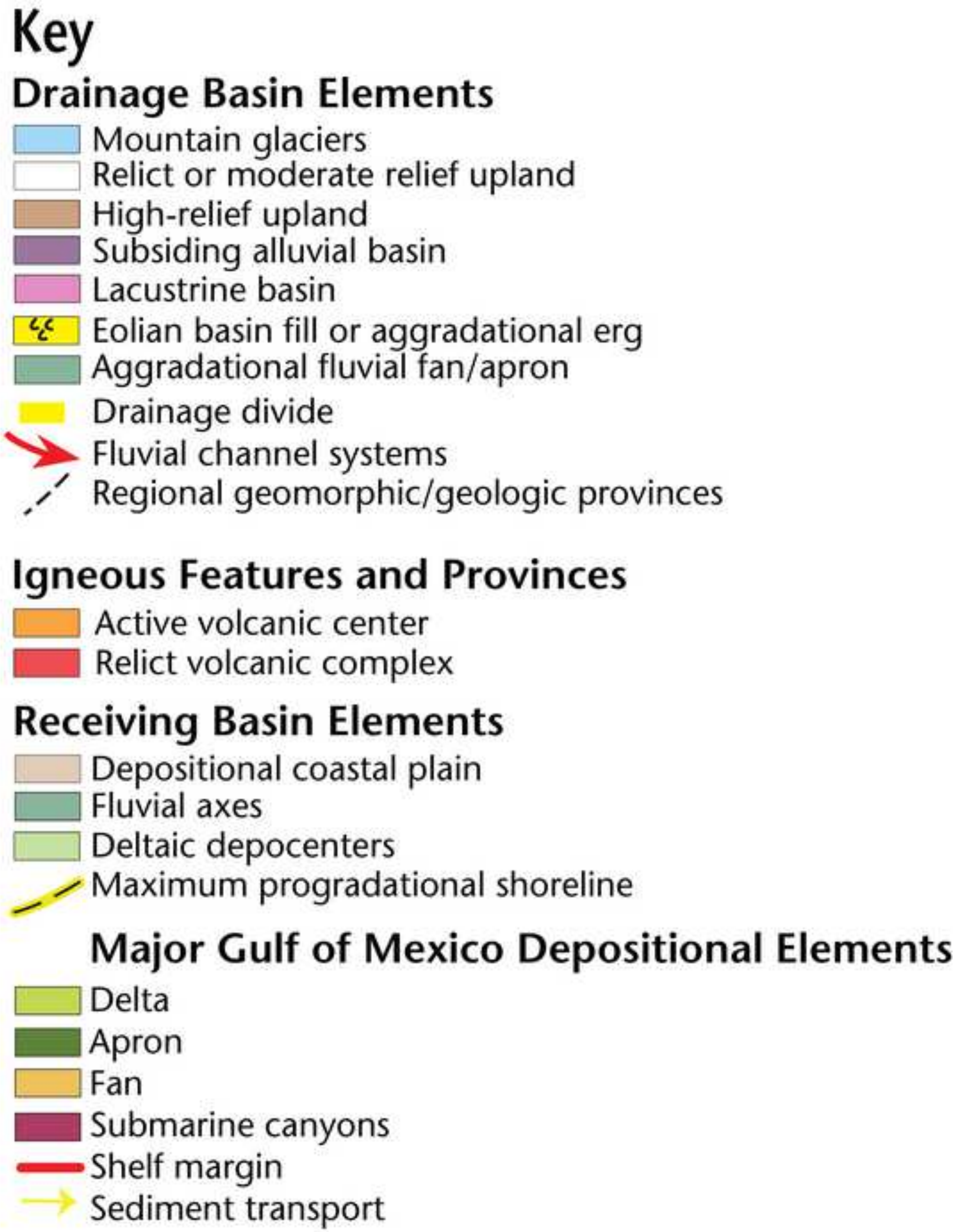
Key
Drainage Basin Elements
Mountain glaciers
Relict or moderate relief upland
High-relief upland
Subsiding alluvial basin
Lacustrine basin
Eolian basin fill or aggradational erg
Aggradational fluvial fan/apron
Drainage divide
Fluvial channel systems
Regional geomorphic/geologic provinces
Igneous Features and Provinces
Active volcanic center
Relict volcanic complex
Receiving Basin Elements
Depositional coastal plain
Fluvial axes
Deltaic depocenters
Maximum progradational shoreline
Major Gulf of Mexico Depositional Elements
Delta
Apron
Fan
Submarine canyons
Shelf margin
Sediment transport

Figure 3b

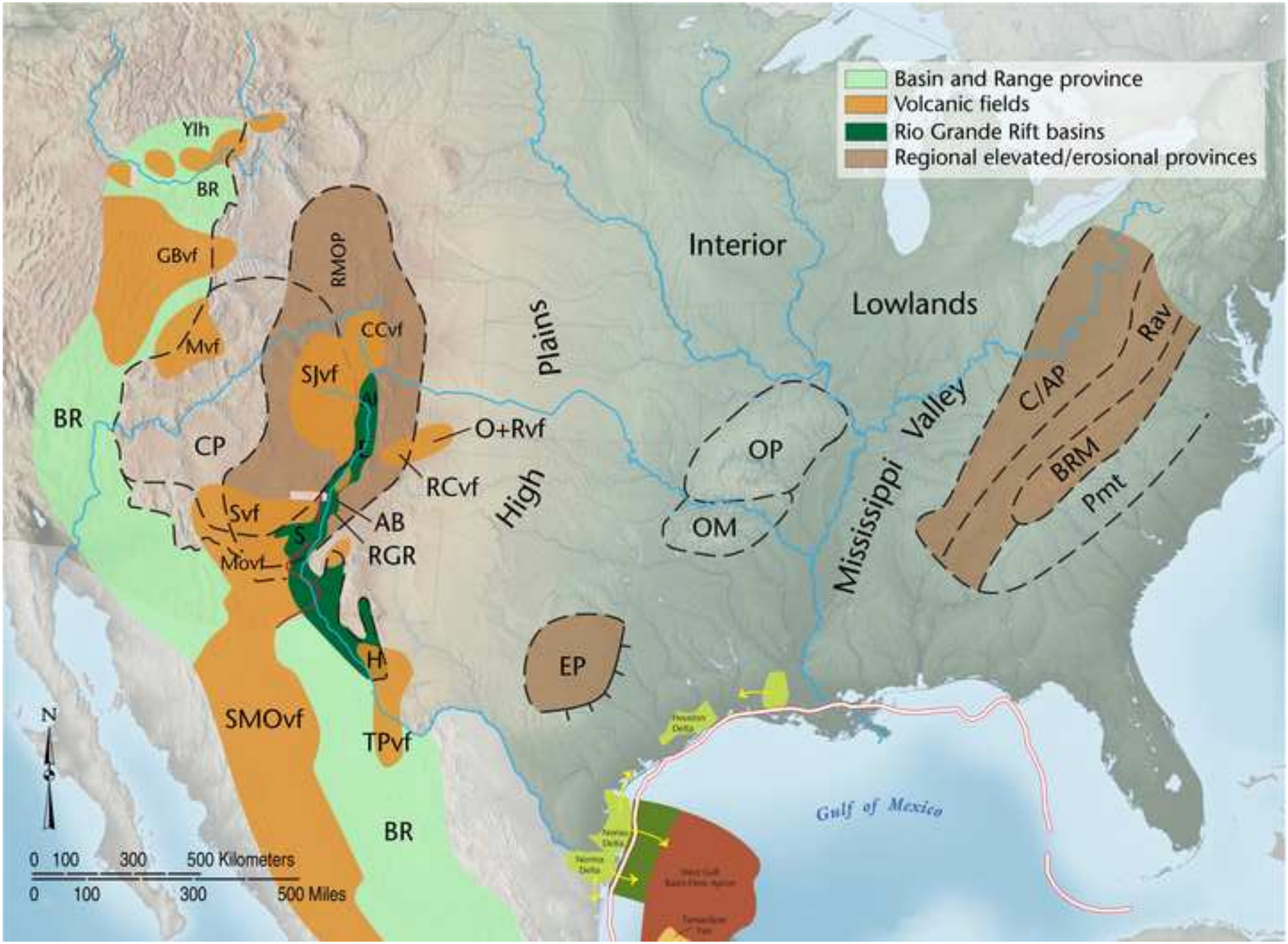

Basin and Range province
Volcanic fields
Rio Grande Rift basins
Regional elevated/erosional provinces
Ylh
BR
GBvf
RMOP
Mvf
CCvf
SJvf
BR
CP
O+Rvf
RCvf
Svf
AB
S
RGR
Movf
H
SMOvf
TPvf
BR
High
Plains
Interior
Lowlands
OP
OM
Mississippi
Valley
C/AP
Rav
BRM
Pmt
EP
Gulf of Mexico
N
0 100 300 500 Kilometers
0 100 300 500 Miles

Figure 4 110215

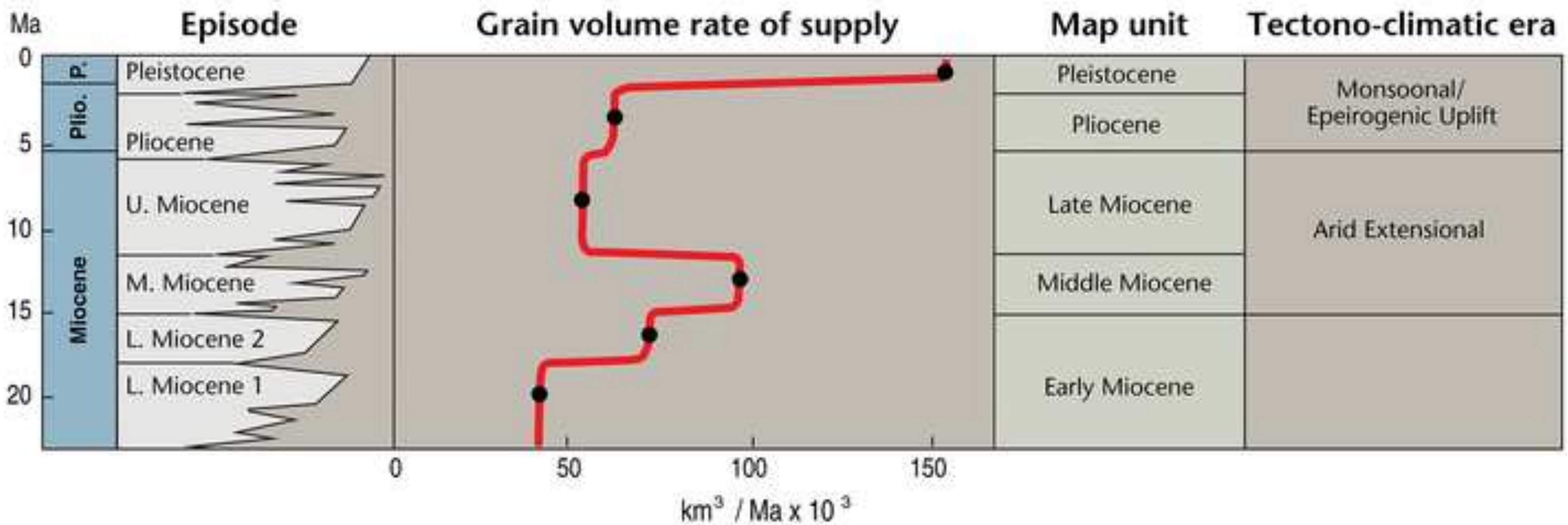

Figure 5

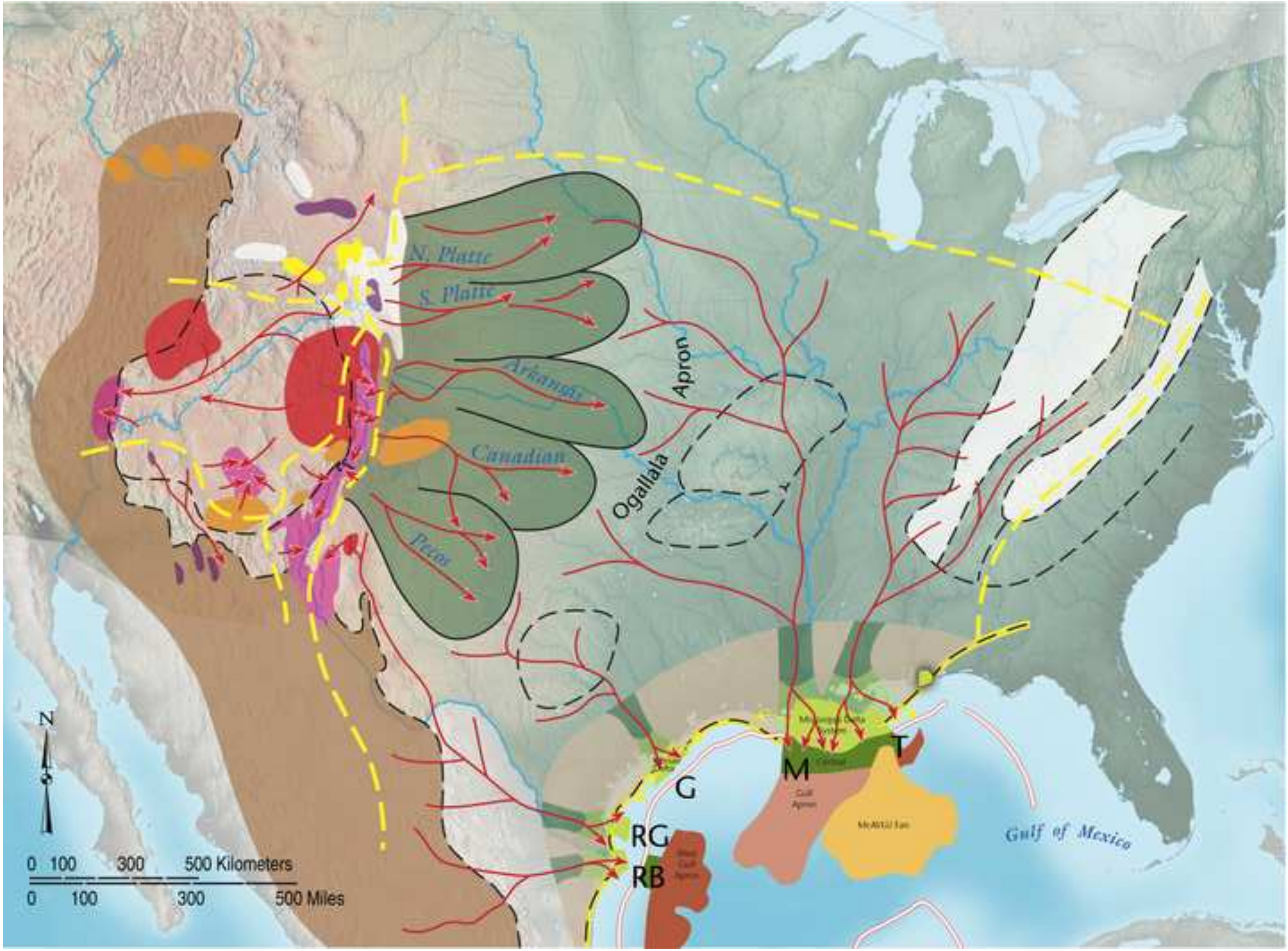

N. Platte
S. Platte
Arkansas
Canadian
Pecos
Apron
Ogallala
G
RG
RB
M
T
Gulf of Mexico
N
0 100 300 500 Kilometers
0 100 300 500 Miles

Figure 6

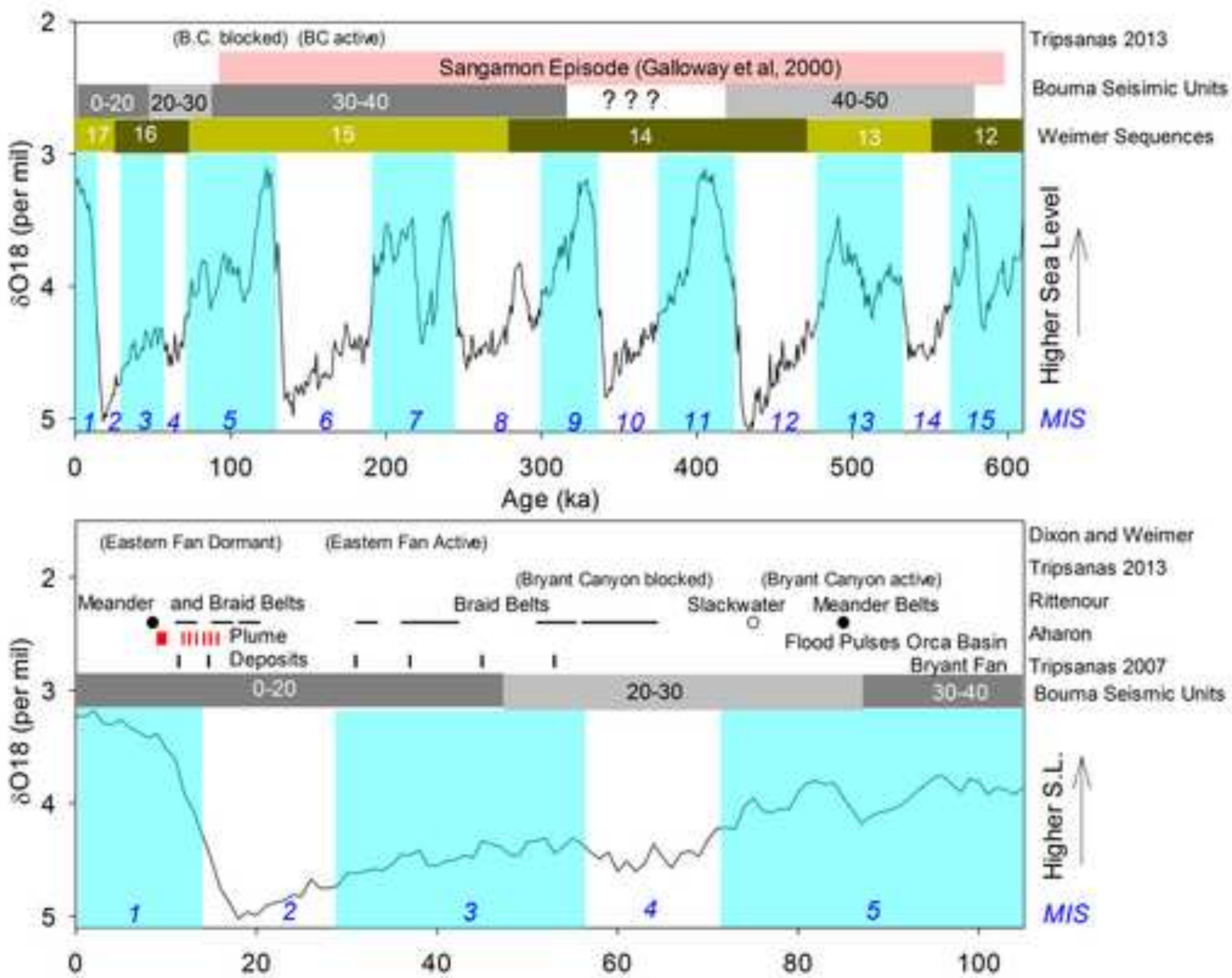

(B.C. blocked) (BC active)
Tripsanas 2013
Sangamon Episode (Galloway et al, 2000)
Bouma Seismic Units
0-20 20-30 30-40 ? ? ? 40-50
Weimer Sequences
17 16 15 14 13 12
δO18 (per mil)
Higher Sea Level
MIS
1 2 3 4 5 6 7 8 9 10 11 12 13 14 15
0 100 200 300 400 500 600
Age (ka)
(Eastern Fan Dormant) (Eastern Fan Active)
Dixon and Weimer
Tripsanas 2013
(Bryant Canyon blocked) (Bryant Canyon active)
Meander and Braid Belts
Braid Belts
Slackwater
Meander Belts
Rittenour
Plume
Aharon
Deposits
Flood Pulses Orca Basin
Bryant Fan
Tripsanas 2007
0-20 20-30 30-40
Bouma Seismic Units
δO18 (per mil)
Higher S.L.
MIS
1 2 3 4 5
0 20 40 60 80 100

Figure 7

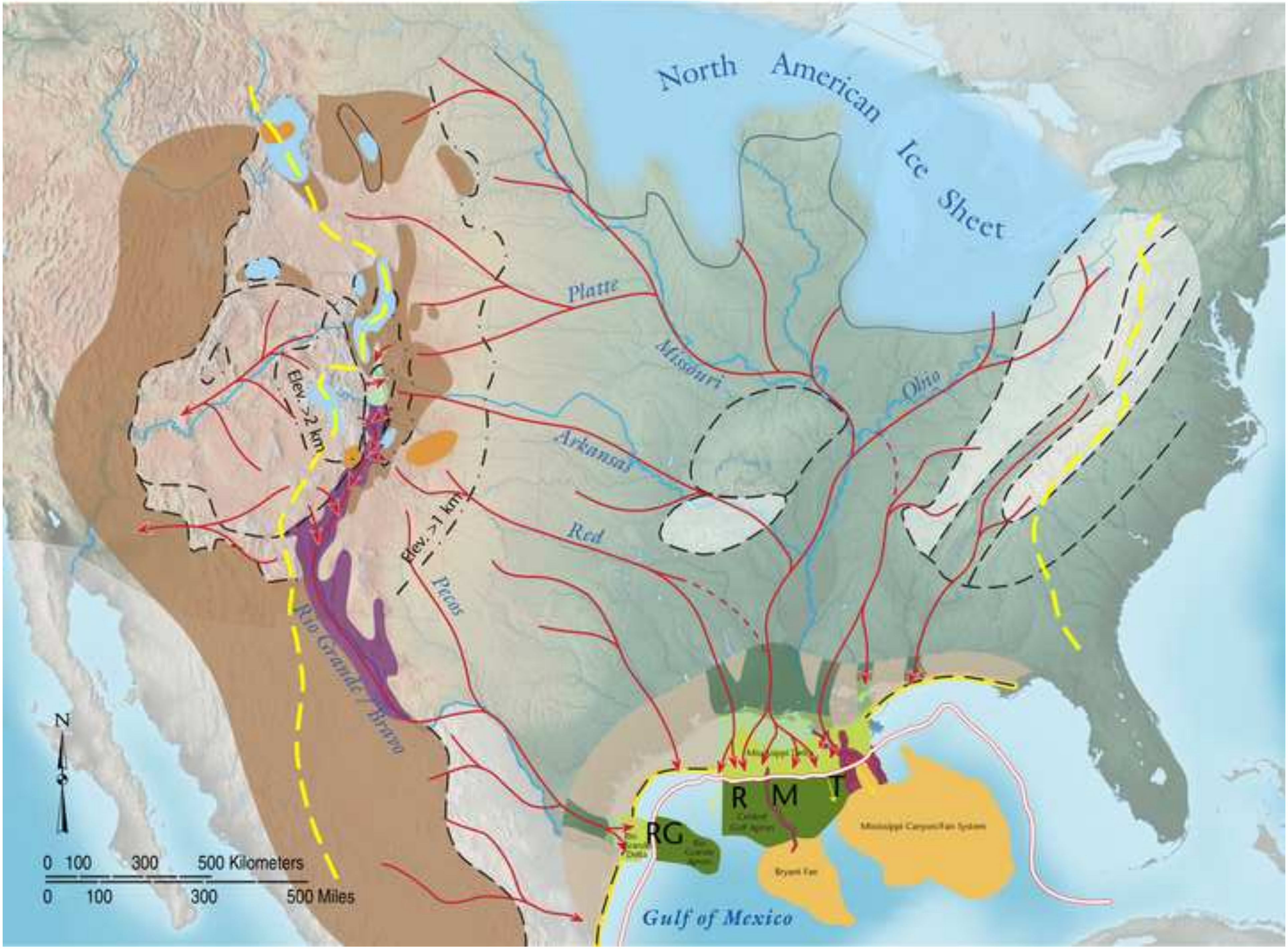
North American Ice Sheet
Platte
Missouri
Ohio
Arkansas
Red
Pecos
Rio Grande / Bravo
Elev. >2 km
Elev. >1 km
R
M
T
RG
Mississippi Canyon/Fan System
Bryant Fan
Gulf of Mexico
N
0 100 300 500 Kilometers
0 100 300 500 Miles

Figure 8

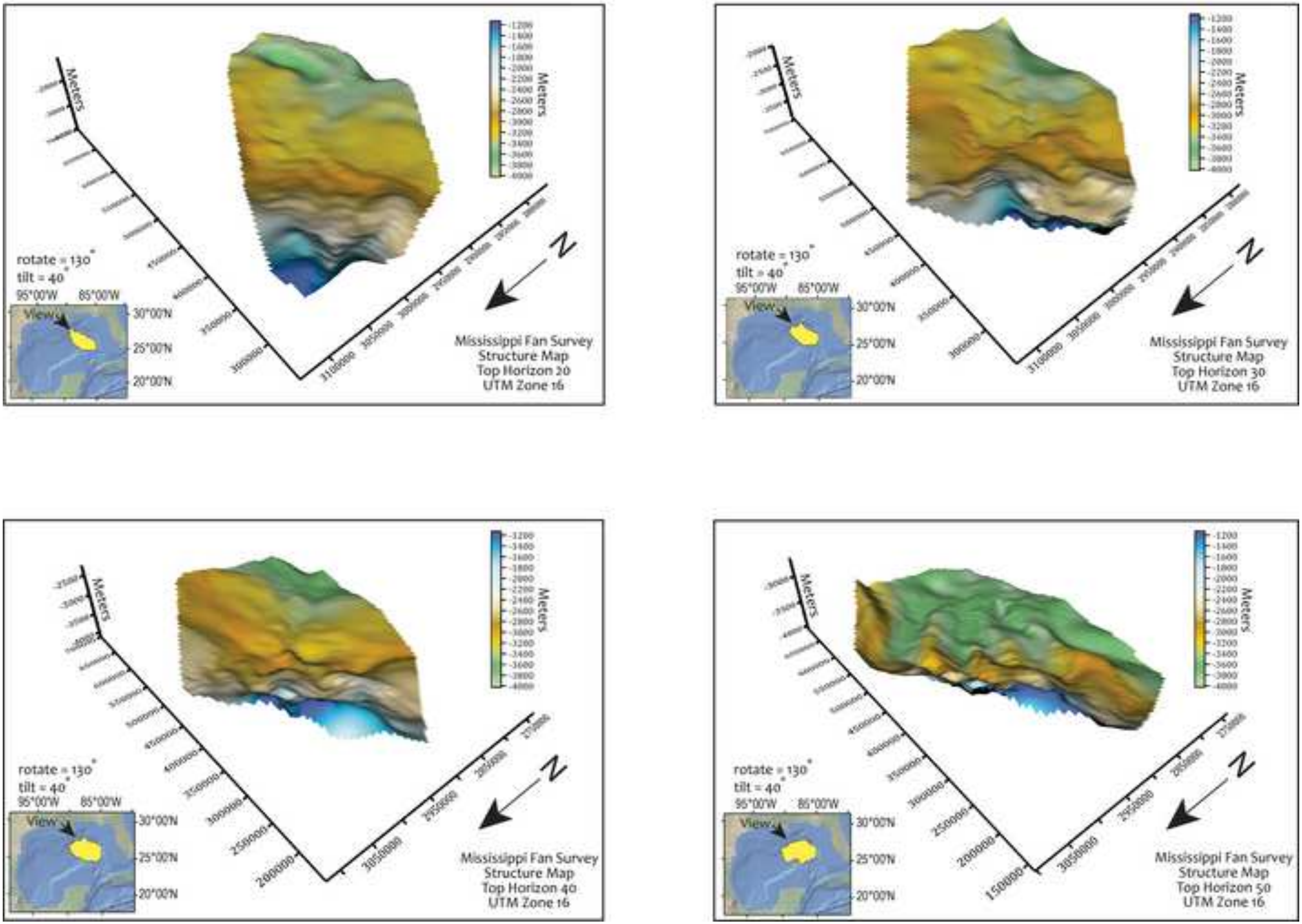
Meters
rotate = 130°
tilt = 40°
95°00'W
85°00'W
View
30°00'N
25°00'N
20°00'N
Mississippi Fan Survey
Structure Map
Top Horizon 20
UTM Zone 16
Meters
rotate = 130°
tilt = 40°
95°00'W
85°00'W
View
30°00'N
25°00'N
20°00'N
Mississippi Fan Survey
Structure Map
Top Horizon 30
UTM Zone 16
Meters
rotate = 130°
tilt = 40°
95°00'W
85°00'W
View
30°00'N
25°00'N
20°00'N
Mississippi Fan Survey
Structure Map
Top Horizon 40
UTM Zone 16
Meters
rotate = 130°
tilt = 40°
95°00'W
85°00'W
View
30°00'N
25°00'N
20°00'N
Mississippi Fan Survey
Structure Map
Top Horizon 50
UTM Zone 16

Figure 9

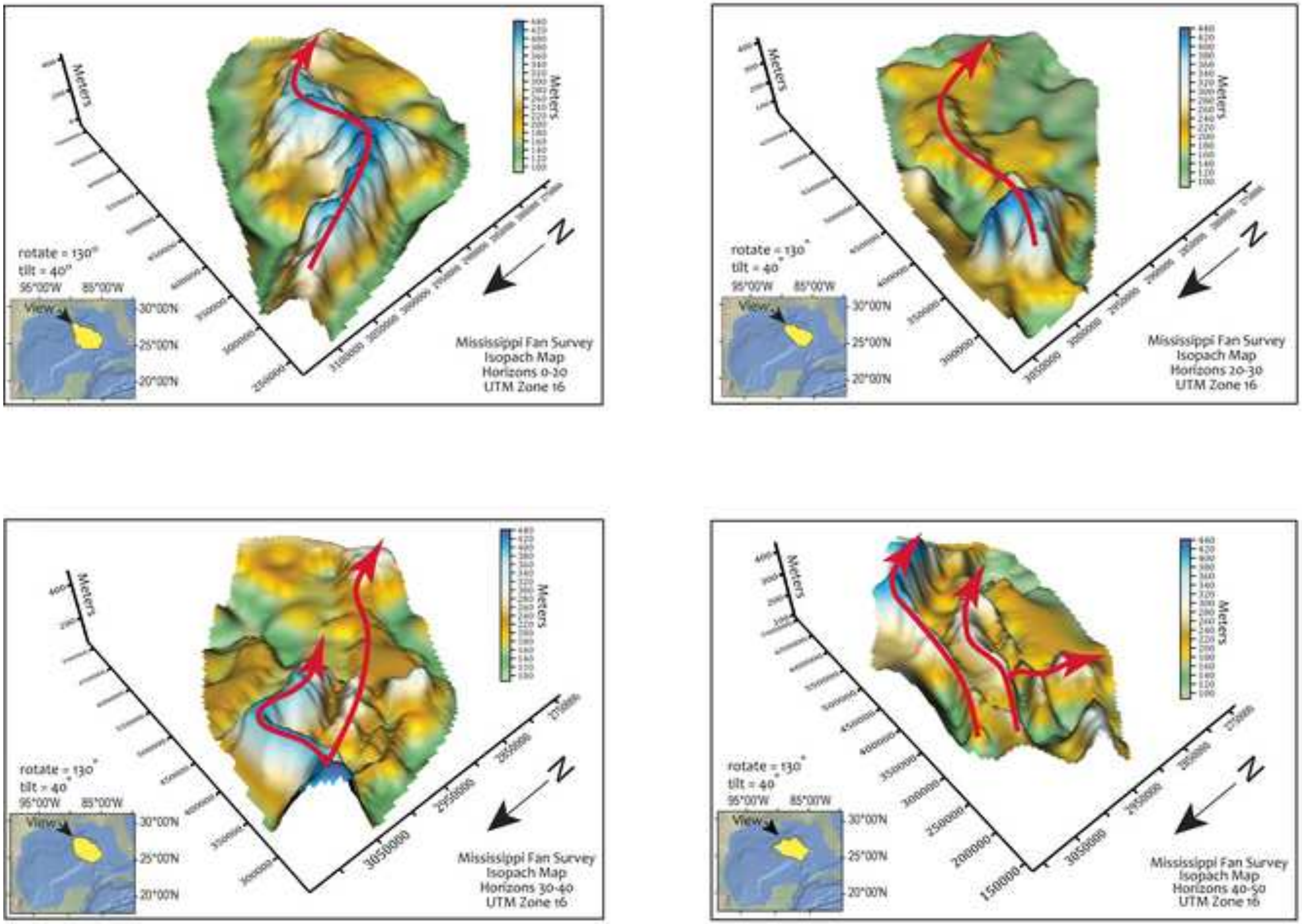

Mississippi Fan Survey
Isopach Map
Horizons 0-20
UTM Zone 16
Mississippi Fan Survey
Isopach Map
Horizons 20-30
UTM Zone 16
Mississippi Fan Survey
Isopach Map
Horizons 30-40
UTM Zone 16
Mississippi Fan Survey
Isopach Map
Horizons 40-50
UTM Zone 16

Figure 10

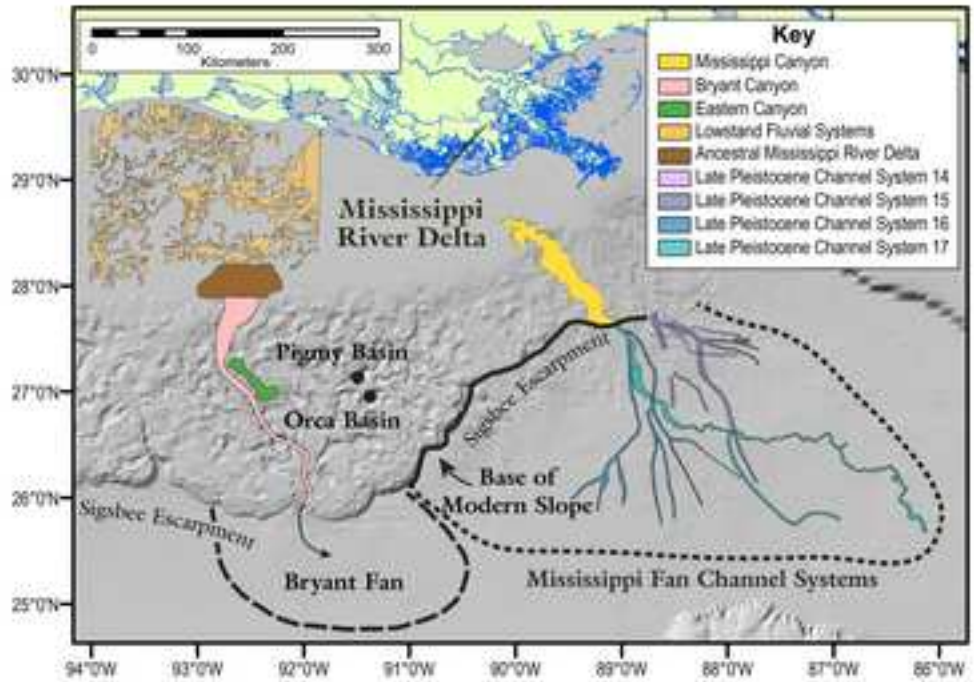

0 100 200 300
Kilometers
Key
Mississippi Canyon
Bryant Canyon
Eastern Canyon
Lowstand Fluvial Systems
Ancestral Mississippi River Delta
Late Pleistocene Channel System 14
Late Pleistocene Channel System 15
Late Pleistocene Channel System 16
Late Pleistocene Channel System 17
Mississippi River Delta
Pigmy Basin
Orca Basin
Sigsbee Escarpment
Base of Modern Slope
Sigsbee Escarpment
Bryant Fan
Mississippi Fan Channel Systems
30°0'N
29°0'N
28°0'N
27°0'N
26°0'N
25°0'N
94°0'W
93°0'W
92°0'W
91°0'W
90°0'W
89°0'W
88°0'W
87°0'W
86°0'W

Figure 11

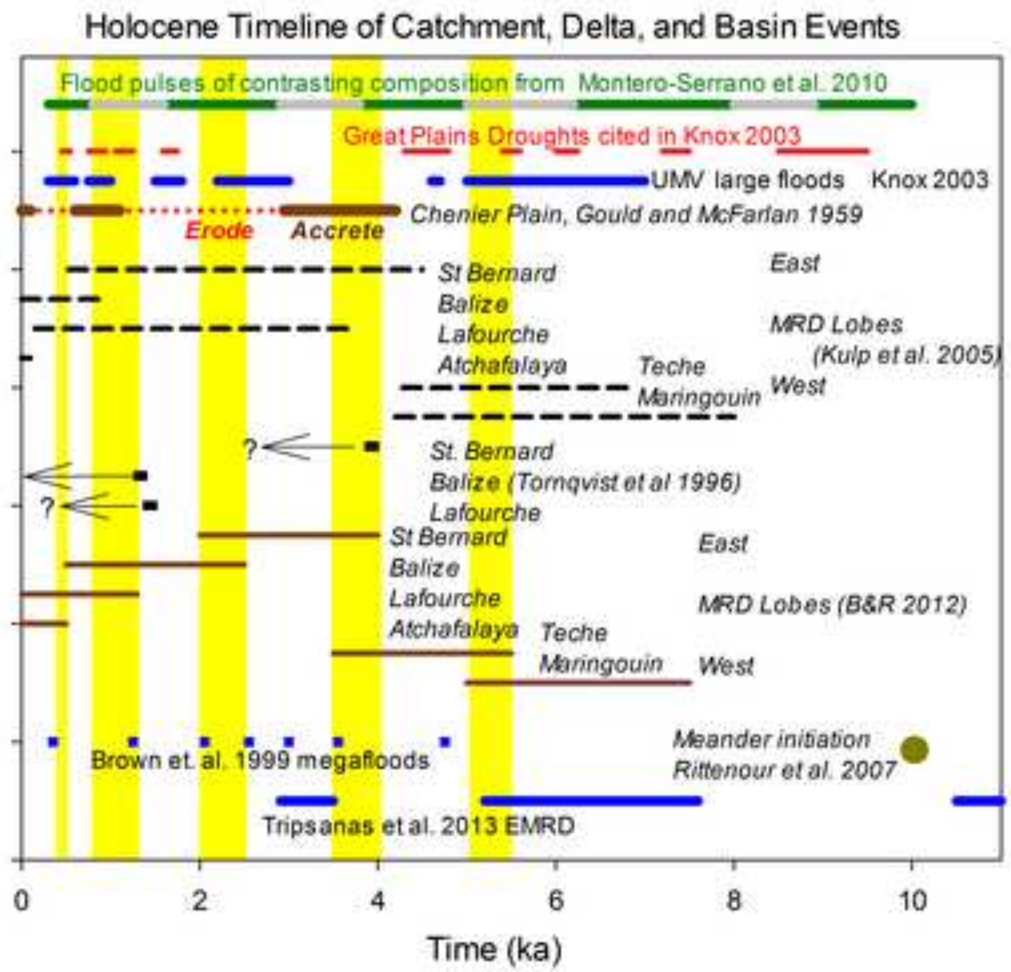

Holocene Timeline of Catchment, Delta, and Basin Events
Flood pulses of contrasting composition from Montero-Serrano et al. 2010
Great Plains Droughts cited in Knox 2003
UMV large floods Knox 2003
Chenier Plain, Gould and McFarlan 1959
Erode
Accrete
St Bernard
Balize
Lafourche
Atchafalaya
Teche
Maringouin
East
MRD Lobes
(Kulp et al. 2005)
West
?
?
St. Bernard
Balize (Tornqvist et al 1996)
Lafourche
St Bernard
Balize
Lafourche
Atchafalaya
Teche
Maringouin
East
MRD Lobes (B&R 2012)
West
Meander initiation
Rittenour et al. 2007
Brown et. al. 1999 megafloods
Tripsanas et al. 2013 EMRD
0
2
4
6
8
10
Time (ka)

Figure 12

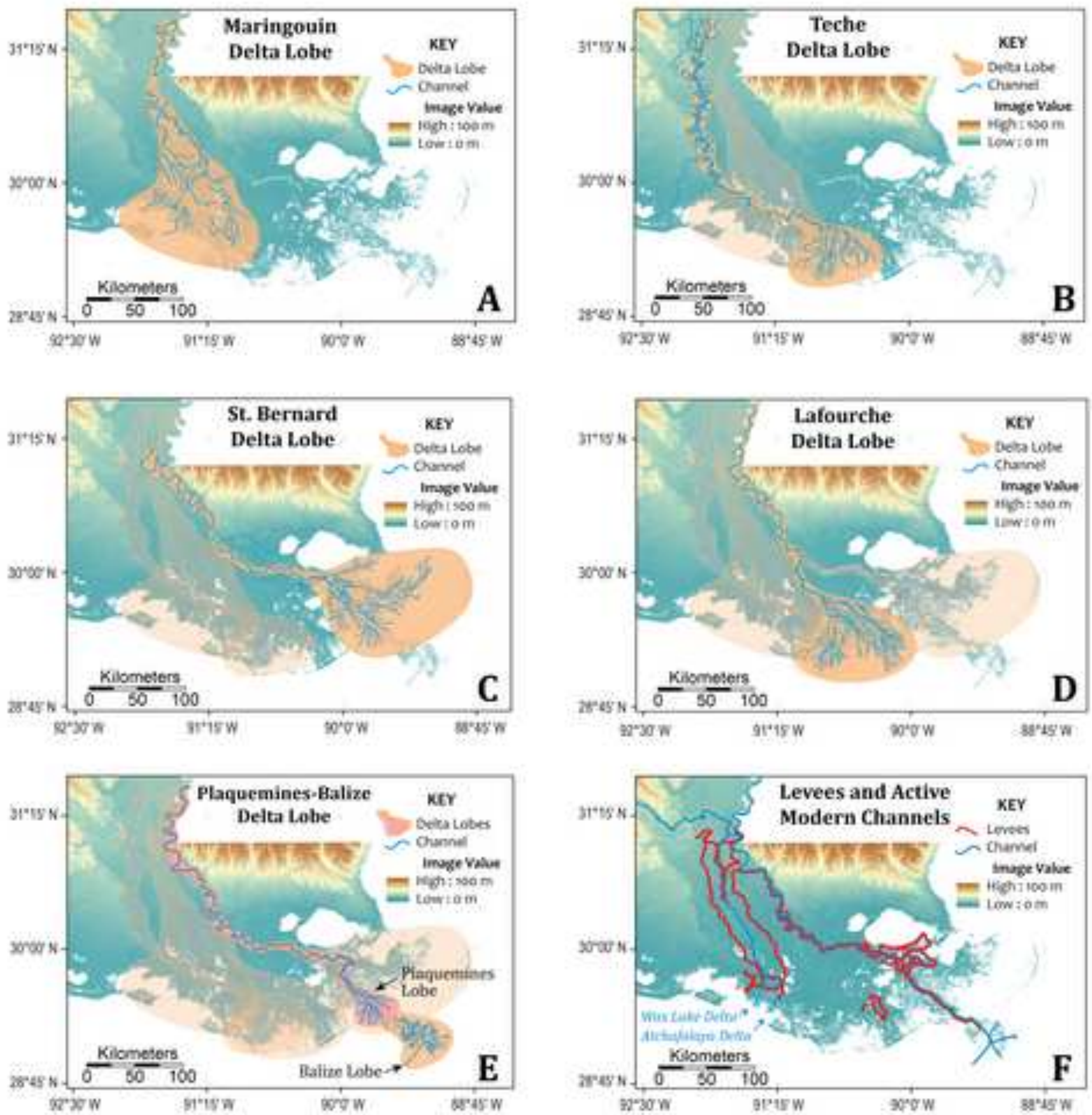
Maringouin
Delta Lobe
KEY
Delta Lobe
Channel
Image Value
High : 100 m
Low : 0 m
Kilometers
0 50 100
A
Teche
Delta Lobe
B
St. Bernard
Delta Lobe
C
Lafourche
Delta Lobe
D
Plaquemines-Balize
Delta Lobe
Delta Lobes
Plaquemines
Lobe
Balize Lobe
E
Levees and Active
Modern Channels
Levees
Wax Lake Delta
Atchafalaya Delta
F
31°15' N
30°00' N
28°45' N
92°30' W
91°15' W
90°0' W
88°45' W

Figure 13

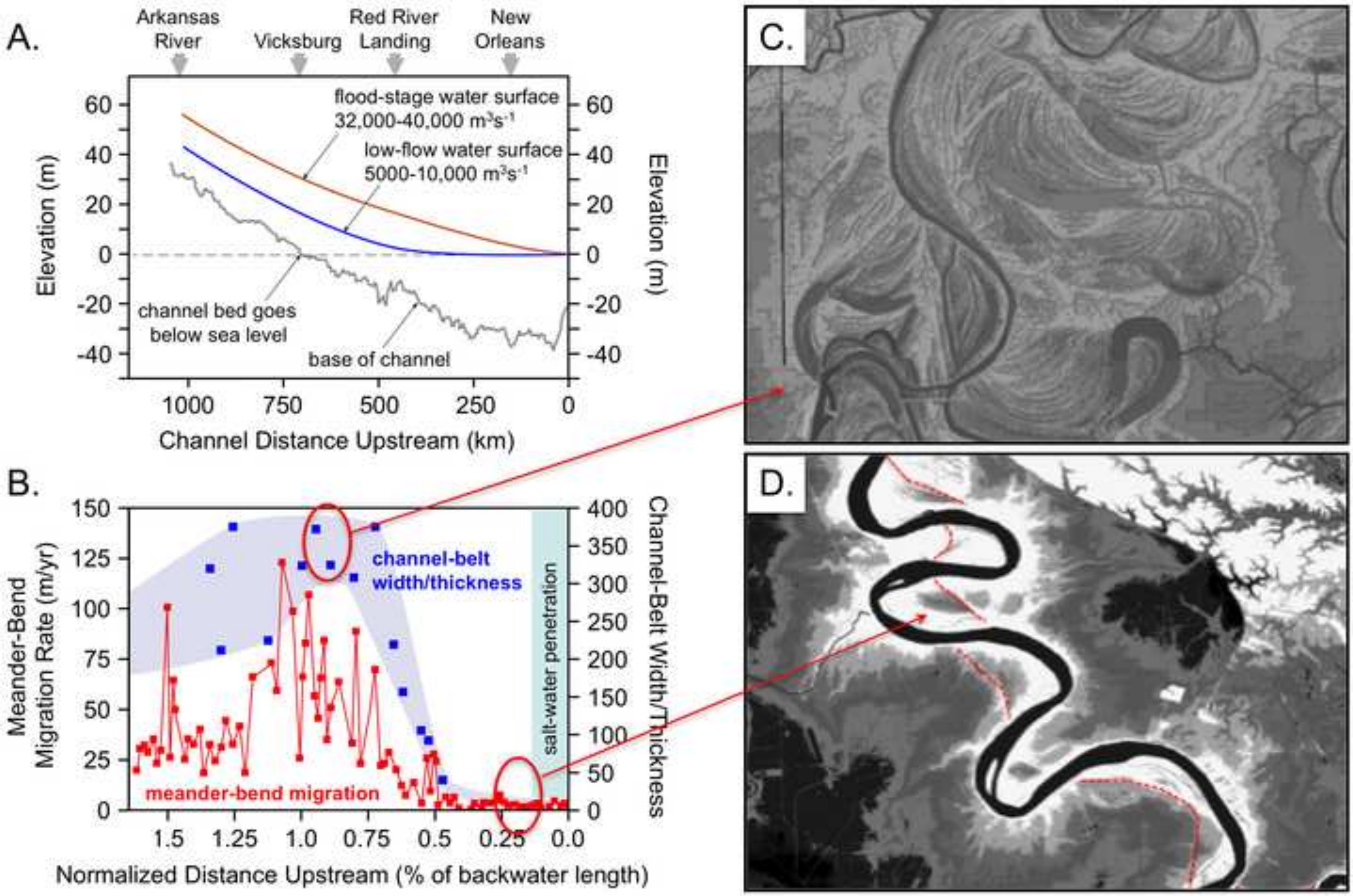

A.
Arkansas River
Vicksburg
Red River Landing
New Orleans
flood-stage water surface
32,000-40,000 m³s⁻¹
low-flow water surface
5000-10,000 m³s⁻¹
channel bed goes below sea level
base of channel
Elevation (m)
Channel Distance Upstream (km)
60
40
20
0
-20
-40
1000
750
500
250
0
B.
150
125
100
75
50
25
0
400
350
300
250
200
150
100
50
0
1.5
1.25
1.0
0.75
0.5
0.25
0.0
channel-belt width/thickness
meander-bend migration
salt-water penetration
Meander-Bend Migration Rate (m/yr)
Channel-Belt Width/Thickness
Normalized Distance Upstream (% of backwater length)
C.
D.

Figure 14a


North Dakota
Montana
Minnesota
South Dakota
Wisconsin
Mississippi River
Missouri River
New York
Michigan
Wyoming
Iowa
Nebraska
Illinois River
Pennsylvania
Indiana
Ohio
Illinois
Ohio River
Colorado
Kansas
West Virginia
Virginia
Kentucky
Missouri
North Carolina
Tennessee
Oklahoma
South Carolina
New Mexico
Georgia
Alabama
Atchafalaya River
Texas
Florida
Gulf of Mexico
N
0
500
Water discharge
in cubic kilometers per year
0 100 200 Kilometers
0 100 200 Miles

Figure 14b

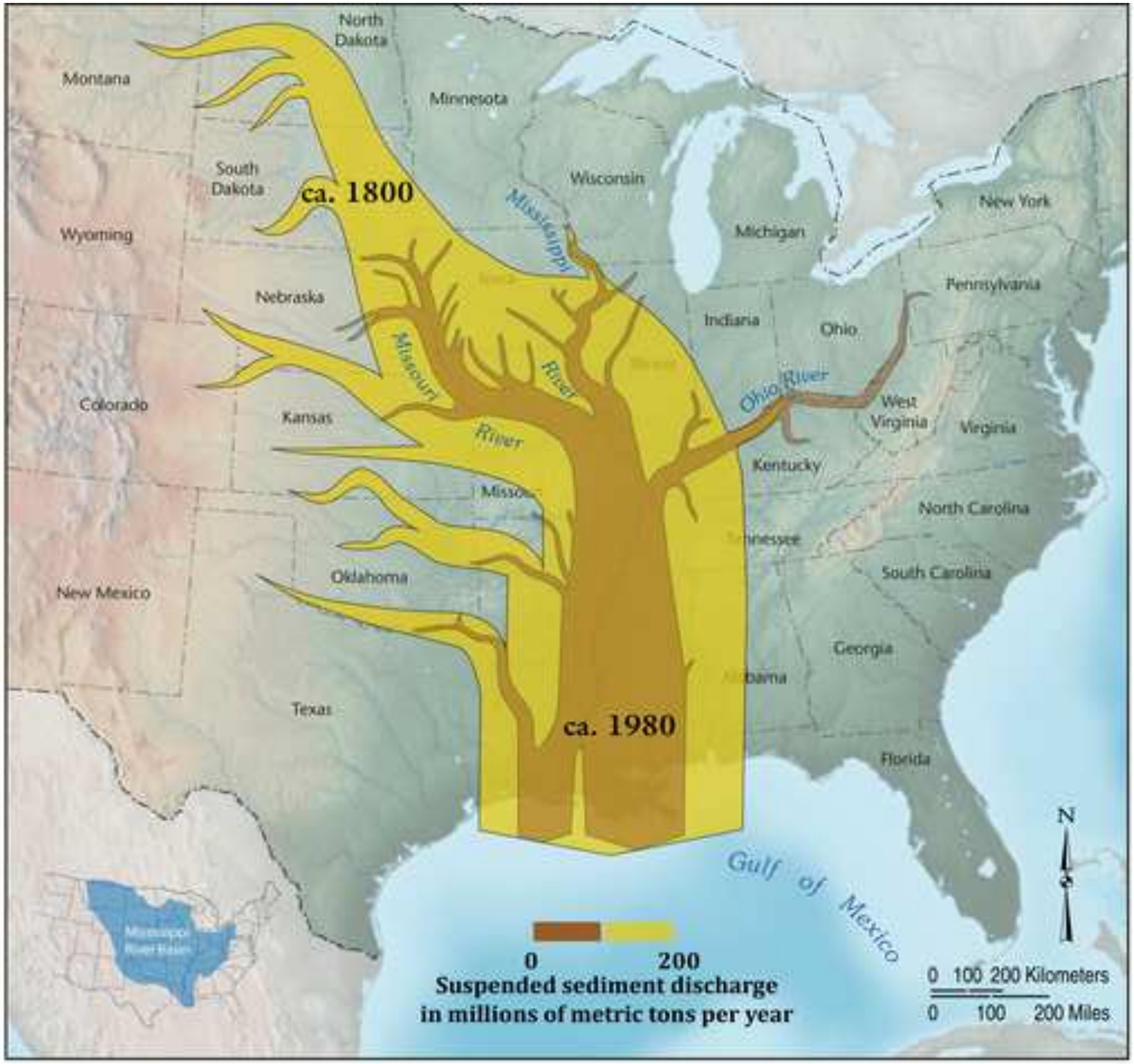

ca. 1800
ca. 1980
Missouri River
Mississippi River
Ohio River
Gulf of Mexico
Montana
North Dakota
Minnesota
South Dakota
Wyoming
Wisconsin
Michigan
New York
Nebraska
Pennsylvania
Indiana
Ohio
Colorado
Kansas
West Virginia
Virginia
Kentucky
North Carolina
New Mexico
Oklahoma
South Carolina
Georgia
Texas
Florida
0
200
Suspended sediment discharge
in millions of metric tons per year
0 100 200 Kilometers
0 100 200 Miles
N

Figure 15

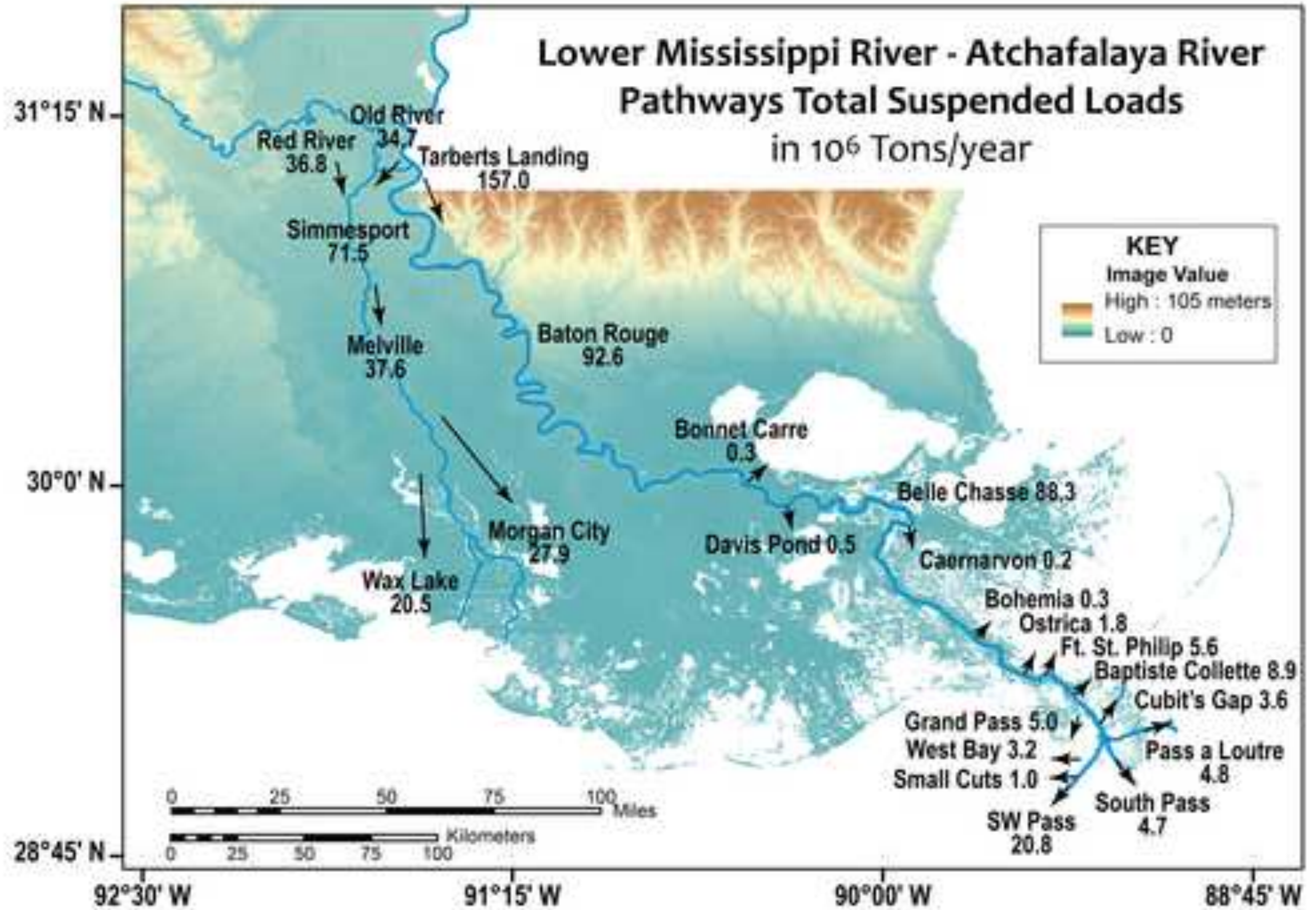

Lower Mississippi River - Atchafalaya River
Pathways Total Suspended Loads
in 10^6 Tons/year
KEY
Image Value
High : 105 meters
Low : 0
Old River 34.7
Red River 36.8
Tarberts Landing 157.0
Simmesport 71.5
Melville 37.6
Baton Rouge 92.6
Bonnet Carre 0.3
Belle Chasse 88.3
Davis Pond 0.5
Caernarvon 0.2
Morgan City 27.9
Wax Lake 20.5
Bohemia 0.3
Ostrica 1.8
Ft. St. Philip 5.6
Baptiste Collette 8.9
Cubit's Gap 3.6
Grand Pass 5.0
West Bay 3.2
Small Cuts 1.0
Pass a Loutre 4.8
South Pass 4.7
SW Pass 20.8
0 25 50 75 100 Miles
0 25 50 75 100 Kilometers
31°15' N
30°0' N
28°45' N
92°30' W
91°15' W
90°00' W
88°45' W

Figure 16

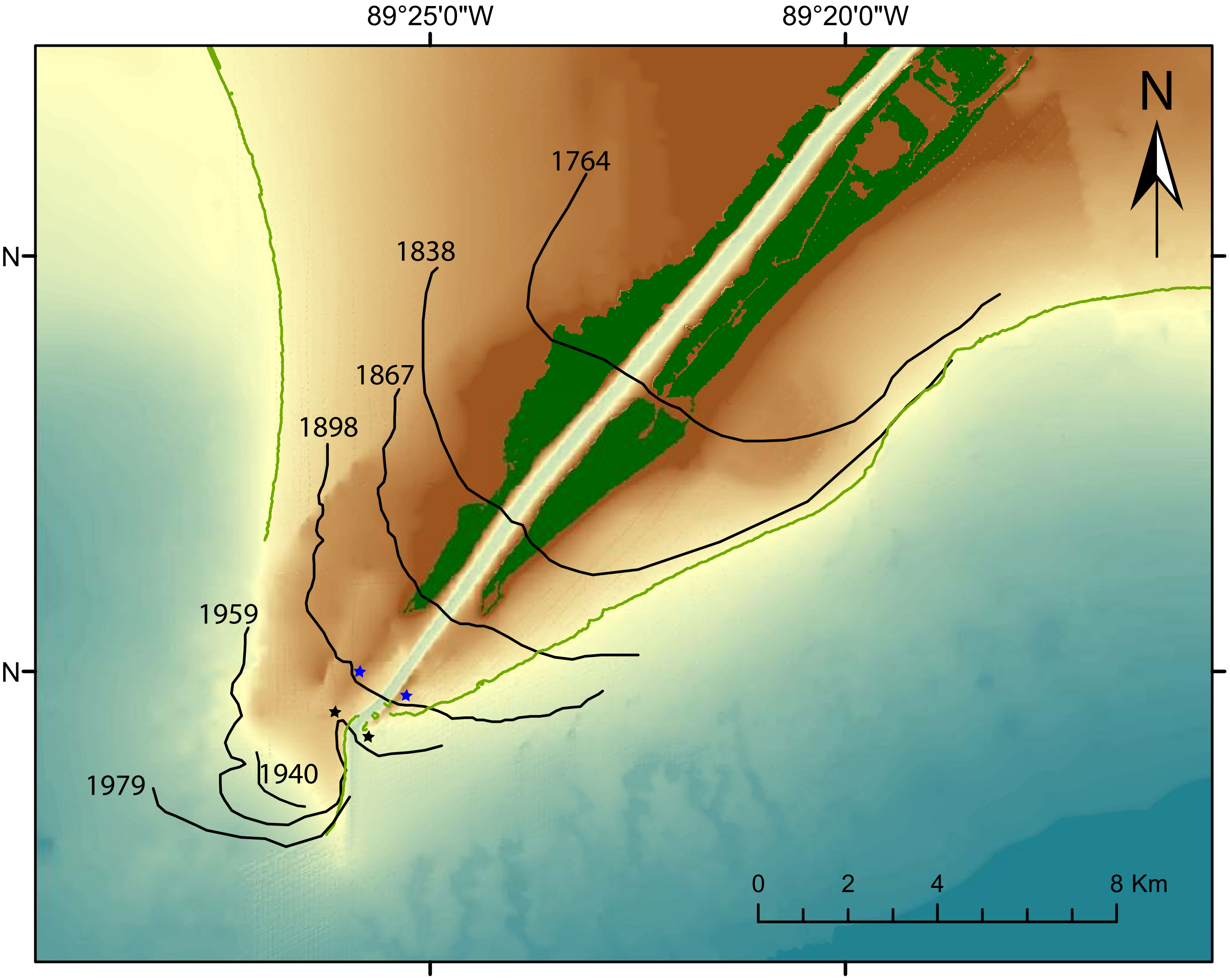

89°25'0"W
89°20'0"W
29°0'0"N
28°55'0"N
N
1764
1838
1867
1898
1959
1940
1979
0
2
4
8 Km

Figure 17

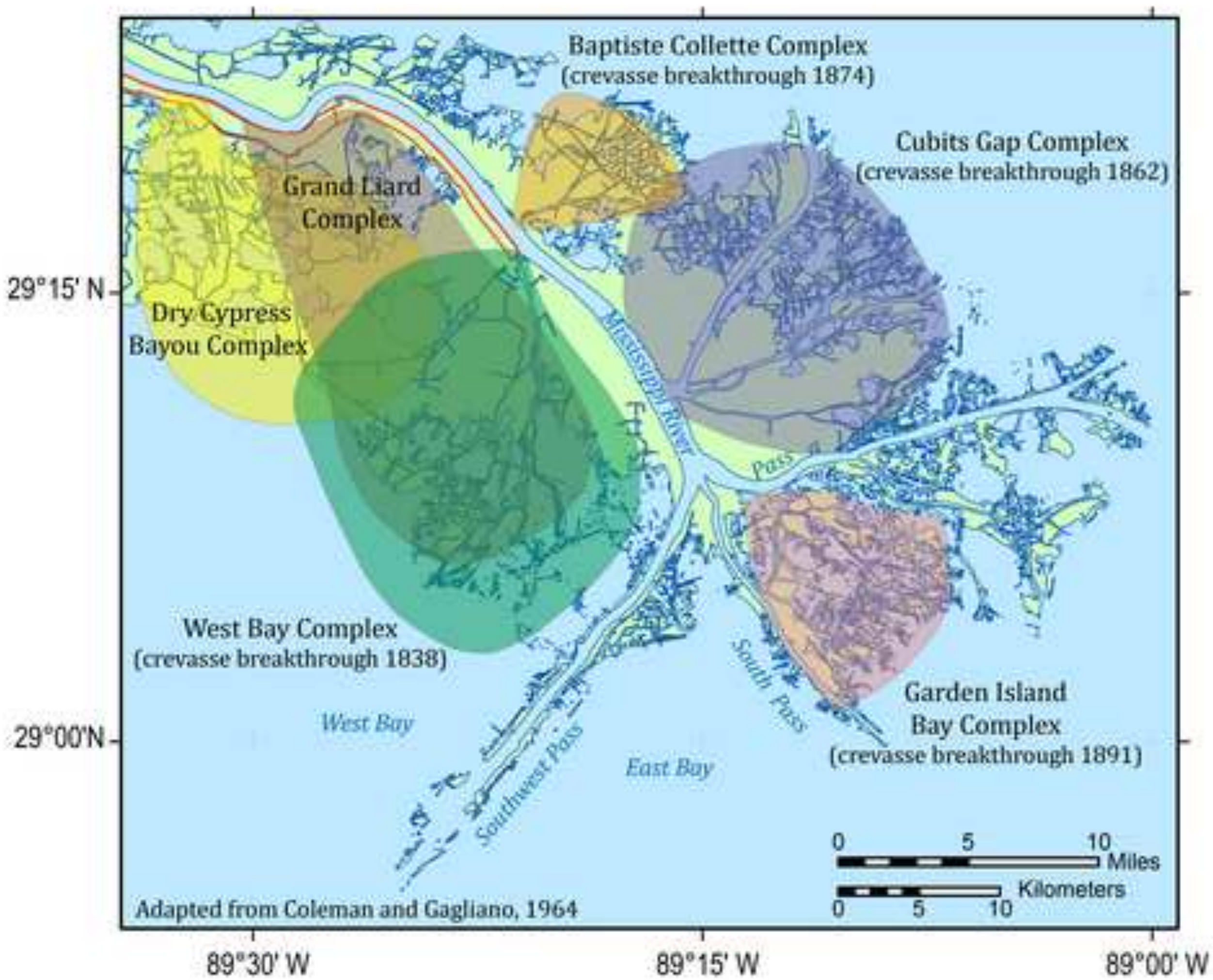

Baptiste Collette Complex
(crevasse breakthrough 1874)
Cubits Gap Complex
(crevasse breakthrough 1862)
Grand Liard
Complex
Dry Cypress
Bayou Complex
Mississippi River
Pass
West Bay Complex
(crevasse breakthrough 1838)
West Bay
Southwest Pass
East Bay
South Pass
Garden Island
Bay Complex
(crevasse breakthrough 1891)
29°15' N
29°00'N
89°30' W
89°15' W
89°00' W
0
5
10
Miles
Kilometers
Adapted from Coleman and Gagliano, 1964

Figure 18

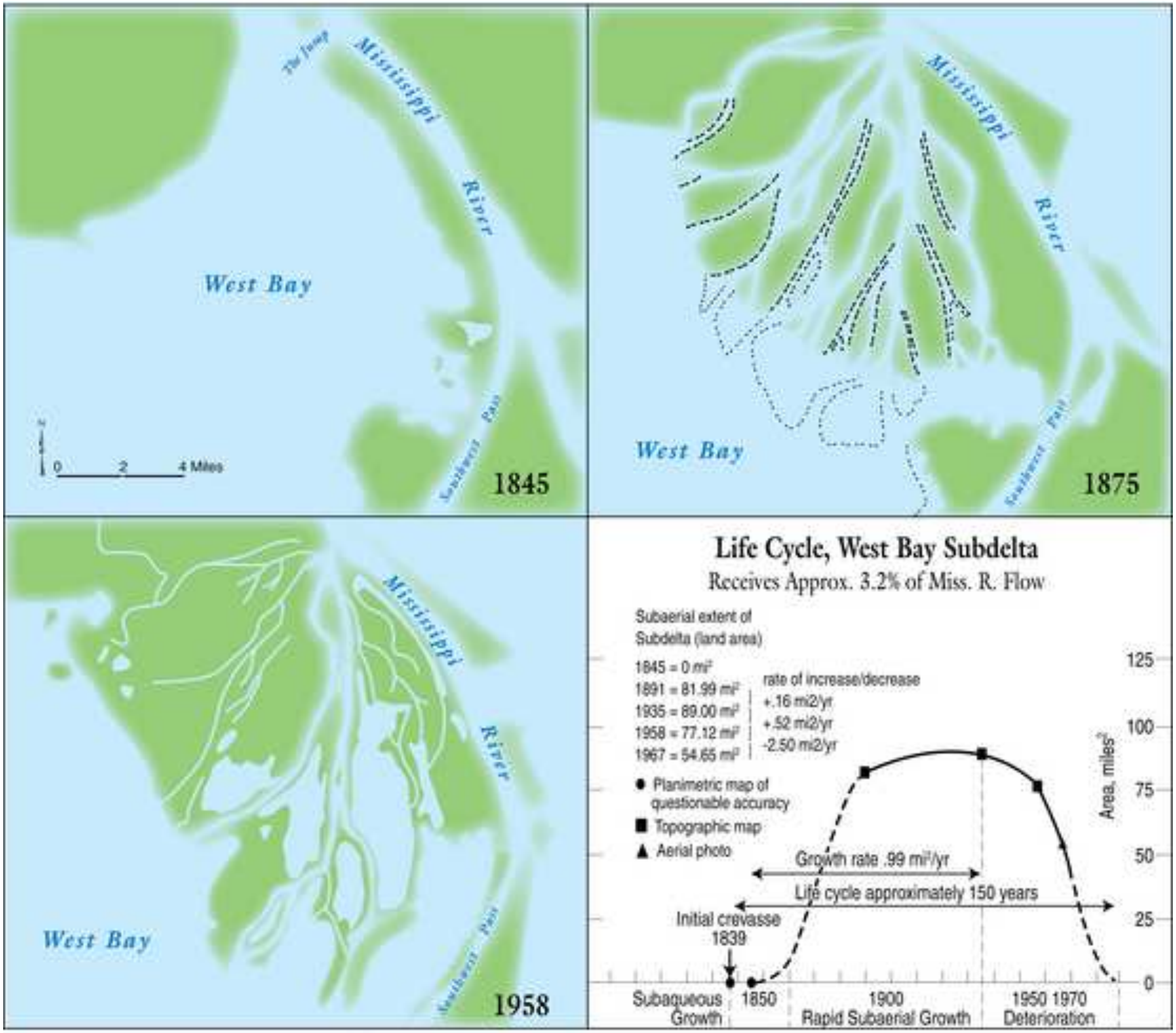

The Jump
Mississippi
River
West Bay
Southwest Pass
0 2 4 Miles
1845
Mississippi
River
West Bay
Southwest Pass
1875
Mississippi
River
West Bay
Southwest Pass
1958
Life Cycle, West Bay Subdelta
Receives Approx. 3.2% of Miss. R. Flow
Subaerial extent of Subdelta (land area)
1845 = 0 mi²
1891 = 81.99 mi²
1935 = 89.00 mi²
1958 = 77.12 mi²
1967 = 54.65 mi²
rate of increase/decrease
+.16 mi2/yr
+.52 mi2/yr
-2.50 mi2/yr
Planimetric map of questionable accuracy
Topographic map
Aerial photo
Growth rate .99 mi²/yr
Life cycle approximately 150 years
Initial crevasse 1839
Area, miles²
125
100
75
50
25
0
1850
1900
1950 1970
Subaqueous Growth
Rapid Subaerial Growth
Deterioration

Figure 19

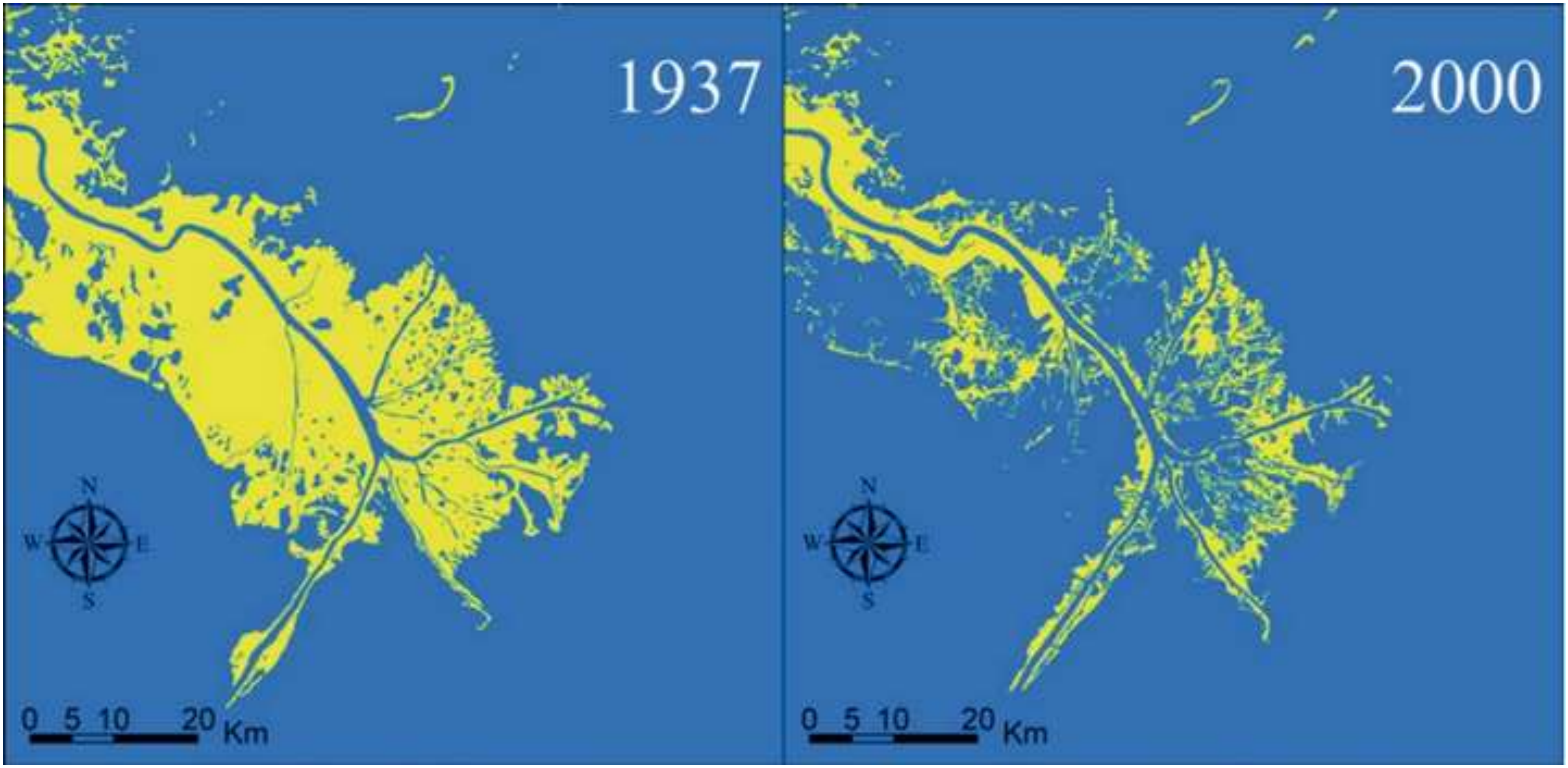

Figure 20

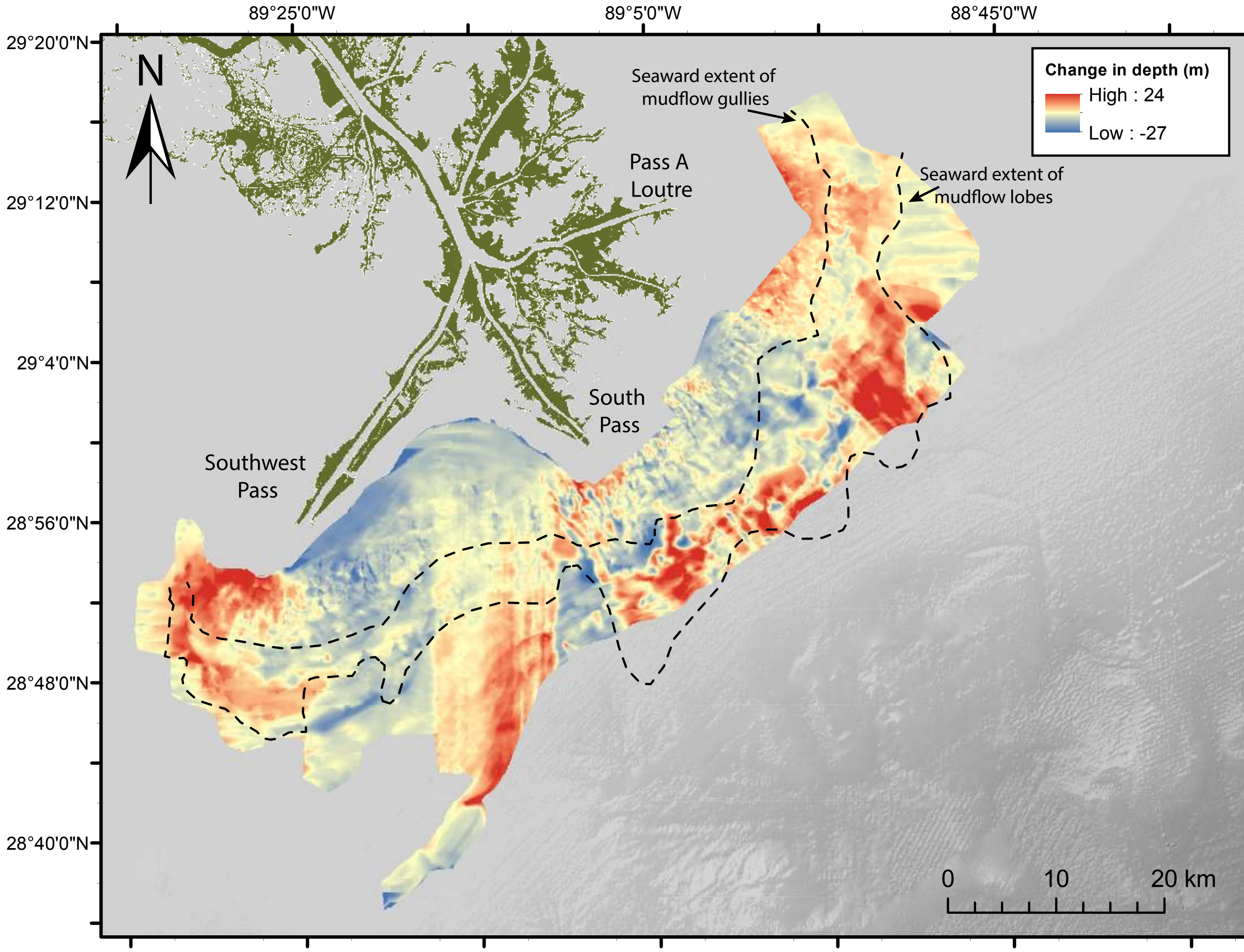

89°25'0"W
89°5'0"W
88°45'0"W
29°20'0"N
29°12'0"N
29°4'0"N
28°56'0"N
28°48'0"N
28°40'0"N
N
Seaward extent of mudflow gullies
Seaward extent of mudflow lobes
Change in depth (m)
High : 24
Low : -27
Pass A Loutre
South Pass
Southwest Pass
0
10
20 km

Figure 21

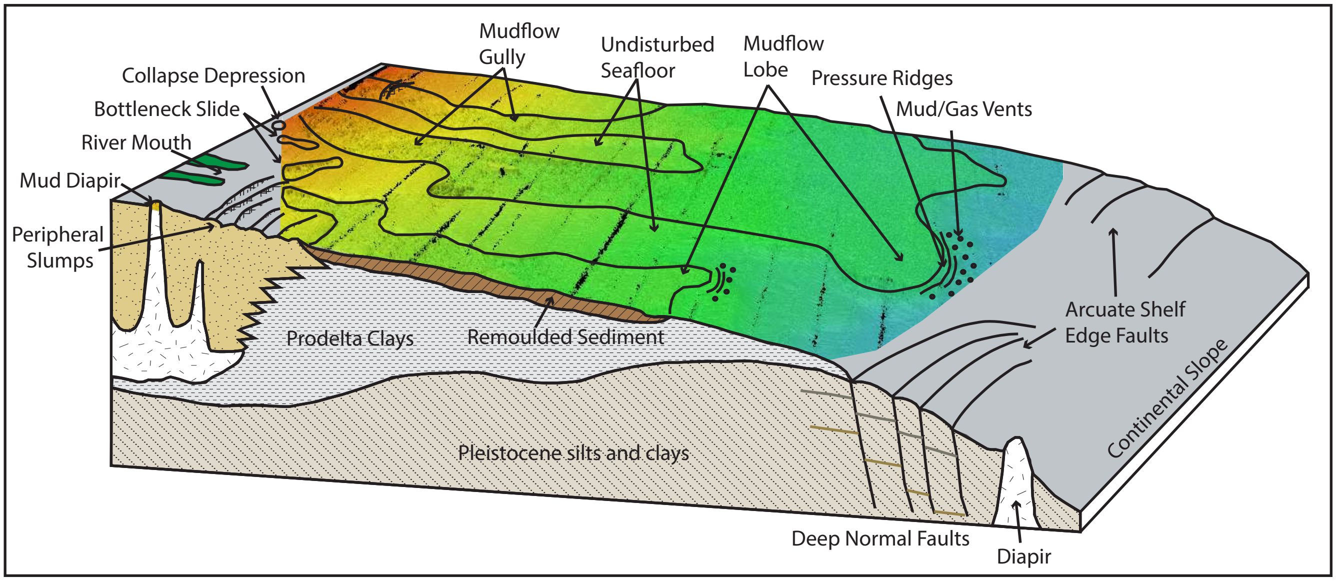

Mudflow Gully
Undisturbed Seafloor
Mudflow Lobe
Pressure Ridges
Mud/Gas Vents
Collapse Depression
Bottleneck Slide
River Mouth
Mud Diapir
Peripheral Slumps
Prodelta Clays
Remoulded Sediment
Arcuate Shelf Edge Faults
Continental Slope
Pleistocene silts and clays
Deep Normal Faults
Diapir

Figure 22

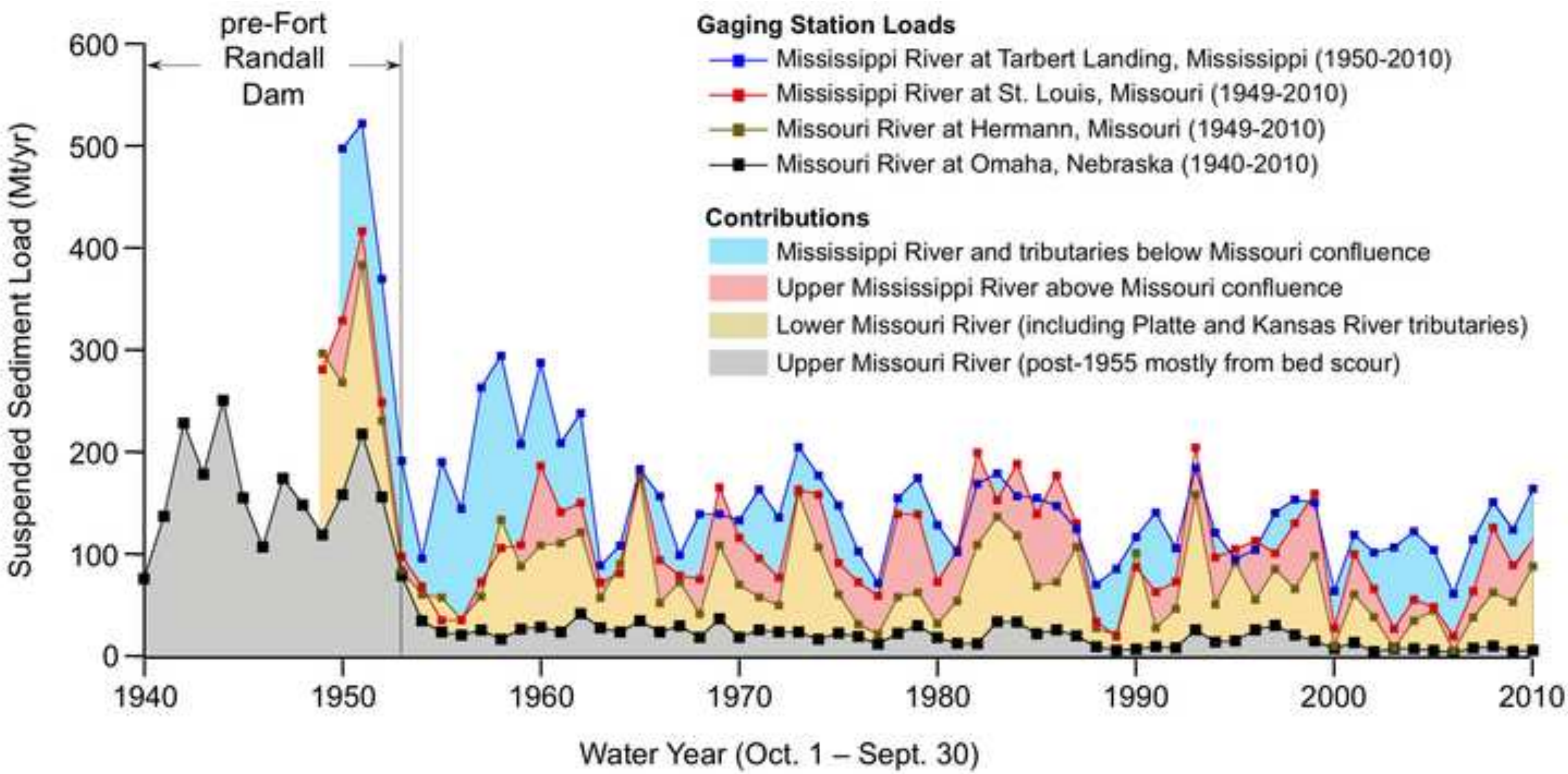

pre-Fort Randall Dam
Gaging Station Loads
Mississippi River at Tarbert Landing, Mississippi (1950-2010)
Mississippi River at St. Louis, Missouri (1949-2010)
Missouri River at Hermann, Missouri (1949-2010)
Missouri River at Omaha, Nebraska (1940-2010)
Contributions
Mississippi River and tributaries below Missouri confluence
Upper Mississippi River above Missouri confluence
Lower Missouri River (including Platte and Kansas River tributaries)
Upper Missouri River (post-1955 mostly from bed scour)
Suspended Sediment Load (Mt/yr)
0
100
200
300
400
500
600
1940
1950
1960
1970
1980
1990
2000
2010
Water Year (Oct. 1 – Sept. 30)

Figure 23

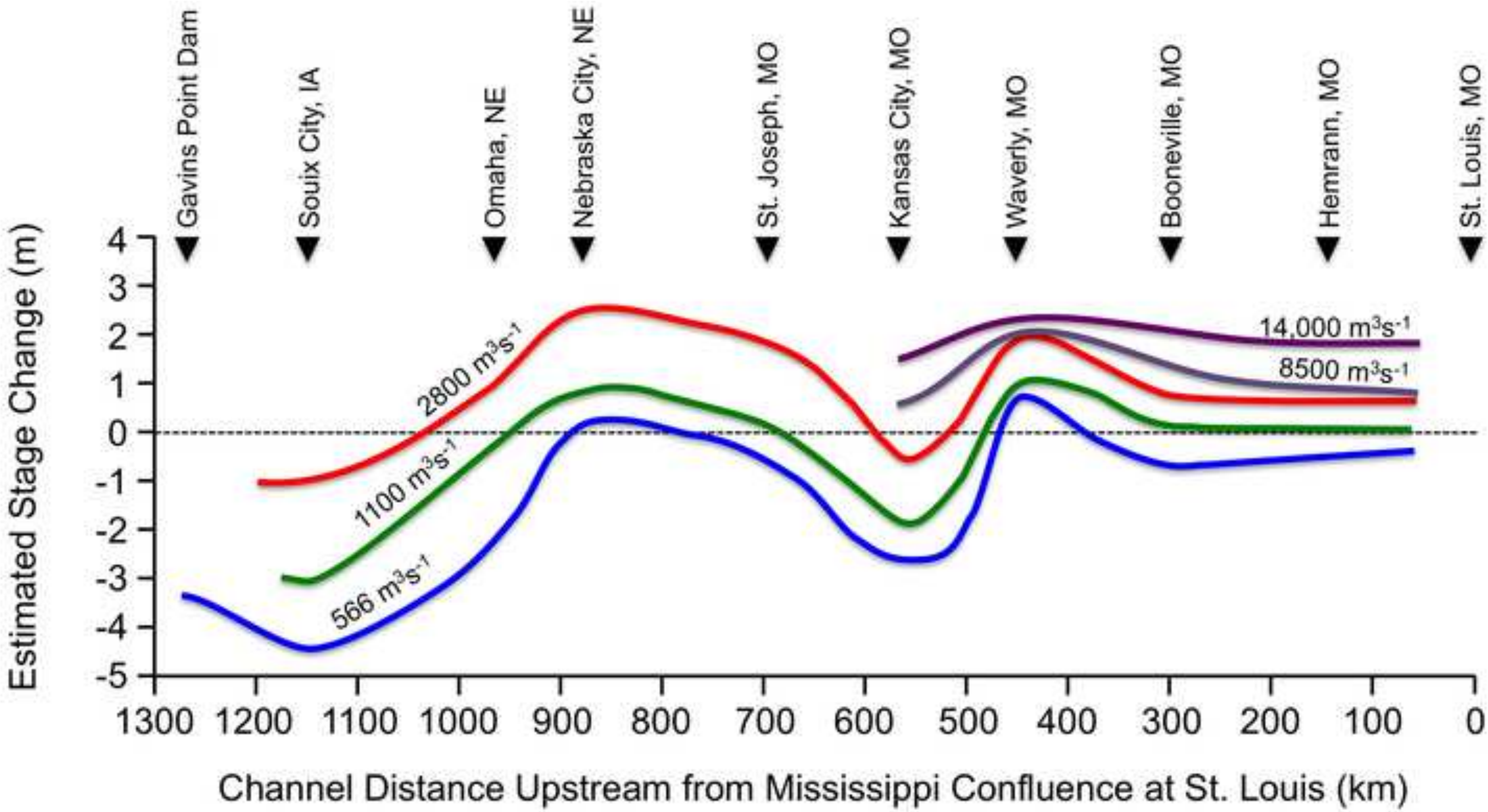

Gavins Point Dam
Souix City, IA
Omaha, NE
Nebraska City, NE
St. Joseph, MO
Kansas City, MO
Waverly, MO
Booneville, MO
Hemrann, MO
St. Louis, MO
Estimated Stage Change (m)
4
3
2
1
0
-1
-2
-3
-4
-5
2800 m3s-1
1100 m3s-1
566 m3s-1
14,000 m3s-1
8500 m3s-1
1300
1200
1100
1000
900
800
700
600
500
400
300
200
100
0
Channel Distance Upstream from Mississippi Confluence at St. Louis (km)

Figure 24

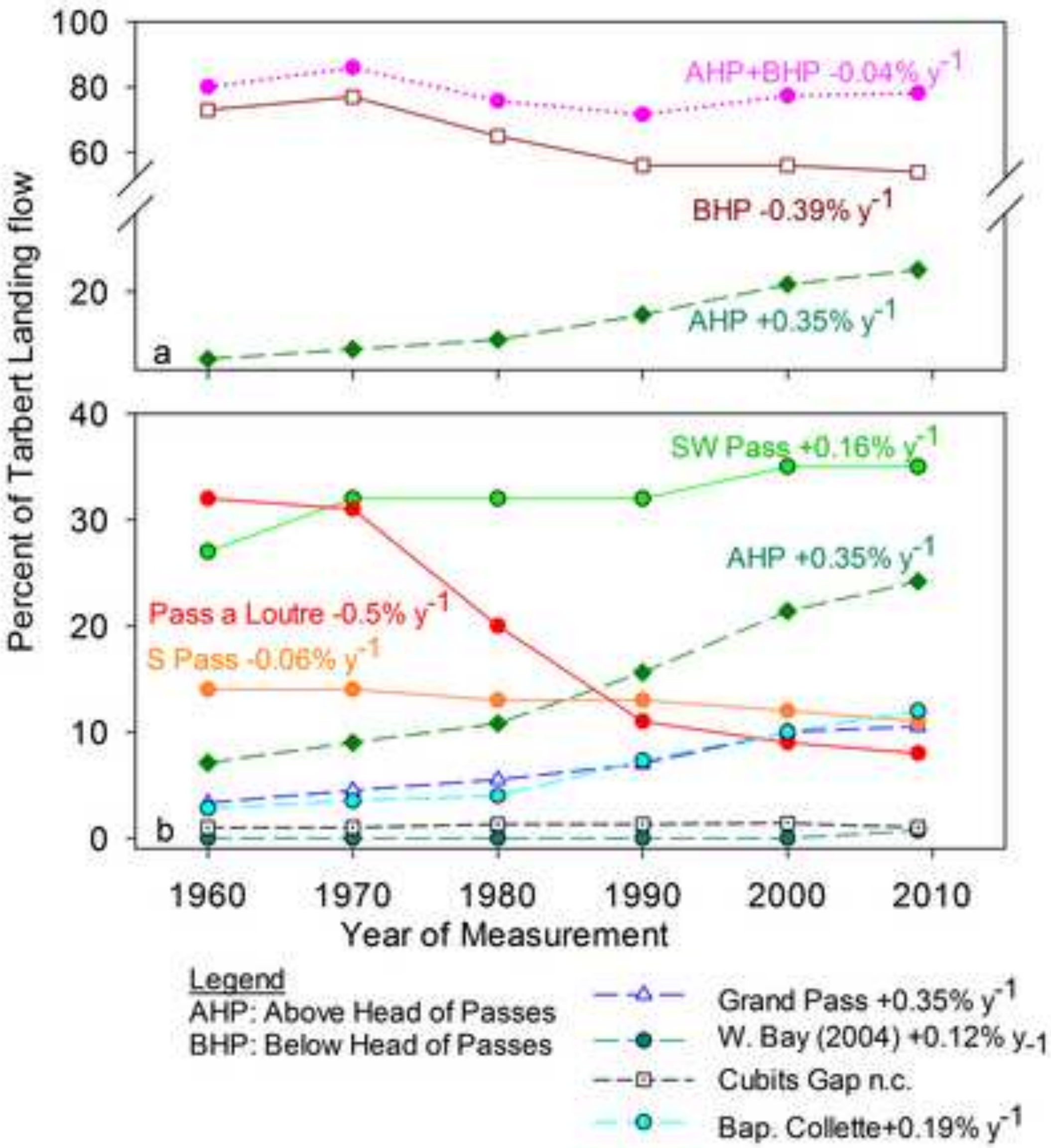

100
80
60
20
a
AHP+BHP -0.04% y-1
BHP -0.39% y-1
AHP +0.35% y-1
40
30
20
10
0
b
SW Pass +0.16% y-1
AHP +0.35% y-1
Pass a Loutre -0.5% y-1
S Pass -0.06% y-1
Percent of Tarbert Landing flow
1960
1970
1980
1990
2000
2010
Year of Measurement
Legend
AHP: Above Head of Passes
BHP: Below Head of Passes
Grand Pass +0.35% y-1
W. Bay (2004) +0.12% y-1
Cubits Gap n.c.
Bap. Collette+0.19% y-1

Figure 25

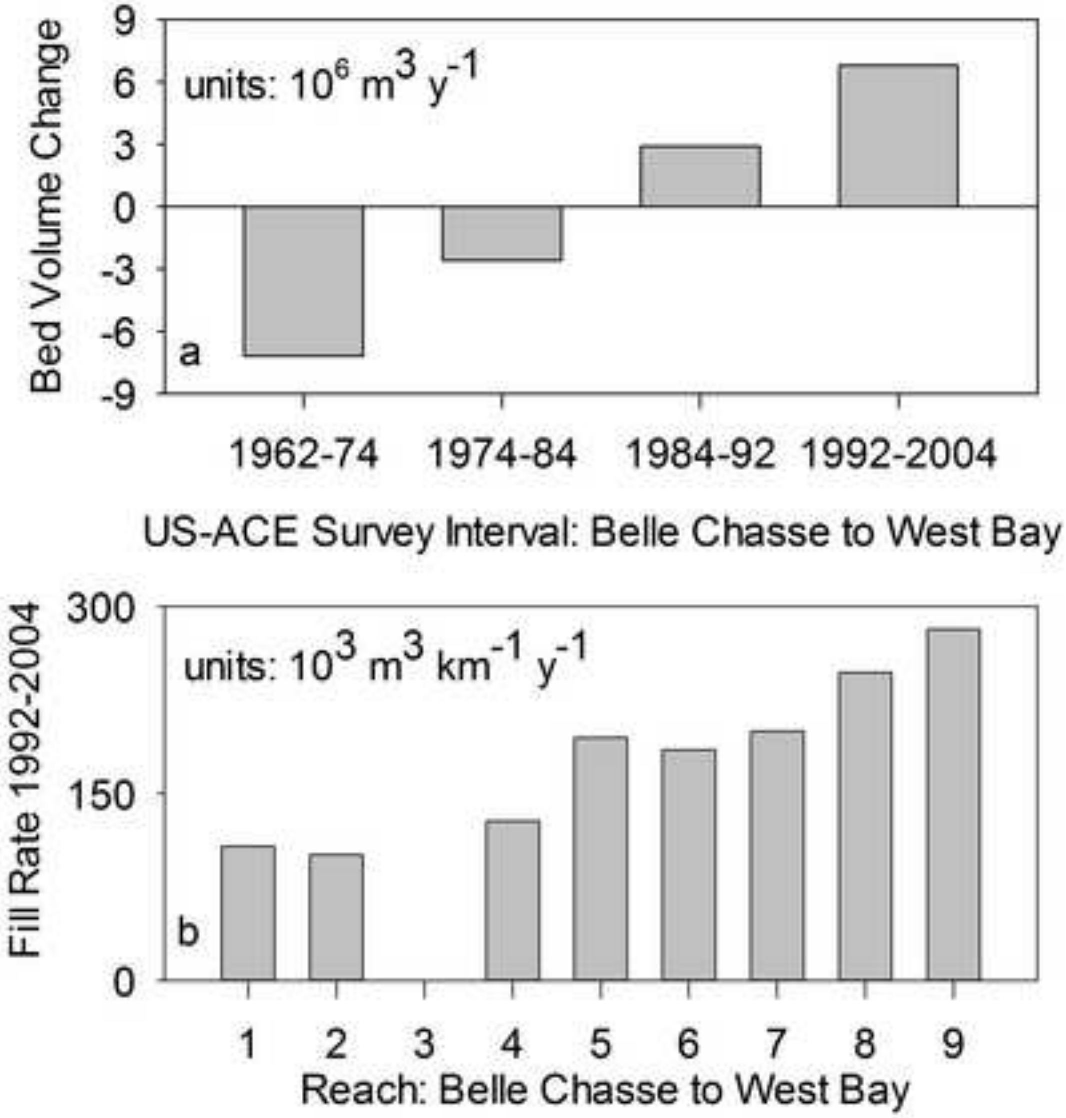

units: 10^6 m^3 y^{-1}
Bed Volume Change
9
6
3
0
-3
-6
-9
a
1962-74
1974-84
1984-92
1992-2004
US-ACE Survey Interval: Belle Chasse to West Bay
units: 10^3 m^3 km^{-1} y^{-1}
Fill Rate 1992-2004
300
150
0
b
1
2
3
4
5
6
7
8
9
Reach: Belle Chasse to West Bay

Figure 26

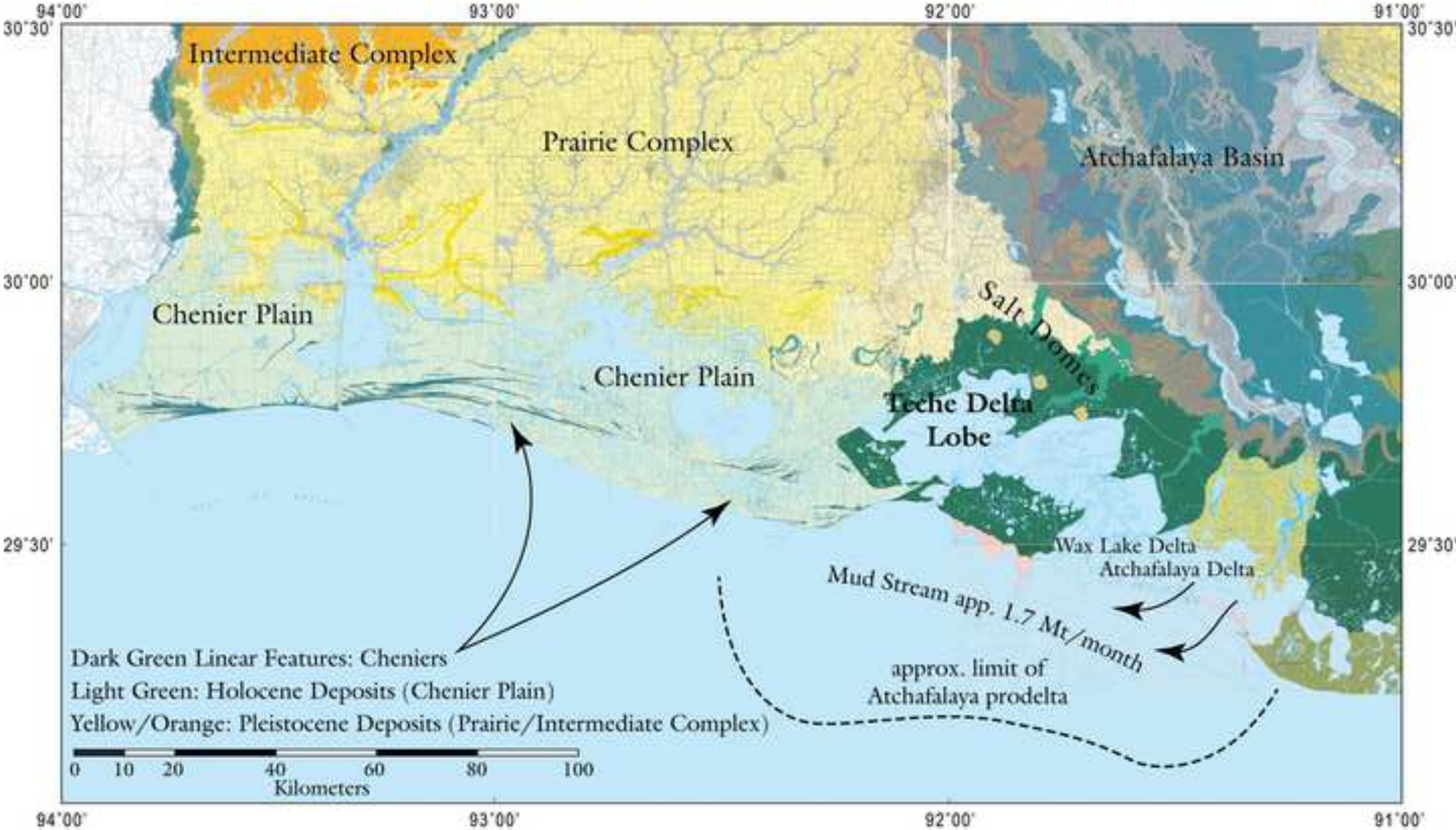
94°00'
93°00'
92°00'
91°00'
30°30'
30°00'
29°30'
Intermediate Complex
Prairie Complex
Atchafalaya Basin
Chenier Plain
Chenier Plain
Salt Domes
Teche Delta Lobe
Wax Lake Delta
Atchafalaya Delta
Mud Stream app. 1.7 Mt/month
approx. limit of Atchafalaya prodelta
Dark Green Linear Features: Cheniers
Light Green: Holocene Deposits (Chenier Plain)
Yellow/Orange: Pleistocene Deposits (Prairie/Intermediate Complex)
0 10 20 40 60 80 100
Kilometers

Figure 27

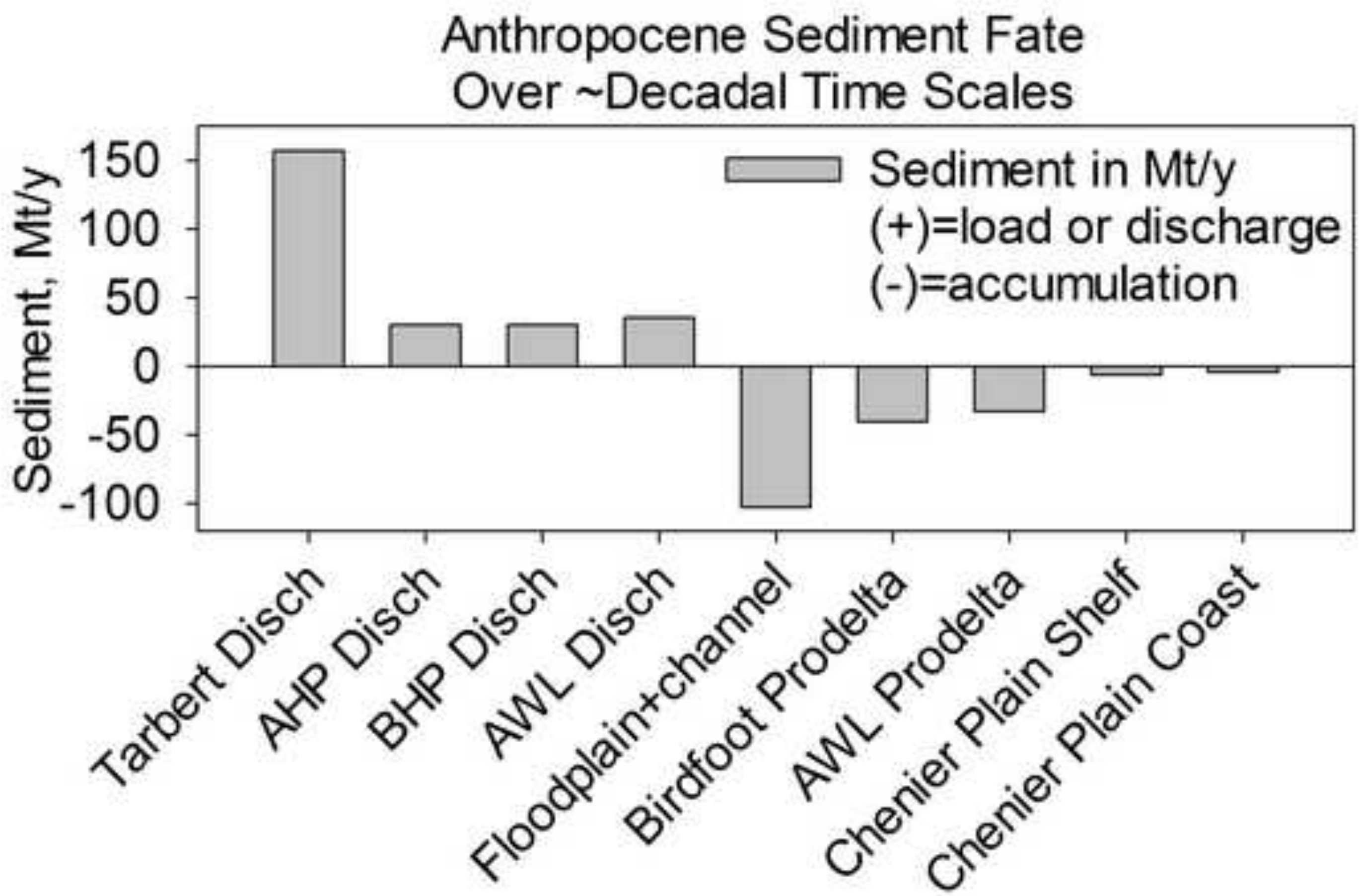

Anthropocene Sediment Fate
Over ~Decadal Time Scales
Sediment in Mt/y
(+)=load or discharge
(-)=accumulation
Sediment, Mt/y
150
100
50
0
-50
-100
Tarbert Disch
AHP Disch
BHP Disch
AWL Disch
Floodplain+channel
Birdfoot Prodelta
AWL Prodelta
Chenier Plain Shelf
Chenier Plain Coast

Figure 28

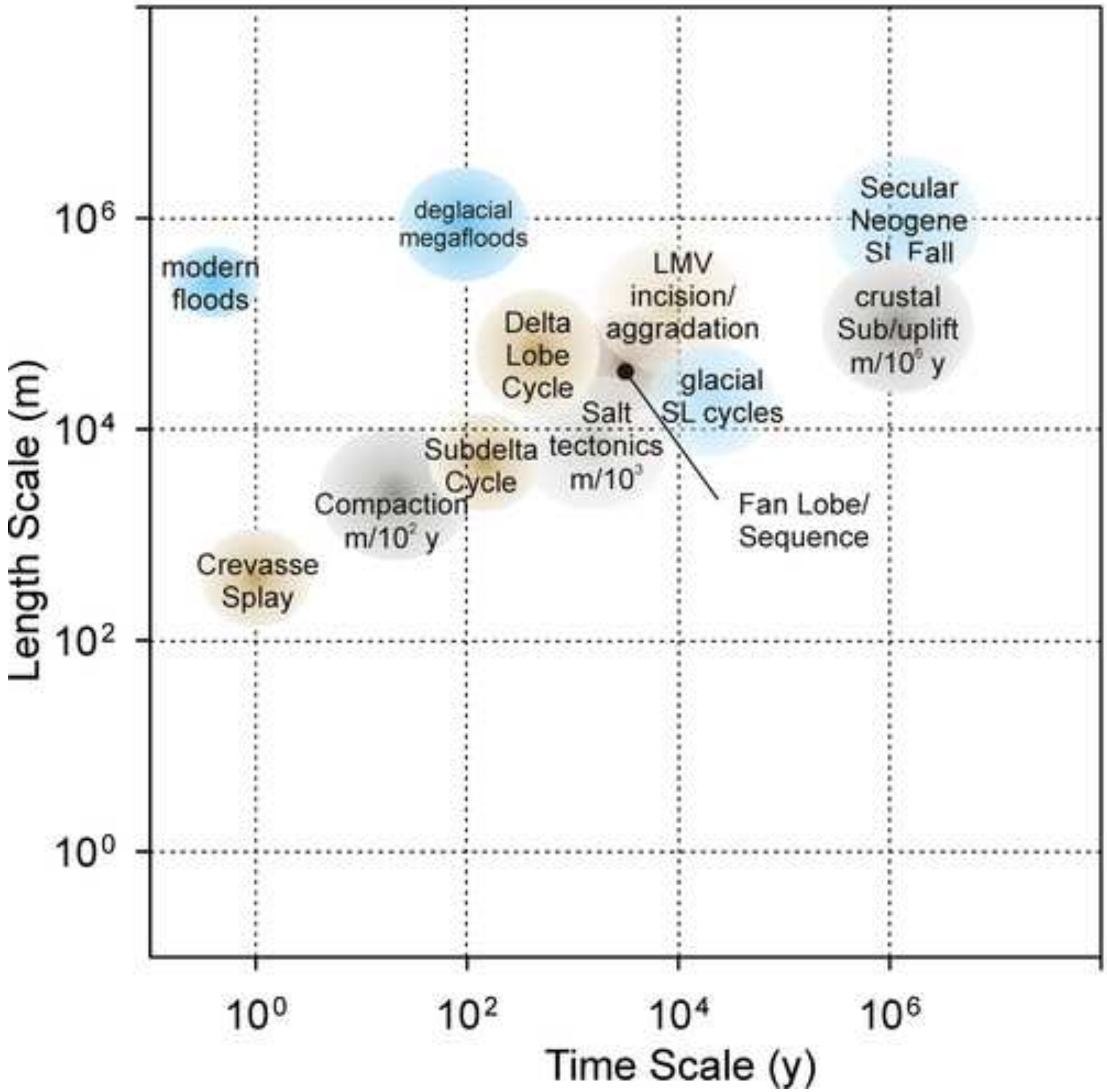

Length Scale (m)
10^6
10^4
10^2
10^0
Time Scale (y)
10^0
10^2
10^4
10^6
modern floods
deglacial megafloods
Secular Neogene SL Fall
LMV incision/ aggradation
crustal Sub/uplift m/10^6 y
Delta Lobe Cycle
glacial SL cycles
Salt tectonics m/10^3
Subdelta Cycle
Compaction m/10^2 y
Fan Lobe/ Sequence
Crevasse Splay

Tables

Table 1. Abbreviations used in this paper

MRS	Mississippi River Source to Sink System, from upper tributary catchments to Gulf of Mexico basin floor
GoM, NGOM	Gulf of Mexico, northern Gulf of Mexico
RMOP	Rocky Mountain orogenic plateau
MIS	Marine Isotope Stage
Ma	Specific calendar year in millions of years before present
My	Duration of a period of time in millions of years
ka	Specific calendar year in thousands of years before present
ky	duration of a period of time in thousands of years
MRD	Mississippi River Delta
LGM	Last Glacial Maximum
LMV	Lower Mississippi Valley, from near New Madrid,Missouri, south to the northern edge of the delta near Baton Rouge, Louisiana
UMV	Upper Mississippi Valley, north from near New Madrid, Missouri
ORCS	Old River Control Structure
MR&T	Mississippi River and Tributaries Project, US Army Corps of Engineers
AWL	Atchafalaya and Wax Lake outlets of the Atchafalaya River

Table 2. Synthesis of Miocene climate and sediment delivery

<table>
<tr><th rowspan="2">Miocene Epoch Time Intervals and Ages[1]</th><th colspan="4">Conditions and Processes by Region</th><th rowspan="2">Deposode (6,7)</th></tr>
<tr><th>Rocky Mountains Great Plains</th><th>Appalachians</th><th>Delta coast and shelf</th><th>Slope and basin</th></tr>
<tr><td>End Miocene (ca. 5.3 Ma)</td><td>Climate: monsoonal precipitation and catchment erosion
Tectonics: regional doming from mantle processes
Sed. Proc: river incision, catchment erosion and high discharge (2,3)</td><td>Climate: sufficient precipitation for broadleaf forests interspersed with grasslands (4)
Tectonics: broad uplift
Sediment Supply: nd</td><td rowspan="2">Continued delta growth along MM trends; eastern lobes become dominant
Possible Mississippi/Tennessee divide (6, 11)</td><td rowspan="2">Continued fan development and syndepositional faulting and subsidence; basin isopachs consistent with multiple fluvial axes active, perhaps simultaneously (12)</td><td rowspan="2">UM
(ca. 12-6 Ma) maximum isopach thickness ~4.9 km</td></tr>
<tr><td>Late (LM; Tortonian and Messinian, 11.6-5.3 Ma)</td><td>Climate: cooler, dryer, less variable than MM
Tectonics: slow regional and local syndepositional subsidence
Sed. Proc.: fluvial aggradation and low discharge (2,3)</td><td>Climate: cooler and dryer than MM, temperate gymnosperm+angiosperm forests and grasslands(4,5)
Tectonics: broad uplift
Sediment Supply: high (5, 8,9)</td></tr>
<tr><td>Middle (MM; Langhian and Serravalian, 16.0-11.6 Ma)</td><td>Climate: Relatively warm, wet, but less than EM (2)
Tectonics: slow regional and local syndepositional subsidence
Sed. Proc.: fluvial aggradation and low-medium discharge (2-3)</td><td>Climate: relatively warm and wet but less than EM, subtropical-warm temperate angiosperm forests (5)
Tectonics: broad uplift
Sediment Supply: moderate to high (8,9)</td><td>Modern Mississippi Axis largely developed; Extensive delta plain composed of heterolithic aggradational and progradational lobes, muddy prodelta (10)
Possible Mississippi/Tennessee divide (6,11)</td><td>Thick muddy apron overtopped by prograding shelf deposits, activates growth faults; basin margin collapse, shelf retreat, resumed progradation; Mississippi and McAVALU Fans develop (10)</td><td>MM
(ca. 15.6-12 Ma) maximum isopach thickness ~2600m (10)</td></tr>
<tr><td>Early (EM; Aquitanian and Budigalian, 23.0-16.0 Ma)</td><td>Climate: relatively warm, wet, seasonal (2)
Tectonics: slow regional and local syndepositional subsidence
Sed. Proc: medium to high discharge (6)</td><td>Climate: nd
Tectonics: quiescent
Sediment Supply: low (pre-uplift)(8,9)</td><td>Red and Mississippi fluvial axes developing extensive fluvially dominated deltas, with marginal strandplains</td><td>Slope apron progrades across slope and basin floor (6)</td><td>LM2
(ca. 18-16 Ma)
LM1 (ca. 25-18 Ma)</td></tr>
</table>

1 Walker et al., 2012

2 Retallack, 2007; Note that this locally derived paleoclimatology for the Rockies and Plains matches local palynological and paleontological data, but does not match the more global perspective of Zachos et al. (2001).

3 Chapin, 2008

4 Desantis and Wallace, 2008
5 Pazzaglia et al., 1997
6 Galloway et al., 2000
7 Galloway et al., 2011
8 Gallen et al., 2013
9 Miller et al., 2013
10 Combellas-Biggot and Galloway, 2005
11 Craddock and Kylander-Clark, 2013
12 Wu and Galloway, 2002.
13 McMillan et al., 2006

Table 3. Synthesis of late Pleistocene/early Holocene processes and conditions by regions within the MS2S system.

Pleistocene Marine Isotope Stage/Time Interval[1]	Conditions and Processes by Region			
	Northern LMRV and tributary valleys	Southern Lower MR valley	Delta and Shelf	Slope and Fan
5 (130-71 ka)	(upper LMRV) meander belts and slackwater deposits documented 92-76 ka (3)	(lower LMRV)MR aggrades to form portions of Prairie Complex coastal/floodplain surface (2), suggesting SL control on fluvial aggradation up to 500 km inland from modern coast.	At peak MIS 5 transgression, coast inland and elevated above modern coast; deltaic and coastal facies develop, mapped by (6) as the Prairie Allogroup	SL above shelf edge, trapping fluvial sediments; MR fan hemipelagic condensed section forms (ca. 75 ky)(8); Bryant Canyon active in MIS 6, deformed into isolated basins from salt movement by 84 ka (7); eastern fan inactive 400-71 ka (9)
4-3 (71-29 Ka)	Switch to braided regime by 64-50 ka, with aggradation in MRV(15-19m, Dudley braid belts) (2,3) and tributary valleys(2,4,5) due to enhanced ice-edge sediment supply;	(post 80-69ka) SL fall drives rapid incision, as MR becomes detached from Prairie Complex (2,3), extending up to ~600 km upstream from modern coast; extensive braid belt development (2)	Incision and planation of MIS 5 alluvial and coastal deposits (2,3); analogous Lagniappe Delta to the east (10,11), cross-shelf progradation with falling SL;	SL above shelf edge; MR Fan Sequence 16 develops; infrequent turbidity current delivery due to shelf failure or large floods feeding Bryant Canyon basins (7); Eastern Fan sequences 14, 15, and early 16 develop (9).
2 (29-14 ka)	Aggradation shifts to incision with continued falling SL,	Morehouse and equivalent braid belts mark latest LMV braid formation (3); large MW floods scour valley (2003)	Prograding deltas and channel networks reach shelf edge (10-12), deliver turbidity currents to fans and intraslope basins (7, 9); probable massive resculpting of shelf-edge deposits by MW floods; canyon incision of shelf edge and slope. Southernmost incised valley scoured to 20-30 m depth below surrounding shelf, ~100 km wide;	Eastern Fan sequence 16 develops (9), then eastern fan goes dormant ; Mississippi Fan sequence 17 deposits, downlapping Eastern Fan sequence 16; Possible sequence boundary at base of large MW flood deposits; MW flood deposits probably blanket fan and reach distal basin (13)
Early MIS 1 (14-9,16 ka)	Advances and retreats of ice lobes drive episodic rerouting of discharge, between Atlantic and GoM outlets (13); maximum fluvial incision 10-13 ka (3); large MW	Maximum incision depths for southern LMV reach > 40 mbsl	Incised valley floods before surrounding shelf regions. transgression in outer shelf incised valley marked at 15-10 ka by marine sediments and fossils	Sediment delivery has shifted from earlier turbidity current mode to suspension settling from plumes; decrease in grain size and decline in supply of clay, reworked

	floods scour valley (4,13)			continental sediments, through last meltwater flood ca. 9.16 ka

(1) Lisiecke and Raymo, 2005
(2) Shen et al., 2012
(3) Rittenour et al., 2007
(4) McKay, D., and Berg, D., 2008.
(5) McVey, K.J., 2005.
(6) Heinrich, 2006
(7) Tripsanas et al., 2007
(8) Weimer, 1991
(9) Dixon and Weimer, 1998
(10) Sydow et al., 1992
(11) Roberts et al., 2004.
(12) Suter and Berryhill, 1985.
(13) Aharon 2003

Table 4. Estimates of sediment volumes, masses, and average accumulation rates for Mississippi Fan sediments bounded by seismic reflectors and age estimates of Bouma et al. (1986). Original maps of Bouma et al. (1986) were digitized in UTM coordinates, and volumes calculated using GIS software. Sediment volumes were converted to sediment masses using grain density of 2,650 kg/m^3, porosities from DSDP Leg 96 core data (Bryant et al., 1986) for core depths of 0-200 m below sea floor (bsf) , and depth-porosity relationships of Nobes et al. (1986) for greater depths. Sediment accumulation rates (SAR) are uncorrected for porosity. Mass accumulation rates (MAR) are estimated as total sediment mass/duration (y) of depositional period, and account for porosity change with depth.

Seismic Unit	Volume (km^3)	Sed. Mass (10^9 t)	SAR km^3/y	MAR Mt/y	Duration (ky)	depth bsf (m)	Porosity
0 to 20	17,500	23,221	0.32-0.44	**422-581**	40-55 ky	242	50
20 to 30	3,500	5,146	0.06-0.18	**85-468**	20-60 ky	462	45
30 to 40	11,200	17,837	No absolute age for reflector 40			595	40
40 to 50	16,000	29,763				859	30
30 to 50	27,270	47,600	0.05-0.07	**89-181**	400-525 ky		

Table 5. Details of discharge and duration for meltwater flood pulses (MWF) of Aharon (2003) and pauses in meltwater discharge to the GoM (P), with approximations of sediment delivery per pulse, using sediment concentration of 0.4 kg/m^3 for prehistoric loads, and 0.2 kg/m^3 for the 2011 flood (conservative ssc estimate from Heimann et al, 2011, and water discharge from US-ACE, 2012). Flood sediment discharge calculations are based on Aharon's (2003) assumption that suspended sediment concentrations (ssc) in meltwater floods were comparable to pre-1950 Mississippi concentrations (~0.4 kg/m^3)(Heimann et al., 2011).

Flood name of Aharon (2003)	Event start (ka)	Event duration (ka)	Water Flux (Sv, 10^6 m^3/s)	Volume per vent (km^3)	Sediment discharge per event (10^9 t)	Discharge rate during event Mt/y
MWF-1/a	16	0.55	0.09	1,561,000	624	1135
MWF-1/c	15	0.3	0.09	851,000	341	1135
MWF-1/e	14.46	0.46	0.08	1,161,000	464	1009
P-1	14					
MWF-2	13.6	0.4	0.15	1,892,000	757	1892
P-2	13.2					
MWF-3	12.9	0.4	0.1	1,261,000	505	1261
P-3	12.5					
MWF-4	12.25	1	0.15	4,730,000	1,892	1892
P-4	11.2					
MWF-5/a	9.97	0.1	0.07	221,000	88	883
MWF-5/c	9.74	0.08	0.07	177,000	71	883
MWF-5/e	9.45	0.16	0.1	505,000	202	1261
MWF-5/g	9.16	0.26	0.08	656,000	262	1009
				Mean:	Mean: 520	
				Total:	Total: 5,205	
Approximation for Mississippi River Flood 2011		~60 d	0.065 (max)	168	0.17	
		Assumes mean flow=max flow/2, and ssc of 0.2 kg/m^3				

Table 6. Timeline of major developments for the Anthropocene MRS. All dates are CE.

1717-1727	First manmade enhancements of natural MR levees for flood control, privately maintained. (2)
ca. 1800-1825	In the UMV, increase in floodplain aggradation from earlier rates of 0.2-0.9 mm/y to 2-20 mm/y, for small and large tributary catchments, respectively. (6)
1814	Bayou Manchac (distributary of the Mississippi River) is closed off from the river for defense purposes, at the recommendation of one-time pirate Jean Lafitte (2).
Ca. 1830-Present	80-99.9% decline in extent of North American prairie mostly due to agricultural development (i.e., landscape for most of the UMV and western tributaries); largest vegetative province in N. America. (8)
1835-1838	Captain Henry Miller Shreve completes first phase of removing a log jam >150 km long (the Great Raft) from the Red River (1,3)
1844-1892	Major LMR floods in 1844, 1850, 1858, 1862, 1865, 1867, 1874, 1882, and 1892 combined with impacts of the Civil War, overwhelm and weaken levee system, setting stage for ongoing and later policy developments (5)
1859	Levee breach in New Orleans produces major flooding; Congress passes the Swamp Act, and initiates surveys of the LMR, sparking the debate on how to control the river (levees only versus outlets and spillways) that develops between Humphreys and Eads
ca. 1873	US-ACE Lieutenant Eugene Woodruff completes removal of logjams from Red and Atchafalaya River (1)
1875-1876	J. B. Eads constructs levees at South Pass which help maintain a 26-30 ft channel at the time of construction. Tonnage shipped from South Pass increases from 6,875 t (1875) to 453,681 t(1880)(2)
1879	Mississippi River Commission created to replace previous State Board of Levee Commissioners. MRC works with the US-ACE to deepen the Mississippi, lessening flood potential and increasing navigability (2)
1885	US-ACE, under A.A. Humphreys, adopts “levees-only” policy, begins to strengthen levee system and close off distributaries to the LMR. (2)
1908-1923	Eads’ technique is used by the US-ACE to construct levees for a deeper channel entrance (35 ft) at Southwest Pass, later deepened to 45 ft . (2)
1904	The Mississippi River connection to the Bayou Lafourche is closed off (7)
1917	Flood Control Act authorizes MRC to expand flood control system with cost sharing by states and local interests (5)
1927	Great Flood inundates ~70,000 km^2 of the MR, tributary, and distributary floodplains, displaces 700,000 people, and remains in flood for 153 consecutive days. 17 major crevasses form in levees, and the levee south of New Orleans is opened intentionally to diminish flood crest at New Orleans (ironically, after the flood had already started to subside). Carnarvon residents remained generally uncompensated for property damage, despite prior assurances (2,5)
1928	US Congress passes the Flood Control Act (updated in 1936 and 1944) that initiates the Mississippi River and Tributaries system, including levees, flood gates, and bank revetments, by which floodwaters and navigation are maintained in the LMR.(2)
1929-1931	Bonnet Carre Spillway constructed upstream of New Orleans, to ease flood pressure on New Orleans, with a designed capacity of 250,000 cfs (5). This is represents a stepwise retreat from the levees-only policy adopted by the US-ACE 44 years earlier.
1937-2011	Bonnet Carre Spillway opened in 1937, 1945, 1950, 1973, 1975, 1979, 1983, 1997, 2008, and 2011 (up to 2014), with peak discharge of 316,000 cfs in 2011. (5)
1952	Fisk publishes analysis of likely imminent capture of Mississippi by Atchafalaya River
	dams
1963	Old River Control Structure (ORCS) completed at the confluence of the Red, Atchafalaya and Mississippi rivers, to maintain Atchafalaya flow at 30% of combined flow of Red and Mississippi (4)
1973	Major flooding on the MR weakens and nearly undermines the ORCS, resulting in redesign and expansion of the ORCS during subsequent years.

(1) Tyson, 1981
(2) Barry, 1997.
(3) Reuss, 2004
(4) McPhee, 1989
(5) US-ACE, 2012
(6) Knox, 2006
(7) LBSE, 1904
(8) Sampson and Knopf, 1994

Table 7. Holocene and Anthropocene sediment budgets. Estimates of Holocene shelf and slope accumulation are based on accumulation rates and spatial extent of Coleman and Roberts (1988a), who determined the average thickness of the MIS-1 sediment isopach (8.9 m) in 471 borings from the shelf and slope (area of ~6500 km^2), from δ18O and physical stratigraphy. Their average isopach thickness is not spatially weighted for core distribution, but borings are widely distributed and include both locations distal to main delta lobes (thin deposits) and locations proximal to Holocene deltaic depocenters (thick deposits). For our conversion of sediment volume to mass, porosity of 0.6 and grain density of 2,650 kg/m^3 were assumed.

Holocene	Sediment Load, Mt/y	Depocenters	Storage Rate, Mt/y	Timescale, y
	400-500 (1)	Alluvial valley and delta plain	230-290 (1)	11,000
		Chenier Plain	3 (2,3)	4,200
		Shelf and slope	5 (4,5)	14,000 (MIS-1)(6)
		Total storage rate over ky timescales:	238-298 Mt/y (sum of above rates)	
Latest Anthropocene				
Total load at Tarbert Landing, 2008-2010	157 (7)	Net channel and floodplain storage below Tarbert Landing	103 (7)	3
Mississippi discharge above Head of Passes, 2008-2010	30.1 (7)	Birdsfoot prodelta storage	40.3 (8)	~100
Mississippi discharge below Head of Passes, 2008-2010	30.3 (7	AWL prodelta storage	33 (9)	~100
Atchafalaya discharge, 2008-2010	35.5	Chenier Plain inner shelf	6 (10)	~100
		Chenier Plain coastal/intertidal	1.5-6 (11)	~20

(1) Blum and Roberts, 2009
(2) Gould and McFarlan, 1959
(3) This study
(4) Coleman and Roberts, 1988a
(5) Coleman and Roberts, 1988b
(6) Lisiecki and Raymo, 2005
(7) Allison et al., 2012
(8) Corbett et al., 2006
(9) Neill and Allison, 2005
(10) Draut et al., 2005a
(11) Draut et al., 2005b

Table 8. Regional responses to allogenic forcing on the system, after Coleman and Roberts (1988) and Autin et al. (1991), and other references cited.

	Response									
Forcing		Sea level	Uplands	Tributaries	Lower valley	Coast/delta	Shelf	Slope	Basin/fan	Example timeframe
Glacial Cycle										
Interglacial	Interglacial	Highstand	Slow degradation, soil formation	Stability and soil formation	aggradation	Deltaic and chenier plains	Forced regression, delta and subdelta progradation	Hemipelagic drape, rare flood-driven plumes	Hemipelagic drape, condensed section, sequence boundary	MIS 1
		Minor oscillations	Soil formation	Meander belt formation	Meander belts, soil formation	Minor degradation	Transgresssive/ Regressive adjustments			MIS 5
Glaciation	Waxing glaciation	Falling	Slow and increasing degradation	Increasing discharge, possibly strongly episodic	Shift from meandering to braided regime	Stream entrenchment and extension, terrace formation	Shelf exposure, forced regression	Enhanced plume/ rare turbidite sedimentation, MTCs Canyon/channel/fan reactivation		MIS 3-4
	Glacial Maximum	Lowstand	Major erosion and dissection		Incision, planation, outwash deposition	Shelf-edge delta development	Broad exposed shelf	Canyon erosion, MTCs	Channel-levee complexes, sand rich	MIS 2, 6
	Waning Glaciation	Rising	Loess deposition	Aggradation, possible	Valley train development	Incised valley infill,	Deltaic reworking by	Meltwater flood events,	Channel-levee	MIS 2-1 transition

				alluvial drowning in lower reaches		landward sediment trapping, transgression, erosion	marine processes	turbidity currents then nepheloid or buoyant plumes	deposits fine over time, delivery rate declines	
River Training	Isolation of river from floodplain; increased stages due to reduction of floodplain area; localized channel aggradation due to loss of stream power at diversions; localized scour due to reduced sediment cover such as downstream from dams.					Focused sediment delivery to selected outlets where local progradation may occur; marine processes and subsidence dominate elsewhere		Prodelta deposits limited to regions proximal to river outlets		Anthropocene
Catchment Subsidence	Reduced sediment supply									Early Miocene
Catchment Uplift	Increased sediment supply, if sufficient stream power is available to transport material. The Late Miocene RMOP was an example of reduced stream power during a time of regional uplift, with modest sediment delivery. In the Late Miocene Appalachians, regional uplift coupled with adequate stream flow produced marked increase in sediment delivery									Late Miocene
Salt Migration	Driven by differential sediment loading. Produces changes in bed level ranging from modest regional subsidence rates to localized intraslope basin formation, deep-sea canyon steering and closure, and fan realignment.									Jurassic to Recent